



Canavan, James W. (2017) The effects of drying on the dimensional stability of spruce wood. PhD thesis.

<http://theses.gla.ac.uk/8134/>

Copyright and moral rights for this work are retained by the author

A copy can be downloaded for personal non-commercial research or study, without prior permission or charge

This work cannot be reproduced or quoted extensively from without first obtaining permission in writing from the author

The content must not be changed in any way or sold commercially in any format or medium without the formal permission of the author

When referring to this work, full bibliographic details including the author, title, awarding institution and date of the thesis must be given

Enlighten:Theses  
<http://theses.gla.ac.uk/>  
theses@ gla.ac.uk



THE EFFECTS OF DRYING ON THE DIMENSIONAL  
STABILITY OF SPRUCE WOOD

James W Canavan

BSc. (Hons)

Submitted for the degree of Doctor of Philosophy

School of Chemistry  
College of Science and Engineering  
University of Glasgow

April 2017

## Abstract

Sitka spruce (*Picea sitchensis* (Bong.) Carr.) has been the most common forestry species in UK plantations for many decades. It is generally fast grown in short rotation, which has implications for quality. The harvested timber has a number of end-use applications. Of these, sawn construction grade timber is at the high end of market value. Currently, under one third of home grown sawn timber processed by sawmills achieves the required C16 or higher grading for construction class timber. Presently there is significant standing stock of 40 years old or under. Improvements in timber quality would create significant benefits for growers and processors.

Distortion in kiln dried sawn timber is a considerable barrier to improving grading classification and marketability. Twist in particular accounts for around six percent of the rejections after kiln drying. Additional twist when timber dries further; in storage, at construction sites or in-service, is perceived as a marketing issue. The focus of this work was to better understand the evolution of twist during the drying process and seek to improve quality by examining the key properties in sawn timber that contribute to the formation of twist.

Samples of regularly processed full size (3 m in length) sawn timber were kiln dried with no restraint to promote maximum twist. This was done in three stages to assess the impact of intermittent drying. Measurements of twist, moisture content, acoustic velocity and basic dimensions were taken before and after each drying cycle. The results showed highly significant differences between battens containing the pith and those that did not. Drying in stages did not seem to affect the linearity of the moisture content against twist relationship. Twist was seen to develop at a consistent rate throughout the process regardless of the final amount of twist accrued or the position from which the batten was sawn. Where timber is likely to dry to lower moisture content after sale it is therefore possible to predict the additional twist from the moisture content expected and allow for it by stricter grading than the twist standard demands.

Twist was seen to decrease slightly during a lengthy period of storage in controlled conditions between drying cycles. This may allude to a relaxation effect which could have

implications for timber distortion in-service but this would require a more extensive study before any such conclusions could be drawn.

A second batch of unrelated samples, were kiln dried to 12% MC under restraint. All of these samples contained the pith along their length and all developed significant amounts of twist. This suggests that battens containing the pith will twist regardless of restraint.

A method was developed to measure longitudinal shrinkage. This required the batten size to be reduced to fit the method and battens were sawn into 3 x 1 m sections. Battens were re-saturated and measured daily throughout air drying until an equilibrium moisture content was achieved. Measurements of transverse shrinkage were also taken concurrently. No relationship could be found between the longitudinal and transverse results. When plotted against the data for twist a positive relationship was found with longitudinal shrinkage.

Acoustic tools were used to calculate dynamic stiffness. As the values for acoustic velocity squared correlated well with dynamic stiffness, other possible relationships were explored. Good agreement was found with twist and longitudinal shrinkage. This suggests it may be possible to predict twist in sawn timber directly or as a function of microfibril angle, using acoustic tools.

A simple method for measuring grain angle was devised. Discs taken from the trees used in the drying experiment were measured for grain angle to compare with other measured properties. The measurement method worked well but the sample size was small and the discs too thin to provide good quality data quality. The results were not as instructive as expected. A vague relationship with twist was found. A repeat of the experiment with an improved method could yield more conclusive results.

A method was developed to measure radial and tangential shrinkage in discs. Discs of Sitka spruce from a different source were used. Discs were saturated and allowed to dry with the expectation of cracks developing. The intention was to explore the nature of internal stresses present in intact discs and why tangential and radial shrinkage differs. As only one disc cracked the scope of comparison was limited but it was apparent that the greater shrinkage tendency in the tangential direction was responsible for radial cracking.

## Table of contents

1	Introduction	13
1.1	Sitka spruce ( <i>Picea sitchensis</i> Bong.) Carr.)	14
1.2	Anatomy	15
1.2.1	An overview of conifer anatomy	15
1.2.2	Tracheid cell structure	18
1.2.3	Juvenile wood	21
1.2.4	Knots	21
1.2.5	Compression wood	22
1.3	Distortion	22
1.3.1	Twist	24
1.4	Grading of sawn timber	24
1.5	Drying sawn timber	26
1.6	Longitudinal, radial and tangential shrinkage	28
1.7	Grain angle	29
1.8	Aims of this study	32
2	The development of twist due to kiln drying: unrestrained and restrained drying	33
2.1	Introduction	33
2.2	Methods and materials	34
2.2.1	Sampling	34
2.2.2	Unrestrained kiln drying	36
2.2.3	Measurement of twist: FRITS Frame	40
2.2.4	Calculation of degree of twist: FRITS Frame	43
2.2.5	Measurement of twist: calibrated wedge	44
2.2.6	Calculation of degree of twist: calibrated wedge	46
2.3	Results	47
2.3.1	Measurements	47
2.3.2	Method choice; FRITS Frame and wedge method	47
2.3.3	Drying cycles	48
2.3.4	Between tree variation	49
2.3.5	Between log variation	52
2.3.6	Between position variation	56
2.3.7	Storage period	59
2.4	Kiln drying of Sitka spruce under restraint	61
2.4.1	Introduction	61
2.4.2	Methods and materials	61
2.4.2.1	Sampling	61
2.4.2.2	Kiln drying under restraint	62
2.4.3	Results	64
2.4.3.1	Comparing restrained and unrestrained drying	65
2.5	Predicting twist	67
2.6	Discussion	68
2.6.1	Measuring twist	68
2.6.2	Kiln drying	69
2.6.3	Unrestrained drying	69
2.6.4	Restrained drying	70
2.6.5	Comparing unrestrained and restrained drying	71
2.6.6	Storage	71
2.6.7	Predicting twist	72

3	Longitudinal and transverse shrinkage	73
3.1	Introduction	73
3.2	Methods and materials	73
3.2.1	Samples	73
3.2.2	Method validation	74
3.2.3	Preparation of samples	74
3.2.4	Saturation of battens and moisture content	75
3.2.5	Measuring frame	76
3.2.6	Timescale of recorded measurements	78
3.2.7	Longitudinal shrinkage measurements	78
3.2.8	Transverse shrinkage measurements	80
3.3	Results	81
3.3.1	Variation in longitudinal shrinkage	81
3.3.1.2	Between and within tree variation	82
3.3.1.3	Between log variation	84
3.3.1.4	Positional variation	86
3.3.2	Longitudinal shrinkage and decreasing moisture content	88
3.3.3	Transverse shrinkage	95
3.3.4	Longitudinal shrinkage, transverse shrinkage and twist	96
3.4	Discussion	99
3.4.1	Method	99
3.4.2	Variation in longitudinal shrinkage	100
3.4.3	Longitudinal shrinkage and decreasing moisture content	101
3.4.4	Transverse shrinkage	101
3.4.5	Shrinkage in relation to twist	102
4	Acoustic velocity	104
4.1	Introduction	104
4.2	Methods and materials	104
4.2.1	Samples	104
4.2.2	Equipment	105
4.2.3	Calculation of modulus of elasticity	106
4.3	Results	106
4.3.1	Modulus of elasticity	106
4.3.2	Twist and acoustic velocity	108
4.3.3	Longitudinal shrinkage and acoustic velocity	110
4.4	Discussion	112
5	Grain angle	114
5.1	Introduction	114
5.2	Methods and materials	114
5.2.1	Samples and sample preparation	114
5.2.2	Measurement	116
5.2.3	Determination of grain angle	117
5.3	Results	119
5.3.1	Agreement between measurements	119
5.3.2	Grain angle values	120
5.3.3	Grain angle and twist	123
5.4	Discussion	124
5.4.1	Method	124
5.4.2	Grain angle data	125
5.4.3	Grain angle and twist	126

6 Radial and tangential shrinkage	128
6.1 Introduction	128
6.2 Methods and materials	128
6.2.1 Experiment 1	129
6.2.1.1 Sample preparation	129
6.2.1.2 Measurement	131
6.2.2 Experiment 2	132
6.2.2.1 Sampling	132
6.2.2.2 Sample preparation	133
6.2.2.3 Measurement and drying procedure	134
6.3 Results	135
6.3.1 Experiment 1(Preliminary)	135
6.3.2 Experiment 2	138
6.3.2.1 Radial and tangential shrinkage with decreasing moisture content	138
6.3.2.2 Comparing radial and tangential shrinkage	149
6.4 Discussion	151
6.4.1 Method	151
6.4.2 Experiment 1	152
6.4.3 Experiment 2	153
6.4.3.1 Moisture content	153
6.4.3.2. Shrinkage in intact discs	153
6.4.3.3 V cracks and shrinkage	153
7 Discussion	155
7.1 Conclusions	155
7.2 Future work	158
List of references	160

## List of Tables

2.1	Total means values of twist per metre for all trees with standard deviations	50
2.2	Between tree differences in twist with LSD 5% grouping	50
2.3	Fisher post hoc analysis of accrued twist at each drying target	51
2.4	Covariance matrix comparing slopes between butt and crown logs at four drying targets	55
2.5	ANCOVA (analysis of covariance) test to establish difference in slope between butt and crown logs at four drying targets	55
2.6	Percentage change in degrees twist per metre after six week conditioning period	60
3.1	Mean values of longitudinal shrinkage for tree, log and position for trees 1-6	82
3.2	Fisher post hoc analysis of between tree variation	83
3.3	Interquartile range and Butt: Crown ratio (%) for butt and crown logs by tree	85
3.4	Mean values and interquartile range for batten positions A, B and C in butt and crown logs	87
3.5	All Pearson correlation values for moisture content against longitudinal shrinkage taken from the estimated FSP and below	94
4.1	Dynamic modulus of elasticity (MoE) values for trees 1-6 at four drying targets	107
6.1	Mean percentage moisture content by disc position (top table) and by tree (bottom table) showing values for start (saturated state) and end (equilibrium moisture content)	139

## List of Figures

1.1	Log of a conifer detail showing radial layers of anatomical structure	15
1.2	Microscopic image showing earlywood and latewood cells	17
1.3	A disc of Sitka spruce in cross section showing heartwood and sapwood	18
1.4	Radial section of a conifer showing cellular organisation and cross fields	19
1.5	Detail of a wood cell showing basic structure of cell walls	20
1.6	Diagram of four types of distortion; bow, twist, spring and cup	24
1.7	Schematic of a typical steam kiln	27
1.8	The three directions of shrinkage shown in a quartered log	29
1.9	A tool to measure grain angle	31
2.1	Felling of samples at Spadeadam Forest, Cumbria	34
2.2	Labelling of battens to identify position within log	36
2.3	Processing of logs at BSW Carlisle	36
2.4	Image of kiln and kiln peripheral control unit	37
2.5	Samples stacked in kiln prior to drying	38
2.6	FRITS Frame	41
2.7	Detail of FRITS Frame features	42
2.8	Batten showing the dimensions used to calculate degree of twist	44
2.9	Images of wedge measurement set up and operation	45
2.10	Measuring wedge and labelled batten end	46
2.11	Scatter plot of FRITS Frame against wedge measurements	48
2.12	Comparing the percentage accrued twist at different drying targets	51
2.13	Accrued twist in thirty-six battens after drying to 20% moisture content	52
2.14	Mean twist per metre showing butt and crown log variation	53
2.15	Scatter plot of mean twist per metre for butt against crown logs	54
2.16	Individual scatter plots of butt against crown by position in log	54
2.17	Detail of sawing pattern used to remove three battens	56
2.18	Mean twist per metre for all A,B and C battens at four drying targets	57
2.19	Percentage increase in twist by batten position at each drying target	58
2.20	Percentage of total twist at each drying target by batten position	58
2.21	Change in mean degrees of twist per metre after storage period	59
2.22	Images of batten ends showing positioning of pith	62
2.23	Stack arranged in frame for restrained drying	63
2.24	Scatter plot of measured twist in restrained battens at Green and 12% moisture content	64
2.25	Scatter plot of twist in restrained battens at 12 and 18% moisture content	65
2.26	Column charts of change in twist per metre from five drying cycles	66
2.27	Column charts of change in twist per metre from five drying cycles with grading limits	66
2.28	Scatter plot of relationship between twist per metre at 20% moisture content and twist per metre at 15 and 8% moisture content as a predictive model	67
3.1	Image of inflatable pool with battens undergoing re-saturation	76
3.2	Overview of longitudinal shrinkage measuring frame	77
3.3	Detail of positioning end of measuring frame with marked batten	79
3.4	Image showing detail of method for transverse shrinkage measurements	80
3.5	Image of cutting pattern detail to produce three battens from each log	81
3.6	Individual value plot of between tree variation	83
3.7	Box plots of individual value range in butt and crown logs	84

3.8	Individual value plot showing mean values for each batten in butt and crown logs	85
3.9	Individual value plots for mean shrinkage by position	86
3.10	Box plots of the range of longitudinal shrinkage values by position sorted into butt and crown categories	87
3.11	Individual value plot showing total longitudinal shrinkage for all battens by position within logs	88
3.12	Scatter plot of moisture content against mean daily shrinkage for trees 1-6	90
3.13	Scatter plot of moisture content against mean daily shrinkage showing butt/crown variation for trees 1-3	90
3.14	Scatter plot of moisture content against mean daily shrinkage showing butt/crown variation for trees 4-6	91
3.15	Scatter plot of moisture content against mean daily shrinkage by position; Tree 1	91
3.16	Scatter plot of moisture content against mean daily shrinkage by position; Tree 2	92
3.17	Scatter plot of moisture content against mean daily shrinkage by position; Tree 3	92
3.18	Scatter plot of moisture content against mean daily shrinkage by position; Tree 4	93
3.19	Scatter plot of moisture content against mean daily shrinkage by position; Tree 5	93
3.20	Scatter plot of moisture content against mean daily shrinkage by position; Tree 6	94
3.21	Column chart of mean total transverse shrinkage for batten positions A, B and C for trees 1-6	95
3.22	Column chart of collective mean values for battens A, B and C for transverse shrinkage across the six measured faces	96
3.23	Column chart of mean longitudinal and transverse shrinkage for three 1-6	97
3.24	Scatter plot of mean longitudinal shrinkage against twist at 8% moisture content for trees 1-6	97
3.25	Scatter plot of mean transverse shrinkage against mean twist per metre at 8% moisture content by batten position	98
4.1	Image of the operation of the Hitman HM2000 acoustic tool	105
4.2	Scatter plots of $AV^2$ against dynamic modulus of elasticity at all four drying targets	107
4.3	Scatter plots of twist against $AV^2$ at all drying targets showing predicted $AV^2$ value	108
4.4	Basic predictive model of $AV^2$ against moisture content based on actual measured values	109
4.5	Scatter plot of all thirty-six battens; Longitudinal shrinkage against $AV^2$ at approximately 15% moisture content	110
4.6	Scatter plot of all thirty-six battens with butt and crown log differentiation; longitudinal shrinkage against $AV^2$ at approximately 15% moisture content	111
4.7	Scatter plot of all thirty-six battens with positional differentiation; Longitudinal shrinkage against $AV^2$ at approximately 15% moisture content	111
5.1	Image detailing disc splitting method	115
5.2	Labelled diagram of grain angle measuring apparatus	116
5.3	Diagram detailing the method of measurement on both faces of a disc	118
5.4	Plot of the before and after adjustment of the measured angles and 'zero point'	118
5.5	Scatter plot of relationship between A and B faces of split discs	119

5.6	Standard deviation of variation between faces A and B for each disc by height	120
5.7	Radial profiles of grain angle in degrees for each disc	121
5.8	Radial profiles for each tree of mean grain angle in degrees showing common trends suggesting changes in grain angle direction	122
5.9	Scatter plots of mean grain angle against mean twist at 20% moisture content for trees 1-6	123
6.1	Image of pinned disc used in Experiment 1 with pinning details	130
6.2	Same disc as 6.1 before and after cracking	130
6.3	Sitka spruce disc split into quarters and re-pinned	131
6.4	Image of digital calliper with small drilled hole highlighted	132
6.5	Diagram of sampling procedure to remove discs	133
6.6	Layout of a pinned disc with detail of measurement procedure	134
6.7	Radial and tangential swelling and shrinking during wetting/drying cycle in a disc	136
6.8	Differential radial and tangential shrinkage in a disc at 14% and 20 % moisture content	137
6.9	Differential radial and tangential shrinkage compared as a function of position (inner or outer) within a disc	138
6.10	Interpolated values of moisture content against shrinkage for discs 1A and 1B	140
6.11	Interpolated values of moisture content against shrinkage for discs 1C and 1D	141
6.12	Interpolated values of moisture content against shrinkage for discs 2A and 2B	142
6.13	Interpolated values of moisture content against shrinkage for discs 2C and 2D	143
6.14	Interpolated values of moisture content against shrinkage for discs 3A and 3B	144
6.15	Interpolated values of moisture content against shrinkage for discs 3C and 3D	145
6.16	Difference in total volumetric shrinkage in trees 1-3 showing variation with height (disc position)	148
6.17	Scatter plot of mean values of total radial against total tangential shrinkage in eleven of the twelve discs (excluding cracked disc)	149
6.18	Images of crack development in disc 3D over eight days	150

## Acknowledgements

As with any piece of work of this nature there are a number of organisations and individuals without whose assistance none of the following would have been possible.

I would like to thank the University of Glasgow, Forest Research and the Engineering and Physical Sciences Research Council for providing the funding which made this work possible. Supervisors have come and gone for a variety of reasons throughout this venture but all have played a role in its completion. Firstly, thanks to Mike Jarvis at the School of Chemistry, University of Glasgow who has been the only constant over the period and who was always available for advice and support when required. At Forest Research thanks to Barry Gardiner who was there at the beginning and to James Pendlebury who stepped in on Barry's departure. Also thanks to Karin de Borst at the School of Engineering, University of Glasgow who also filled a supervisory role.

Thanks for practical assistance and advice to all staff and colleagues at University of Glasgow; Hugh Flowers, Ian Pulford, Harry Duncan, Michael Beglan, Mohammad Ali Salik, Steven Adams, Kate Hudson-McAulay and Adam Boney. A particular mention is due to Mike Yerbury, University of Glasgow and Egger, who was instrumental in arranging site access, harvesting, transportation and processing of samples on more than one occasion which made life much easier for myself. Many thanks for this and your ongoing support throughout, it was very much appreciated.

At Edinburgh Napier University, staff and students past and present, Callum Hill, Dan Ridley-Ellis, Stefan Lehneke, James Ramsay and Tom Drewitt. Thanks for the use of facilities, equipment and personal assistance which contributed to the completion of this work.

A great deal of the practical work for this research was carried out at the Forest Research, Northern Research Station (NRS) at Bush Estate. I am very appreciative of the facilities that were made available to carry out his work namely; the drying kiln, use of buildings for practical work and storage, use of tools and equipment and vehicles for transportation. Many thanks to all at NRS particularly Elspeth Macdonald, John Paul McLean, Carina Convery, Colin McEvoy, Dave Clark, Tom Connolly, Bruce Nicoll and Kate Beauchamp.

Thanks to Kirsty McLean at the SRUC-BioSS CT Unit at Bush Estate for use of their scanner and for providing software for disc analysis.

Processing of samples was carried out at BSW Timber, Carlisle. Thanks to Alex Brownlie of BSW for kindly providing this service and to Dave Miras and his team at Carlisle for their assistance. Thank you also to the staff at BSW Fort William for the use of their facilities and equipment. Further pre-processed samples were obtained from James Jones and Sons, at Lockerbie. Many thanks to David Leslie and all his staff for their help in providing these samples.

Apologies if I've forgotten anyone.

Finally, many thanks to my family and friends for their support and patience over the period of this work, in particular to my Father-in-law Billy and especially to my wife Susie whose support, experience and understanding were invaluable when the going got rough. I couldn't have done it without you.

## **Candidate's declaration**

I declare that the work presented in this thesis is entirely my own and of my own composition unless otherwise stated and that no part of this work has been submitted for any other degree.

James W Canavan

April 2017

## 1. Introduction

It has been shown that wood and wood products have a less significant environmental impact and lower carbon footprint than alternative materials used in the construction industry (Davis, 2009). As a construction material, wood has been shown to be more energy efficient than either steel or concrete (Abimaje and Baba, 2014). Good construction timber is strong, stable, durable and versatile. It also benefits from aesthetic and “natural” qualities that can be appealing and inspirational.

Coniferous species (softwoods) currently account for 95% of the processed timber in the UK. Around 60% of this is sawn timber intended for the construction market. In 2013 softwood deliveries to UK sawmills totalled 6.5 million green tonnes. When processed, 29% of this volume accounts for construction grade timber (Forestry Commission Statistics, 2014) achieving C18 or below strength class within the grading requirements of the European standard EN 14081-1:2005+A1:2011 (CEN, 2011).

Sitka spruce (*Picea sitchensis* (Bong.) Carr.) currently accounts for around one half of the stocked area for coniferous species in the United Kingdom and more than two thirds of the stocked area in Scotland. Historically, it has been identified that the objective of maximising volume yield in this species appears to be compromising batten quality and performance (Macdonald and Hubert, 2002). To this end, understanding existing deficiencies in performance are crucial to implementing improvements in silviculture and processing.

The Strategic Integrated Research in Timber (SIRT) network is a collaborative research initiative between the University of Glasgow, Edinburgh Napier University and Forest Research. Research undertaken by SIRT aims to advance the understanding of wood and wood products to the benefit of the UK forest industries and processors.

Twist distortion in kiln dried battens has been identified as one of the most limiting factors in sawn timber which is intended for use in the construction industry. In this work the dimensional stability of kiln dried sawn timber is assessed by investigating the causes of twist by analysis of measured properties and exploring means by which it can be minimised in the future.

## 1.1 Sitka spruce (*Picea sitchensis* (Bong.) Carr.)

Sitka spruce is a native of the North West Pacific with a coastal range of around 3000km stretching from Northern California in the south to Southern Alaska at its northern extreme. It is named for the town of Sitka on Baranof Island, Alaska where it was first encountered by European explorers. It was introduced to the UK in 1831 by botanist and explorer David Douglas (Samuel et al, 2007). Originally popular as an ornamental in parks and gardens, its suitability to the British maritime climate and propensity to rapid growth quickly established it as a favourite among plantation landowners. It has since become extensively grown throughout the United Kingdom. Sitka spruce will grow in a variety of soil types; alluvial, sandy/coarse textured and deep organic soils. In well drained, permeable soils with an adequately accessible water table, rooting can occur up to 2m in depth. In shallower soils lateral rooting is common to maximise water and nutrient uptake. In its native range it can be found growing from sea level up to an altitude of around 900m in south eastern Alaska (Macdonald, 1967., Harris, 1990).

The provenance of the majority of Sitka spruce growing in Britain today is from the Queen Charlotte Islands (QCI) ( $53^{\circ} 0' 0''$  N,  $132^{\circ} 0' 0''$  W) situated off the west coast of British Columbia, Canada. Similarities in latitude and climatic conditions were the predominant reasons for this choice. Some phenological properties of the QCI provenance have been noted. Susceptibility to early/late frosts and preference to milder, wetter climatic conditions has led to consideration of other provenances. The Alaskan provenance may cope better in the more northern reaches of Scotland while Washington or Oregon may have more potential in Southern England. Experimental trials have indicated a general suitability for Washington and Northern Oregon provenances at selected sites in Wales and South West England (Samuel et al, 2007). A variety of growing trials have been carried out since the 1920s throughout Britain. The mechanical properties of the timber produced are dependent on a number of factors such as growth rate, stem straightness, branching and wood density. In recent years, where mature stocks of trees exhibiting one or more of these enhanced properties were available, progeny have been developed through trials with reference to unimproved species of QCI origin. As a result improved planting stock (plus trees) which maximise growth rate and stem straightness while minimising loss of wood density have been available since the 1990s in an attempt to improve the quality of construction grade timber (Mochan et al, 2008). Current investigation of the impact of climate change will determine the role of this species in the future of UK forestry (Ray et al, 2002). Research in this area is ongoing.

## 1.2 Anatomy

Conifers belong to a group of seed bearing plants called gymnosperms which pre date their angiosperm (hardwood) relatives. Gymnosperms first appear in the fossil record in the late Devonian period around 360 million years ago (Campbell and Reece, 2002a). As may be expected of an evolutionary antecedent, the anatomical structure and reproductive system of gymnosperms is less complex than that of angiosperms. In terms of processing the wood of conifers into useable timber, it is none the less a multifaceted structure where small local differences in anatomical organization can have a considerable bearing on the quality and stability of sawn timber.

### 1.2.1 An overview of conifer anatomy

The basic anatomical layers of a conifer are shown in the labelled diagram in Figure 1.1.

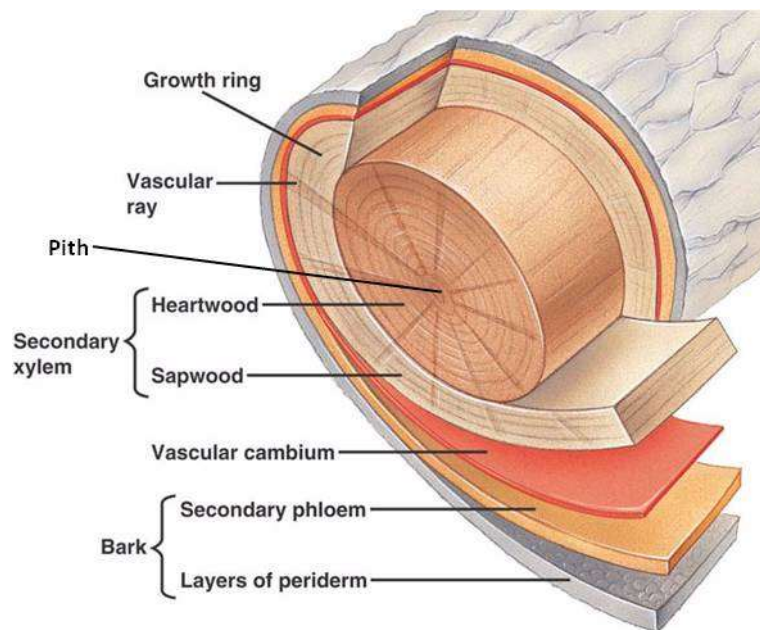


Figure 1.1. Log of a conifer with major sections peeled away and labelled to highlight the radial layers of anatomical structure. The central pith represents the initial growth of the tree. Initial growth consists of primary xylem and primary phloem. Cells are generated from the vascular cambium; secondary xylem in the direction of the pith and secondary phloem in the direction of the bark. (Image: ©Pearson Education Inc. Publishing as Benjamin Cummings, adapted from Campbell and Reece (2002a))

The tissue of the primary apical meristem is comprised of parenchyma cells, the most common ground tissue found in all plants. Around these principal cells, a ring of vascular bundles develops, comprised of primary xylem and phloem cells; thin, elongated conducting cells. This forms the vascular cambium which in turn generates secondary xylem to the inside of the ring and secondary phloem to the outside. The innermost parenchyma cells will develop into the pith of the tree. The pith is normally visible as a small, darker coloured central circle of soft, spongy material around 1-3mm in diameter when seen in cross section. As primary growth continues to elongate the stem, secondary growth from lateral meristems generate secondary xylem between the vascular cambium and the pith and secondary phloem between the vascular cambium and the bark. From this point cell division at the vascular cambium continues to produce secondary xylem which becomes what we know as the wood of the tree. Cell division on the secondary phloem side of the vascular cambium becomes less productive and an additional lateral meristem; the cork cambium, is formed. This produces a layer of cork cells which serve as a protective impermeable barrier. The cork cambium and cork cells are collectively known as the periderm. Combined with the secondary phloem this constitutes the bark of the tree; its outermost layer (Campbell and Reece, 2002<sub>b</sub>). Functionally the secondary phloem transports sap, containing the nutrient by-products (sugars, starches, carbohydrates and proteins) of photosynthesis. Secondary xylem transports water from the roots of the tree throughout its structure to replace water lost due to respiration. This water may also contain soluble organic and inorganic compounds present in soil or ground water.

Outward from the pith, annual growth is visible to the naked eye in the form of added rings of secondary xylem. Each growth ring comprises a light band (earlywood) and a dark band (latewood) which represent one year of growth (Figure 1.2). In temperate climates, earlywood cells are laid down from early spring through to late summer. Earlywood cells are roughly hexagonal in shape when viewed in transverse section. They have thin cell walls and wide lumen and are collectively visible on a transverse surface as the lighter coloured bands in each annual ring. As summer progresses towards autumn the rate of growth decreases. From this point latewood cells, with thicker cell walls and narrower lumen which are more oblong in shape, are laid down until the growing season ends. Latewood cells are visible as the darker and often thinner band in an annual ring. On average, earlywood cells account for 40-80% of cell growth in any year. This is however dependent on site, climatic conditions and water availability (Domec and Gartner, 2002).

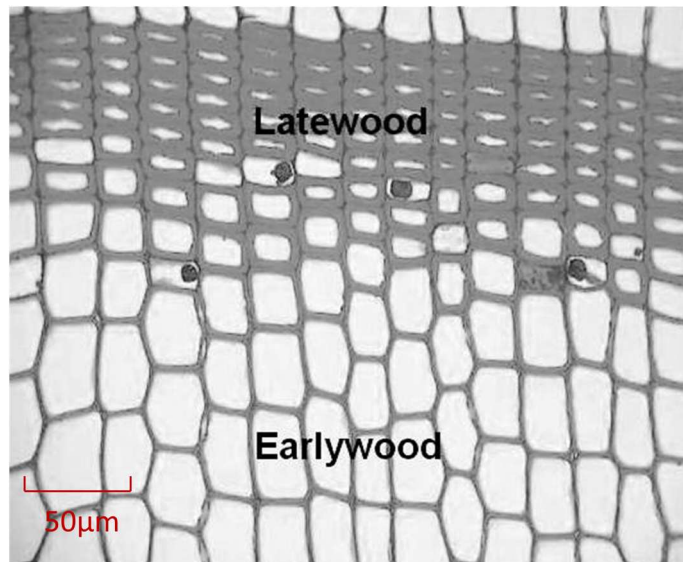


Figure 1.2. Microscopic image showing earlywood and latewood cells. Scale bar represents 50 $\mu$ m.

When viewing a cross section of a log, there is often an observable central, disc shaped area that is a darker in colour than the surrounding outer wood (Figure 1.3). This darker interior wood is termed the heartwood and the lighter surrounding wood the sapwood. In some species, including Sitka spruce, this is not always clearly visible. However, both bands will be present regardless of any obvious colour difference. As a tree matures, cells become lignified and effectively non-living. These dead cells make up the heartwood. This begins in the inner annual rings of the tree at around 7 years of age and progresses at a rate of around 0.5 to 0.7 annual rings per annum thereafter (Beauchamp, 2011). The chemical processes which transform sapwood to heartwood produce extractives which are retained within the heartwood cells. These extractives are of several classes - e.g. lignans, flavenoids, and tannins – and their functions within the tree are diverse. Caron-Decloquement (2010) found there to be at least 34 different extractives in Sitka spruce. Extractives add to the stability of the structure at the core of the tree and are an essential factor in the durability of wood as a working material (Taylor et al, 2002). Heartwood is no longer involved in the transport and exchange of materials. The lighter coloured sapwood is essentially the living part of the tree where water and nutrient transport is facilitated.

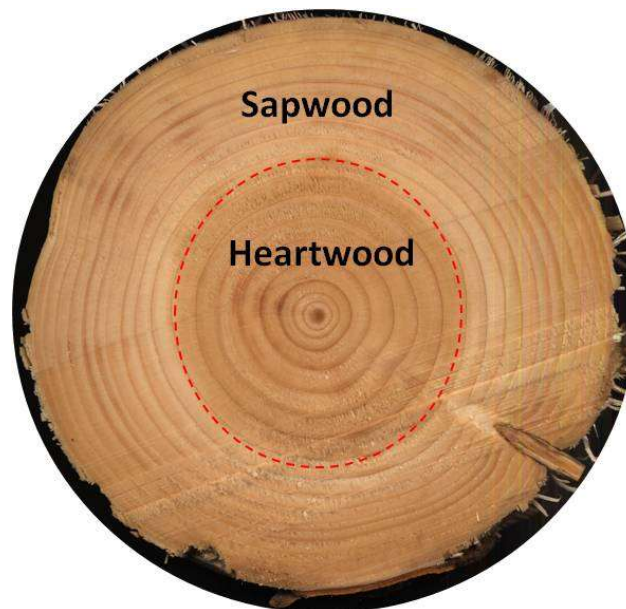
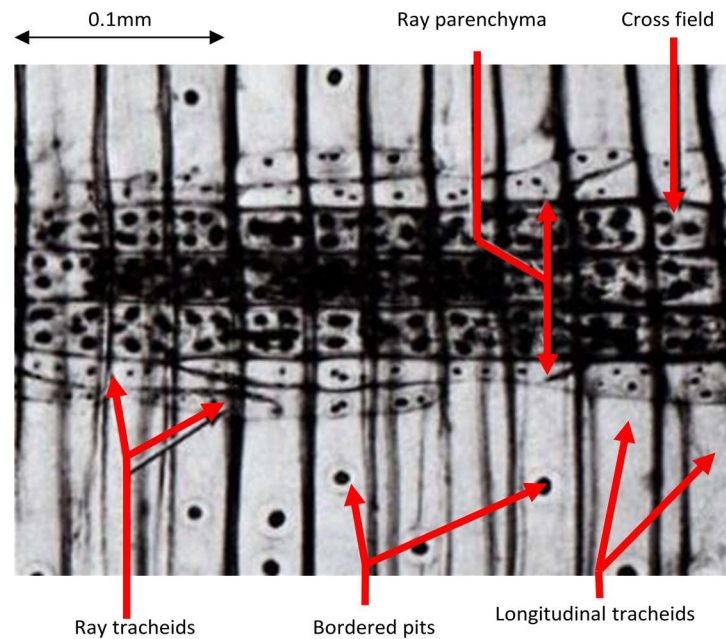


Figure 1.3. A disc of Sitka spruce in cross section showing heartwood and sapwood. The heartwood area is visible as the darker central area within the red dotted line. This is surrounded by the lighter coloured sapwood. The colour differentiation is not always clearly visible to the naked eye in Sitka spruce.

### 1.2.2 Tracheid cell structure

In conifers the primary and secondary xylem and phloem cells take the form of tracheids, the secondary xylem cells being the larger and dominant variety. Tracheids formed from secondary xylem are cylindrical shaped (fusiform) cells with wedged, imperforate ends and are normally no more than 5 mm in length at maturity and around 0.015 – 0.080 mm wide (Wilson and White, 1986a). Pitting occurs regularly in the cell walls creating channels between cells by connecting pit pairs or bordered pits. This is evident along their length and at the tapered ends and facilitates longitudinal transport of water and nutrients between adjoining cells. In the radial direction cells are mostly uniseriate bands of ray parenchyma cells with a number of ray tracheids present in some species. Both systems are connected by various forms of pitting in cell walls. When viewed in radial cross-section bands of interlinked longitudinal and radial cells (cross fields) are clearly visible as shown in Figure 1.4. (Esau, 1977a).



**Figure 1.4. Radial section of a conifer showing longitudinal tracheids with bordered pits perpendicular to ray parenchyma cells and some ray tracheids. Rectangular areas of cross fields are clearly visible (image adapted from Esau, 1977a).**

Tracheids contain a primary and a secondary cell wall, with the secondary wall being additionally divided into three sections. Each cell wall contains bundles of microfibrils with differing orientation. The configuration of these microfibrils within the cell walls has a significant influence on a tree's physical and mechanical strength. The general structure of a wood cell (tracheid) is shown in Figure 1.5.

When a cell divides into two daughter cells they are bonded by an intercellular layer, the middle lamella, which consists mainly of pectic materials. Upon this layer, and often indistinguishable from it, a primary wall is formed on either side made up of pectic and cellulosic material. Microfibrils in the primary wall are of a disordered nature, designed to accommodate cell expansion. The secondary wall does not immediately develop and the primary wall does not become lignified until the secondary wall is laid down (Wilson and White, 1986b).

The secondary wall consists of three layers of cellulose and hemicelluloses. The three layers of secondary wall are defined as the  $S_1$ ,  $S_2$  and  $S_3$ , sequentially inward from the primary wall. This demarcation is largely due to varying layer thickness and the orientation of the microfibrils in each. The  $S_2$  layer is considerably thicker than the  $S_1$  and  $S_3$  layers

and can constitute up to 90% of the secondary wall (Moore, 2011). The  $S_2$  microfibrils are more ordered and steeper in angle to the axis;  $10^\circ$  to  $30^\circ$ , compared with those of the  $S_1$  and  $S_3$  layers which generally have angles of  $50^\circ$  to  $70^\circ$  and  $60^\circ$  to  $90^\circ$  respectively. Microfibrils are wound in a helical fashion around the cell walls. In the  $S_1$  layer this is a mixture of  $S$  (right to left) and  $Z$  (left to right) directions. The  $S_2$  layer has a regular and tightly packed  $Z$  helix. The  $S_3$  layer is also mixed but predominantly takes the form of an  $S$  helix (Walker, 2006a).

This configuration of microfibril angles in the various layers provides structural support for the growing tree, particularly in the juvenile stage – to protect against wind blow and other physical disturbance - and most notably within the  $S_2$  layer (Barnett and Bonham, 2004). Spaces between microfibrils in the cell wall are packed with non-cellulosic molecules (Esau, 1977b).

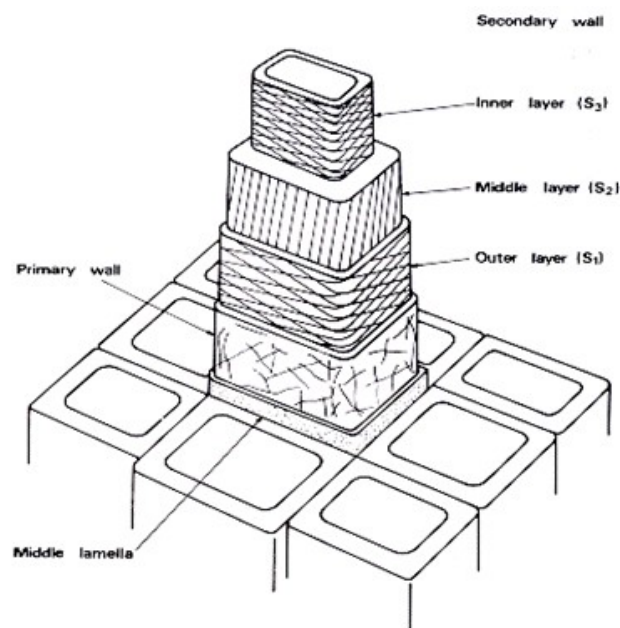


Figure 1.5. Detail of a wood cell (tracheid) showing the basic structure of the middle lamella, primary and secondary walls, and detail of the three layers of the secondary wall (Esau, 1977b).

As the cell matures the cell walls become lignified, causing dimensional modifications in the cell structure. As this process is repeated with annual growth, compressive and tensile stresses develop between adjoining cells (Plomion et al, 2001). The release of these stresses when logs are processed is a source of distortion in sawn timber.

### **1.2.3 Juvenile wood**

In young trees the properties of cells differ from those laid down later in development. Around the central pith is the juvenile wood, which originates in the growing sapling. Juvenile wood in conifers generally grows faster, has lower density and strength, shorter microfibrils and greater microfibril angle than mature wood (Passialis and Kiriazakos, 2004). Cameron et al (2005) found high annual ring width and microfibril angle, low density and low proportions of latewood in the first 12 annual rings of fast grown Sitka spruce. Observations of changes in tracheid length and microfibril angle are identifiers of the transition from juvenile wood to mature wood. It is estimated that on average this is a period of around 15 years (Moore, 2011). The presence of juvenile wood in sawn timber and particularly the influence of the higher microfibril angles found in juvenile wood have been identified as one of the key factors in the development of twist on drying (Vainio et al 2002; Gorisek et al, 2005).

### **1.2.4 Knots**

Knots are regarded as a defect by processors but are an inevitable and indeed essential component of tree growth. Knots arise from the branching process which allows the tree to develop leafy branches to facilitate photosynthesis. There are three main types of knot. They are; (1) fully formed branches where the knot will be an integral part of the structure, (2) partially formed branches that have been cut or died and are present as a loose knot in the wood and (3) branches that have been cut close to the tree trunk where normal growth will continue and surround the knot, leaving it embedded in the trunk (Wilson and White, 1986c). Knotting can impact on the dimensional stability and mechanical properties of sawn timber. This is very much dependant on the type of knot present and the overall volume of knotting in each individual piece of timber. This can be highly variable in any

consignment of logs and sorting to segregate undesirable pieces is time consuming and uneconomical. There appears to be little dedicated literature dealing specifically with the subject of knots. Macdonald and Hubert (2002) discuss the potential management of knot formation in relation to re-spacing and pruning during growth. It concludes that efforts to manage knots do not necessarily increase timber value. Between species variation in the volume of knotting can be considerable. Sitka spruce, by its nature, tends to be at least moderately knotted in general.

### **1.2.5 Compression wood**

During growth, intercellular stresses will develop within the anatomical structure of all trees. This takes place where normal growth is disrupted and occurs in response to growth deviating from the vertical, e.g. when branching take place. This may also occur in response to biophysical factors; wind blow, slope or to optimise branch positioning to maximise access to light. Differently structured cells are laid down to correct this in order that normal growth can be resumed. In conifers this type of growth is termed compression wood (Fang et al, 2008).

Compression wood cells are shorter and rounder than normal wood cells. They have thicker cell walls and higher microfibril angle are more compactly arranged with less space between individual cells (Timell, 1986). When logs are sawn these stresses are released and can be a major influence on distortion in sawn timber. Compression wood is a complex phenomenon. Its effect on distortion is not fully explored in this work.

## **1.3 Distortion**

There are numerous reasons why sawn timber distorts when it is processed. Firstly, it is always worth remembering that trees do not grow for our benefit. What we see as defects or difficulties when processing wood will more often than not have a biological function which is of benefit to the growing tree. When drying and processing wood, the means by which we deal with inherent growth characteristics will determine the final quality of the finished product.

When a tree is harvested it ceases to be a living organism. Immediately moisture will begin to be lost. As logs are further processed into battens, the rate at which this occurs will increase as the surface area exposed to the environment increases. The sawing of logs also separates the structural organization of the tree and releases inbuilt tensions. How the log has been processed to this stage will have a lasting impact on the quality of the final product. Selection of an appropriate cutting pattern will get the most out of the log. It has been shown that battens cut from near the pith or containing juvenile wood are more likely to distort on drying (Klaiber and Seeling, 2004). When processing fast grown small diameter logs it is inevitable that a proportion of battens will be sawn from this section of the log. In such circumstances it is to be expected that a quantity of the final product will not make the grade required for construction timber. In larger diameter logs, a cutting pattern which selects for the highest volume of battens cut from the outer section of the log should maximise the yield of construction grade timber (Danborg, 1994).

Distortion can be evident in freshly sawn green wood. This will most likely be due to the release of growth stresses. It is generally accepted however that sawn green timber is rarely significantly distorted. In most cases the development of increased distortion will occur during drying and will only become apparent as moisture content decreases beyond fibre saturation point (FSP). When the hollow lumens of the cells are drained of free water, only the water bound within the cell walls remains. This is referred to as the FSP and drying beyond this point will lead to a gradual loss of water from the cell walls. When air dried, in ambient conditions, the wood will dry relatively slowly until it comes into equilibrium with its surroundings. Then it is said to have reached equilibrium moisture content (EMC). Drying in kilns accelerates the drying process and as the wood loses moisture more quickly internal moisture gradients will be established from the core of the wood to the surface in contact with the surrounding environment. When wood is kiln dried care must be taken to establish the optimum conditions (see section 1.5). Rapid water loss at high temperatures can create uneven moisture gradients and hence, uneven drying of the wood. This can be a cause of distortion.

There are four key types of distortion that have been identified as problematic to the processing industry. By simple definition they are; bow; lengthwise deviation of a batten along its widest face from end to end, spring; lengthwise deviation of a batten along its edge or narrowest face from end to end, cup; deviation of a batten across its width on its widest face from edge to edge and twist; spiral deviation of a batten along its length. Visual examples of all four types of distortion are given in Figure 1.6.

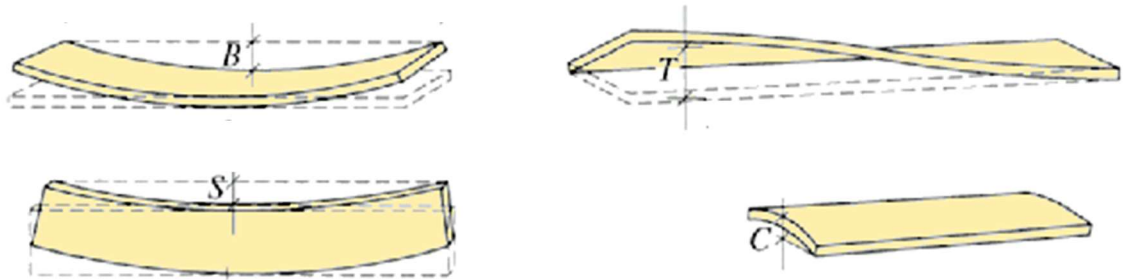


Figure 1.6. Diagrams of four types of distortion; B - bow, T - twist, S - spring and C -cup.

### 1.3.1 Twist

Twist is more formally described by the European Committee for Standardisation in standard EN1310:1997 (CEN, 1997) as “*the rise of the fourth corner from a flat surface*”. From the same standard, the limit for twist in grade C18 or below timber is “*no more than 2mm deviation from a flat surface over 25mm width over the worst 2m in length*”. Twist in UK grown Sitka spruce has been identified as the most limiting factor for increasing its application and marketability as construction class timber (Moore, 2011; McLean et al, 2014).

## 1.4 Grading of sawn timber

Sawmills have traditionally been the major purchaser of UK timber and provide prepared timber products for construction, pallets, packaging and fencing. The construction industry is a large consumer of timber and timber products in the UK and the use of timber in housing construction and other large scale projects has increased in recent years. Construction timber grading is based on three core properties; bending strength (the modulus of rupture), bending stiffness (the modulus of elasticity) and density. Other properties such as distortion, cracking or splitting, collapse or case hardening, knots, fungal or insect infestation, unusual grain angle and any other defects of significance will also be taken into consideration.

Bending strength can only be tested destructively by rupture of the batten but does generally correlate well with stiffness. Bending stiffness can be non-destructively assessed by machine which can grade for elastic modulus. Density can be measured simply by weight and dimensions and this can also be achieved by x-ray scanning however, consideration should always be given to moisture content which can affect values for density. Traditionally, all other properties are visually assessed and graded accordingly by a trained operative.

In recent years a number of x-ray and laser scanners and acoustic tools have become available which have the ability to predict many if not all of these properties. Among these are the Microtec GOLDENEYE x-ray scanner, Microtec Viscan laser scanner (distortion only) and the Brokhuis mtgESCAN. All three can be installed in a sawmill production setting but are quite expensive pieces of equipment. More economical and portable are the Brokhuis Timber Grader MTG and Hitman 2000 hand held acoustic grading tools. The development of these tools continues to progress at pace and they are becoming increasingly popular with processors and researchers.

Testing is done in batches of not less than 450 pieces. Individual pieces are not graded in isolation and the determined grade will be representative of a much larger consignment. A greater number of pieces tested (usually around 1000 pieces) will reduce the uncertainty in the final grade. In the first instance any pieces which have failed visual inspection will be removed. Consideration must be given to the species being tested, the dimensions of the samples and the cutting pattern (Ridley-Ellis, 2011). Any machines in use must be European Committee for Standardization approved to CEN TC 124 TG1 according to timber grading standard EN 14081-3:2012 (CEN, 2012). Each grading class has assigned critical property values and the results, or indicating properties of testing are correlated against these values to determine the pass or fail limits within the standards set by EN 14081-3:2012, EN 384:2010 and EN408:2010+A1:2012 (CEN 2010; 2012b). Softwoods are designated a C classification and most UK Sitka spruce will be machine graded using a C16 /reject setting, the minimum grade for timber intended for use as a construction material. Post grading, each pack from any given population should be made up of predominantly C16 timber but it is likely that some of the pieces will fall either side of this grade. Testing should therefore not be considered as absolute guarantee of piece by piece quality. Current pass rates for this grade are in excess of 90% (Moore et al, 2013).

## 1.5 Drying sawn timber

Drying sawn timber to below 20% moisture content significantly improves its suitability as a working material. In general, strength properties are improved, the timber can be machined and shaped more easily, fastenings and bonding are more secure and applications of paint, varnish or preservatives should be more effective.

Drying in purpose built kilns is the most common method used for the commercial drying of timber. Kilns are normally constructed of brick or sheet metal or a combination of both and insulated to retain heat. Size of load and stacking practices are variable and good practice will take a number of factors into consideration (Cooper and Maun, 2004). Rows of battens are separated in the stack by stickers, small pieces of sawn wood of around 10 x 10 mm and of variable length. These are placed strategically between the rows to ensure an even flow of air through the stack and reduce warping. Species, permeability, initial moisture content, dimensions of boards and final target moisture content will determine the appropriate kiln schedule that should be selected. The kiln schedule is essentially the dry bulb/wet bulb settings most suited to the load. These are often provided by the kiln manufacturer or are published by national forestry or timber regulatory bodies. Comprehensive examples of typical kiln schedules related to species and end use are published by the United States Department of Agriculture (Boone et al, 1988).

In a conventional steam kiln, energy is provided by gas, oil or by the burning of waste wood accumulated on site. Heat is normally delivered via steam filled pipes or coils at ceiling level. Air passes over the heat source and is distributed around the kiln by fans. Humidity may be increased by the addition of steam or by spray atomisers located within the kiln. The control of temperature and humidity are monitored by observing the dry bulb (measure of air temperature) and wet bulb (measure of temperature in relation to moisture content of air) temperatures. The wet bulb temperature will be lower than dry bulb and the difference is referred to as the wet bulb depression. Temperature and humidity can be modified by venting off humid air and introducing cool, dry air to the system and repeating the process. Steam kilns operate at temperatures of up to 82°C with air flow/fan speeds of around 120m/min to produce timber with moisture content of less than 20%. A diagram of a conventional steam kiln and its major components is shown in Figure 1.7.

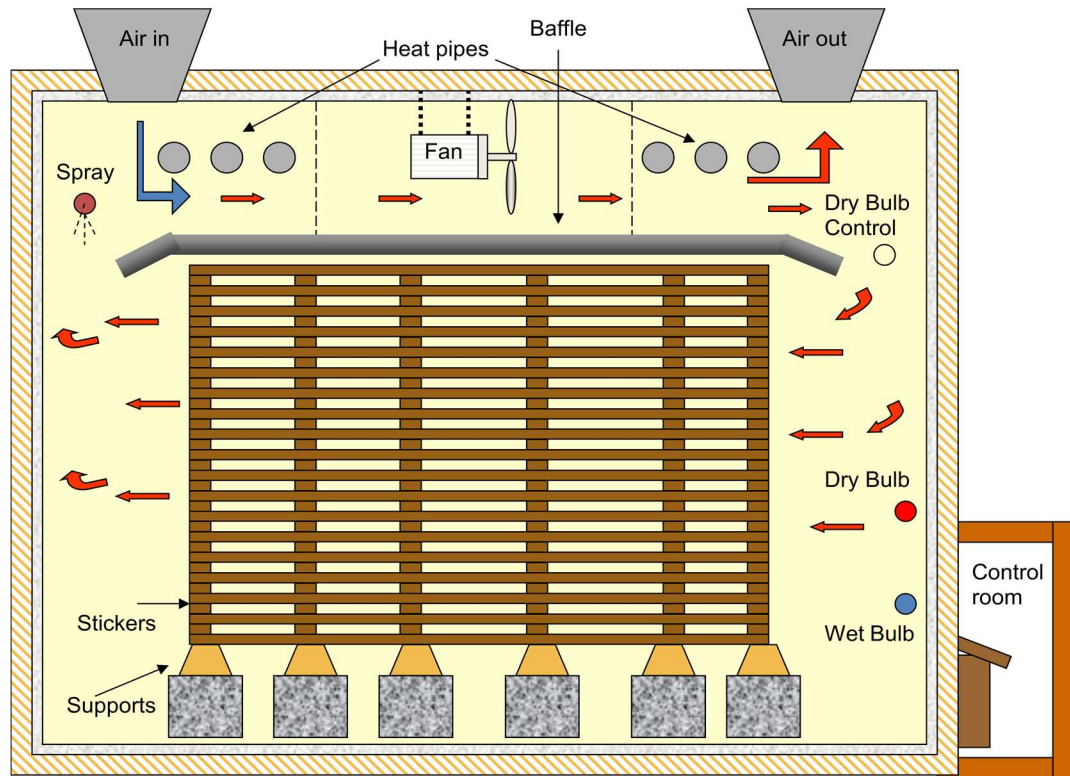


Figure 1.7. Schematic of a typical steam kiln used in a commercial sawmill.

Most softwoods can be dried faster at high temperature (HT). A study commissioned by the Forestry Commission and Scottish Enterprise and undertaken by Building Research Establishment (BRE) and other European partners carried out a number of trials where Sitka spruce sawn timber was dried under a variety of HT conditions and compared with controls dried under conventional conditions. This concluded that in terms of energy efficiency and time, HT drying was more beneficial to processors (Riepen et al, 2004). However, the quality of the final product was dependant on a number of factors. In most cases HT drying produced degrees of twist that were similar or slightly lower than the conventional controls. In some cases the application of top load (weight) and/or additional post-drying steam conditioning was required to achieve the lower levels of twist (Riepen et al, 2004). In the UK most of the volume of Sitka spruce produced is dried in the conventional manner. Drying times can be variable and dependant on end use and producers economic needs. Information obtained from producers suggests shorter drying times (generally a minimum of 48 hours) will provide a high volume output at the cost of a lower yield in construction grade. If a higher yield in grade is required drying can be continued for up to six days.

## 1.6 Longitudinal, radial and tangential shrinkage

The anisotropic shrinkage of wood in the longitudinal, radial and tangential directions is a complex phenomenon which has generated numerous models and theoretical studies of the topic over the years (Barber and Meylan, 1964; Barber, 1968; Cave, 1972; Yamamoto, 1999, 2001). Wood cell walls comprise a lignin hemicellulose matrix with embedded microfibrils of cellulose (Meylan, 1972). The microfibril angle in the S<sub>2</sub> layer of the cell wall is the dominant influence on the anisotropy of shrinkage. The internal amorphous matrix of wood cells has been shown experimentally to shrink and swell isotropically. The cellulose microfibrils embedded within the matrix do not. This confirms the Barber and Meylan (1964) reinforced matrix hypothesis (Yamamoto, 2001). Microfibril angle has implications for timber quality, particularly in terms of stiffness where higher microfibril angle can significantly reduce stiffness. Angles of up to 35° have been reported in Sitka spruce (Reynolds, 2010). Higher microfibril angle is normally found close to the pith and decreases with radial distance towards the bark. Local differences can arise due to the presence of reaction wood (compression wood) and other growth factors. In a study of four provenances of Sitka spruce, Vainio et al (2002) found mean microfibril angle near the pith of 22° which decreased to 11° in the outer rings. Recent work by Mclean et al (2015) found microfibril angle in excess of 30° at the pith which decreased to around 10° by ring 30 in four provenances of Sitka spruce.

As wood dries below FSP, bound water from the cell matrix is gradually lost and cells begin to shrink. Shrinkage has three directions in wood; (1) longitudinal, along the grain throughout the length of the tree; (2) radial, in the transverse direction, perpendicular to the annual rings from pith to bark, (3) tangentially, in the transverse direction, across the annual rings (Figure 1.8). The microfibrils are inflexible and cells shrink at right angles to their orientation. Shrinkage along the grain is therefore small compared to shrinkage across the grain, but this still sets up large stresses when wood of varying microfibril angle is dried. Shrinkage across the grain is considerably greater. Typical oven-dried shrinkage values for medium density wood are reported in Walker (2006b) as; longitudinal: 0.1-0.3%, radial: 2-6% and tangential: 5-10%. However, shrinkage differs from species to species and is also dependant on a number of factors including age at drying, timber dimensions and drying schedule.

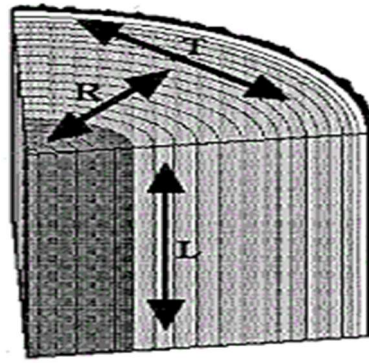


Figure 1.8. The three directions of shrinkage shown in a quartered log. L; longitudinal along the grain, R, radial from pith to bark, T, tangential across the annual rings (image from Wengert and Meyer, 1993).

Longitudinal shrinkage is often regarded as negligible, possibly due to the typically low values of shrinkage reported. Tangential shrinkage is normally greater than radial when internal stresses are released but the mechanisms involved are not fully understood. Leonardon et al (2010) investigated the influence of the cell wall structure by comparing juvenile and mature wood with compression wood. This concluded that to different degrees, longitudinal and tangential shrinkage are governed by the presence of compression wood as well as microfibril angle. As longitudinal shrinkage is often overlooked, the relationship between all three directions of shrinkage still requires further study.

## 1.7 Grain angle

Grain angle can be simply described as the alignment of the longitudinal and radial arrangement of tracheids in relation to the central axis of the pith of the tree from butt to crown. This is seldom, perhaps never parallel to the axis. Grain angle has a tendency to grow in a helical manner with height and as such is referred to as spiral grain. Rather than being seen as a defect or abnormality it is part of the normal growth pattern and common to some degree in every species (Northcott, 1957). Grain angle has been shown to be a significant influence on the development of twist in sawn timber and a major problem for processors to deal with (Balodis, 1972; Forsberg and Warensjo; 2001; Ekevad, 2005, Kubojima et al, 2013).

The angle at which the helix develops is not consistent between individuals and this can be attributed in part to heritable factors (Fonweban et al, 2013) and growth traits (Hallingback et al; 2010a). It is also not consistent in individuals and the direction of the spiral is known to change direction, sometimes more than once, though the length of the tree. In early growth, grain angle will develop in a left handed (S) or right handed (Z) direction. Brazier (1965) found that 30% of a sample population of Sitka spruce had an S spiral in early growth. Macdonald and Hubert (2002) suggest that the typical pattern in the species is S spiral. Whatever the direction of the spiral at origin, it may well change to the opposite direction with age. When, or if, this is likely to occur is not well understood. In fast grown Sitka spruce, the influence of an S shaped spiral in early development is the feature which dominates twist in sawn timber (Harris, 1989a)

Measuring grain angle accurately has previously proved challenging and to date it could be said that there is no definitive method which is widely employed. In Figure 1.9 a simple device to measure grain angle, taken from Brazier (1965), is shown. This is effectively a pivoted, straight edged implement attached to a scale in degrees. When the face of the split disc is placed against the flat edge the angle can be read. This equipment is not dissimilar to methods used more recently by Sall (2002) or indeed, in this work. The current European standard method, as specified in EN1310:1997 (CEN, 1997), is a scribing method. This involves scribing two equidistant parallel lines, along the grain, on the surface of a batten, taking measurements between the two and applying a simple algorithm to calculate the grain angle. A similar method is used by Hallingback et al (2010b) to measure grain angle in Scots Pine. This is more suited to large battens which have low knot volume or as under bark field measurements on standing trees. Light transmission or conduction of light through discs has been used in slightly different formats by Nystrom (2003) and Cown et al (2012), the theory being that the grain angle can be determined by the angle of light transmitted through tracheids. A method to identify grain angle, moisture content and density was developed by Schajer and Orhan (2006). The depolarisation, attenuation and phase shift of a microwave beam passed through the wood were analysed to provide the results.

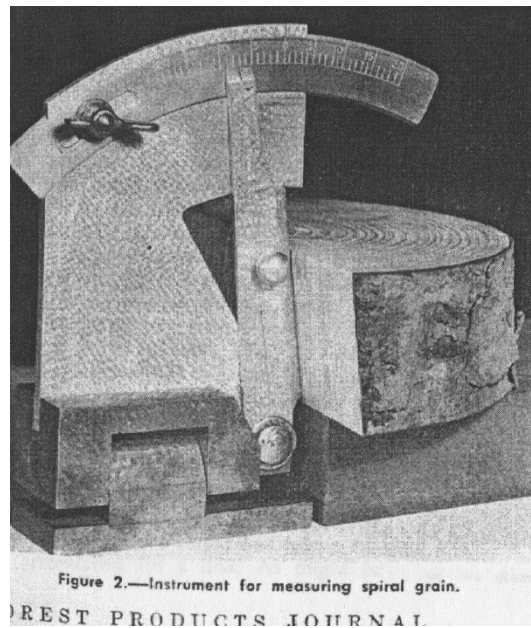


Figure 1.9. A tool to measure grain angle. From Brazier (1965)

Harris (1965) points out that the degree of grain angle alone does not lead directly to abnormal shrinkage behaviour but suggests that it is strongly influenced by the tangential shrinkage behaviour which is translated into the axial direction of the timber. This statement reinforces the hypothesis that twist is not necessarily the result of any one particular property of sawn timber but complex mixture of effects with an almost infinite number of permutations. This is perhaps best expressed in a quotation from Harris (1989b);

*“The interaction of growth layers with different grain angles and varying moisture content, together with internal and external restraints make prediction of the degree of twist that will be encountered for any change in moisture content quite impossible”.*

## 1.8 Aims of this study

This work was commissioned as part of the Strategic Integrated Research in Timber partners; University of Glasgow, Edinburgh Napier University and Forest Research timber improvement programme, which seeks to improve the quality and increase utilisation of UK grown forest products.

The aim of this study was to investigate the properties that might cause distortion in kiln dried sawn timber and seek relationships between them in consideration of developing practical methods of timber quality assessment applicable to the processing industry. The emphasis was focused on twist due to the importance placed on this particular problem by the industry.

This was done by;

1. Designing practical experimental methods to accurately measure the key properties that are known to produce twist in Sitka spruce sawn timber.
2. Testing the hypotheses; (a) Spiral grain angle has an influence on twist (b) Longitudinal shrinkage has an influence on twist (c) Longitudinal shrinkage has a relationship with microfibril angle.
3. Analysing the gathered data to seek out novel relationships between properties related to the development of twist with particular attention to longitudinal, radial and tangential shrinkage and spiral grain angle.
4. Assessing the effectiveness of acoustic tools as predictors of distortion.

## 2 The development of twist due to kiln drying: unrestrained and restrained drying

### 2.1 Introduction

There were two separate experiments carried out to explore how twist develops. The first experiment was designed to assess the impact of drying regularly processed battens without any form of restraint therefore allowing the maximum amount of distortion to develop. This was done in three stages; from the green state down to 20% moisture content (MC), from 20% – 15% MC and from 15% – 8% MC. This should provide information about how twist develops as moisture content decreases. Results are analysed with particular reference to between tree variation and within tree variation with height and radial position. Previous work on this subject has shown that twist is more prevalent in battens sawn close to the pith (Simpson and Tschernitz, 1997; Johansson and Kliger, 2002; Straze et al, 2011). Comparisons are made between battens by (1) position relative to the pith and (2) by position relative to butt or crown to observe any effect of position within the log. The results are considered alongside other measured and observed physical properties from the same samples (longitudinal shrinkage, grain angle, stiffness, see chapters 2, 3 and 4).

In the second experiment two separate batches of battens; one batch in the green state and one pre dried to 18% moisture content, all cut from the centre of logs were dried under restraint to 12% MC. All battens were previously processed in a commercial sawmill and had been rejected as unsuitable for construction grade timber. Drying to 12% MC was carried out in two separate cycles, under the same conditions. All battens were expected to develop significant levels of twist. The aim of this experiment was to compare the resulting twist accrued under restraint in rejected battens with two distinct start points in terms of moisture content (green and dried to 18% MC). Results are also compared with those from the unrestrained drying experiment.

## 2.2 Methods and materials

### 2.2.1 Sampling

Six commercially grown Sitka spruce trees were felled at Spadeadam forest North West of Carlisle, Cumbria, UK (55.04.32 N/ 2.36.44 W, Alt 348m) (Figure 2.1). Trees were selected for their straightness and comparable diameter at breast height (DBH) but otherwise randomly. Mean DBH at 1.3m was 32.15cm across the six trees with a standard deviation of 1.74cm. At the time of felling the samples were approximately 37 years old (planted 1975, felled May 2012).



Figure 2.1. Felling of samples at Spadeadam Forest, Cumbria.

After felling, trees were sawn into two sections (butt end and crown end) of approximately 4m. At this point, three discs were removed; one from the base of the butt end, beyond any basal flare, one from the area of segregation between logs at around 4m and one from the upper section of the crown end but short of the true crown. Mean disc diameters were recorded as 36.2, 23.9 and 21.9cm respectively. The discs were bagged and sealed to preserve green moisture content and transported on the same day to the University of Glasgow and stored in a cold room at 2°C. The logs were stacked by the roadside and transported to the BSW Timber Group sawmill at Carlisle 48 hrs later then processed at this site a further 48 hrs later. During this

time the samples were exposed to ambient temperatures and weather conditions. When referenced with Met Office historical data for the period, mean daily temperatures were approximate to the historical average (8.75°C) and rainfall more than double the historical average (89mm vs. 190mm). It is assumed that given these conditions and the short period of exposure, this would have had a negligible effect on the initial green moisture content at time of processing.

The logs were sawn at BSW Carlisle (Figure 2.3) with a cutting pattern selected to produce three battens with dimensions; 3000 x 148.5 x 102 mm. Each set of three battens consisted of one batten where the pith was completely or mostly contained throughout the batten and two battens where little or no pith was present. For identification each set of three battens from each log were identified as battens A, B and C; batten B being the central batten and battens A and C positioned on either side as shown in Figure 2.2. After processing, the samples were given appropriate identification markings in a manner that preserved their origins and recorded their orientation within the log and tree. The samples were transported on the same day to the Forest Research Northern Research Station (FR NRS), Bush Estate near Roslin. It was not possible to record initial moisture content with a moisture meter due to a malfunction (broken pin) with the equipment but all samples were weighed prior to being put in cold storage at 4°C. All other metered moisture content values reported in this work were taken with a GANN Hydromette M2050 moisture meter (Gann Mess-u. Regeltechnik GmbH, 70839, Gerlingen, Germany). MC was determined by three readings taken on each batten; one at either end and one approximately in the centre of the batten. The mean of the three readings was regarded as the mean moisture content for each batten.

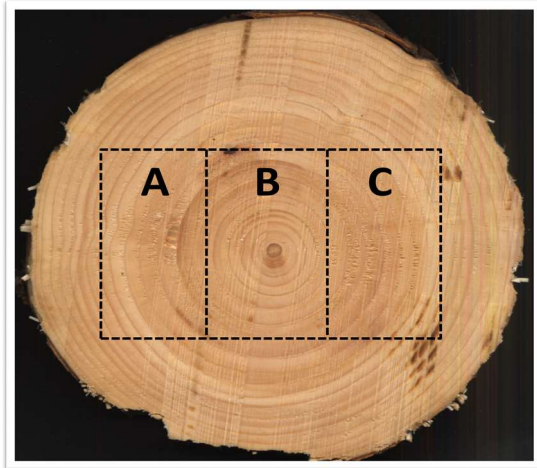


Figure 2.2. Labelling of battens to identify position within the log. The B battens wholly or partially contain the pith. The A and C battens are sawn from either side and will contain some degree of juvenile wood.



Figure 2.3. Processing of logs into battens at BSW Carlisle

### 2.2.2 Unrestrained kiln drying

Samples were dried in an experimental kiln based at FR NRS. This kiln is owned and maintained by the partners of the SIRT project. The kiln, a concrete and metal built structure (Figure 2.4), has an internal load area of 3.1 x 3.6 x 2.2 m and functions in the same manner as a standard steam kiln. It is oil powered and heat is delivered via steam filled coils at a dropped ceiling level and distributed evenly throughout the space. Distribution is controlled by a series of fans and baffles. These can be adapted to suit the size and arrangement of the load. Humidity is increased through the

addition of water by spray atomisers and temperature is controlled by periodic venting of the system. Kiln operation is controlled by a GANN Hydromat TK-MP4032 kiln control system and manually regulated with a MPP 5/TK-MP 501 peripheral unit (Gann Mess-u. Regeltechnik GmbH, 70839, Gerlingen, Germany) (Figure 2.4). The drying schedule used for all the experimental work in this research was the default Sitka spruce cycle suggested by the manufacturer. The planned final drying targets were 20, 12 and 8% moisture content.



**Figure 2.4.** Top: View of kiln showing door to control room and door to load area (behind pallets). Oil tank can be seen on the left of picture and venting flue on top of the building. Loading doors are to the right of picture. Bottom: Peripheral control panel situated in control room.

The commercial drying of sawn timber involves large volumes of battens stacked in several rows, one on top of another, separated by strategically placed stickers to facilitate sufficient circulation of warm air through the stack. It is common practice

to use straps or weight (top load) to secure the stack and minimise any distortion effects brought about by drying.

For the purposes of this experiment no restraint was applied in order to allow for maximum distortion. The samples were arranged lengthwise from the rear to the front of the kiln atop two potato storage boxes (Figure 2.5). This raised the samples from the kiln floor and ensured that the air flow distribution contacted the face of the battens rather than flowing through open channels that would have been created by positioning in the opposite direction. This retains more humidity and temperature within the stack, especially with the enclosed space provided below by the potato boxes, and minimises the chances of the samples drying out too quickly which can produce moisture deficient gaps in the water transport gradient and cause deformation such as case hardening or collapse (Tarvainen et al, 2006). Although these effects are known to happen less frequently in Sitka spruce, the aim of this research was to observe the effects of distortion related to anisotropic shrinkage. Therefore, it was desirable to minimise the possibility of such defects arising.



**Figure 2.5.** Samples stacked in kiln prior to drying.

To assess the ongoing changes in moisture content throughout the drying cycle, monitor probes were attached to four battens. Each probe has two pins that are inserted around 2-3 cm into drilled holes at different positions in each batten (e.g. end, centre, off centre) to give an indication of moisture content changes over the whole length. Moisture content is measured by the electrical resistance between the pins and is therefore comparable to the two pin resistance meter used to measure moisture content at all other stages of the experiment. Four battens of differing initial moisture content were selected to reflect the relative average moisture content covering the range from the highest to the lowest measured moisture content across the batch. The progress and completion of the drying schedule was regulated by the average moisture content of the four battens throughout each drying cycle. As the cycle progressed, the mean moisture content of the monitor battens was displayed on the peripheral unit. As well as monitoring the moisture content of these selected battens as the drying cycle progresses, the kiln is also fitted with two equilibrium moisture content (EMC) sensors. These are fitted with a thin wood strip of the appropriate species in the two static temperature sensors. It is assumed that the wood strip is thin enough to be in effective equilibrium with the kiln atmosphere at all times. The EMC sensors measure the electrical resistance from the ambient air/moisture conditions within the system. When corrected with the internal temperature this provides a measure of the system EMC which can be correlated with the wood MC % to regulate the progress of the drying schedule.

The drying cycle is divided into 17 individual phases. The phases, their function and the intended effects on the load are detailed below:

Phase 1: Heating up (break up). Intended to prepare and “break up” the wood structure in preparation for drying. Low temperature ( $\sim 20^{\circ}\text{C}$ ) maintains relatively high system EMC (close to green moisture content %). Spraying turned on when maximum temperature is achieved to ensure sufficient absorption of water by the air.

Phase 2: Heating up (warming through). A reduction in spraying and interlinked, gradual temperature increase to reduce EMC in preparation for drying phases.

Phases 3 – 15: Drying in 13 stages. System EMC continuously lowered, phase by phase, as wood MC % decreases in accordance with the programme drying gradient (ratio MC %:EMC). Temperature gradually increases as wood MC % decreases. The programme drying gradient is controlled by the mean value generated by the four monitor probes. If any of the parameters are exceeded this can be corrected by venting of the system and/or additional spraying.

Phase 16: Conditioning and Equalising. When the mean target moisture content has been attained from the drying phases, the cycle moves to a phase of conditioning. This seeks to find and maintain the system EMC where the MC % in the wood deviates by no more than 1% from the desired final MC %. This is followed by a short equalising phase which sustains the system EMC for a short period. The aim of both phases is to minimise the effects of any drying stresses and establish an even moisture gradient between the core and shell of the battens.

Phase 17: Cooling down. To reduce the internal temperature the heating is switched off and the system is vented. When a temperature equal to 60% of the programme maximum temperature has been reached the cycle is complete. The programme is closed down. The fans turn off and the vents are closed. Under these conditions the final wood MC % can be maintained for at least 24 hrs.

### **2.2.3 Measurement of twist: FRITS Frame**

The development of twist was measured using two methods: FRITS Frame and calibrated measuring wedge. Both methods can be compared with previous studies into twist (Klaiber and Seeling, 2004; Straze et al, 2011) but are at the same time significantly different.

The FRITS Frame (Freiburg's Improved Timber Scan) (Figure 2.6) is a bespoke piece of equipment which was designed and manufactured at Freiburg University

(Seeling and Merforth, 2000). The apparatus used in this experiment is owned by and was kindly provided by Edinburgh Napier University.



**Figure 2.6. FRITS Frame. Assembled and raised on to blocks for easy access.**

The FRITS Frame is a metal structure with dimensions 4.5 x 1.0 x 0.8 m. It has a motorised conveyor belt attached to one of the upper, lengthwise sections which can be manually operated in a forward or backward direction using a handset. At one end of the belt there are attachment points for two lasers; one vertical and one horizontal. The horizontal laser tracks the incremental distance of each measurement point along the length of the batten while the vertical laser measures the height from the batten face at each of the horizontal increments. The lasers are linked to a laptop via a Bluetooth<sup>®</sup> connection and measurements are automatically logged in a spreadsheet.

A batten is placed face up in the lower, central section of the frame, resting on three bolt head points; one the end where the measurement originated and two at the terminal end, to ensure a stable, three point position (Figure 2.7).

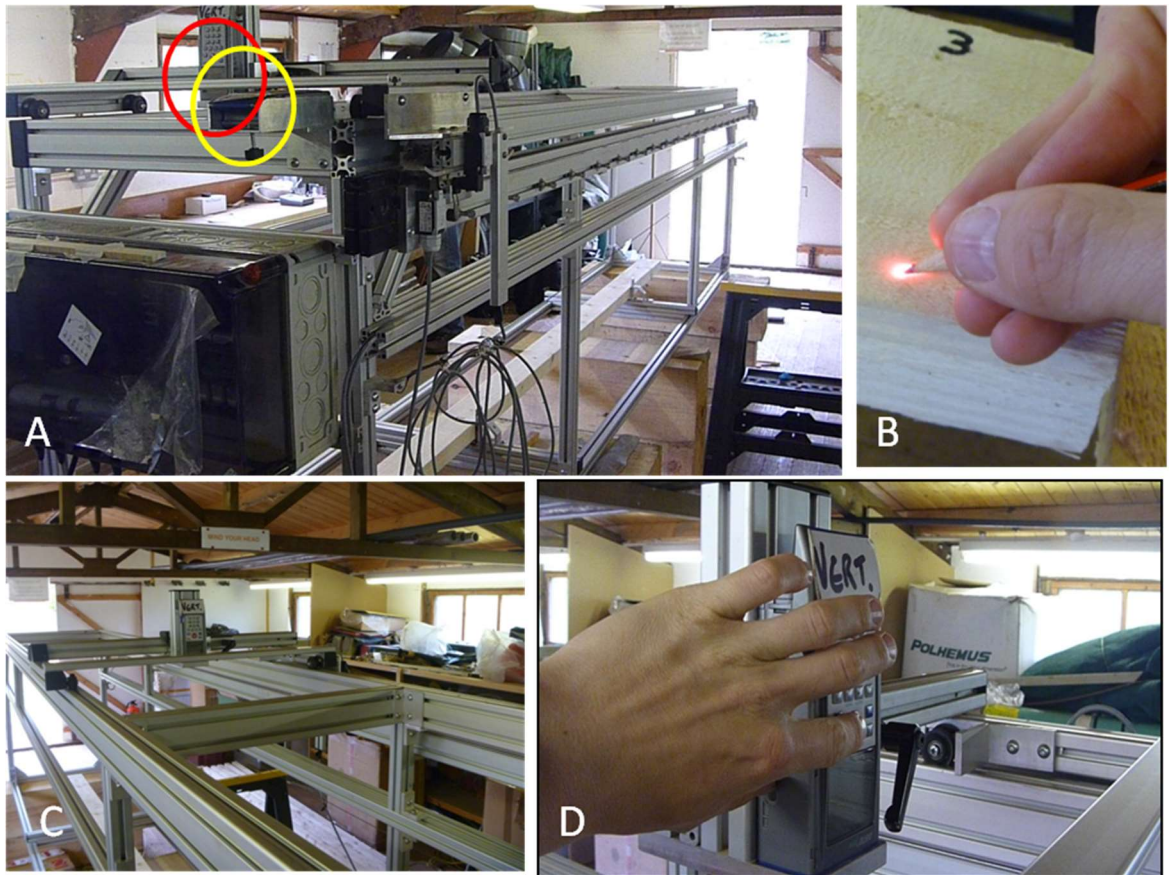


**Figure 2.7.** A: Positioning of lasers; vertical highlighted by red circle and horizontal by yellow, B: Marking the end of a sample to identify the start point, C: Vertical laser in operation, mid frame, D: Moving laser into position for repeat measurement on opposing edge.

The vertical laser spot was positioned approximately 2 cm from the end of the batten and 1 cm in from the edge. The laser was then allowed to run along the length of the batten to ensure there was no deviation from the edge. Once established, a mark was made on the batten to identify the start point (Figure 2.7B). Sixteen measurements were taken along the 3m length. The distance of each horizontal increment was variable due to the irregular movement of the conveyer belt. The anticipated distance was 20cm and the results show a standard deviation of  $\pm 0.01$ cm from this value. This process was then repeated along the opposing edge of the batten by shifting the vertical laser laterally into position on the opposite side by sliding along the rail and locking into position (Figure 2.7D). On completion the distance between the two points of measurement origin, the path gap, was recorded using digital callipers.

## 2.2.4 Calculation of degree of twist: FRITS Frame

A simple Pythagorean algorithm was used to calculate the degree of twist ( $^{\circ}Tw$ ). It should be noted that the standard method of measuring twist at industry level would be in millimetres per metre as per standard EN 1310:1997 (CEN). When working with long battens designed to produce maximum twist this system tends to become rather non-linear. For the purposes of this work it was decided to use degrees of twist per metre. At each measurement increment along the length of the batten, the difference ( $D$ ) between each parallel vertical measurement ( $hA_1 - hA_2$ ) was determined and converted to the appropriate units, i.e. from metres to millimetres (Equation 2.1). The length of the path gap ( $pg$ ; the gap between the two marked spots) recorded at the initial measurement point was corrected for each of the sixteen measurement points to provide an amended path gap for each point ( $pg_a$ ) (Equation 2.2). The degree of twist for each point was then calculated from the inverse tangent function of each right angled triangle (Equation 2.3). Degrees of twist per metre ( $^{\circ}Tw/m$ ) can then be calculated from the correlation between the individual twist values and the incremental distance between each measurement and the standard deviation of both (Equation 2.4). Visual details of the elements of the equations are shown in Figure 2.8.

$$\text{Equation 2.1} \quad D = (hA_1 - hA_2) 1000$$

$$\text{Equation 2.2} \quad pg_a = \sqrt{pg^2 - D^2}$$

$$\text{Equation 2.3} \quad ^{\circ}Tw = \tan^{-1} \{D/pg_a\}$$

$$\text{Equation 2.4} \quad ^{\circ}Tw/m = \text{Corr} (^{\circ}Tw, dist) \left\{ \frac{{}^{\circ}Tw_{SD}}{dist_{SD}} \right\}$$

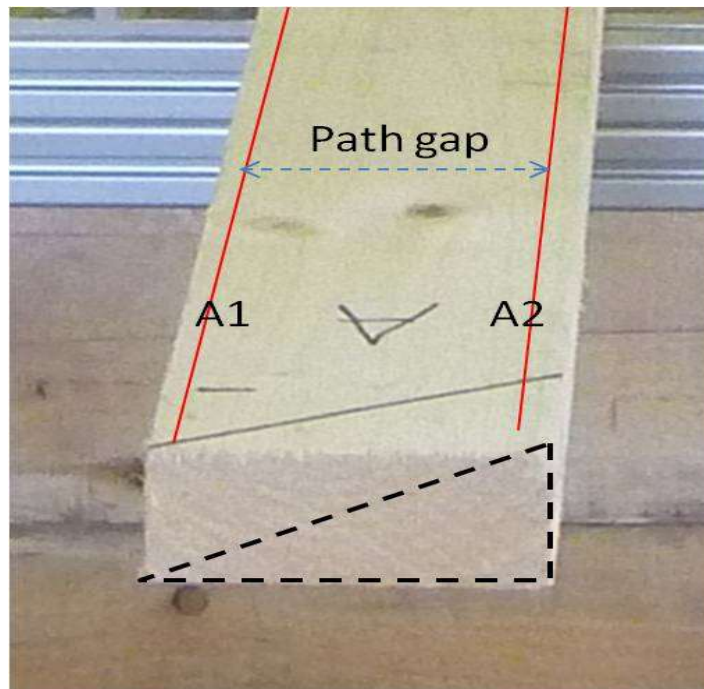
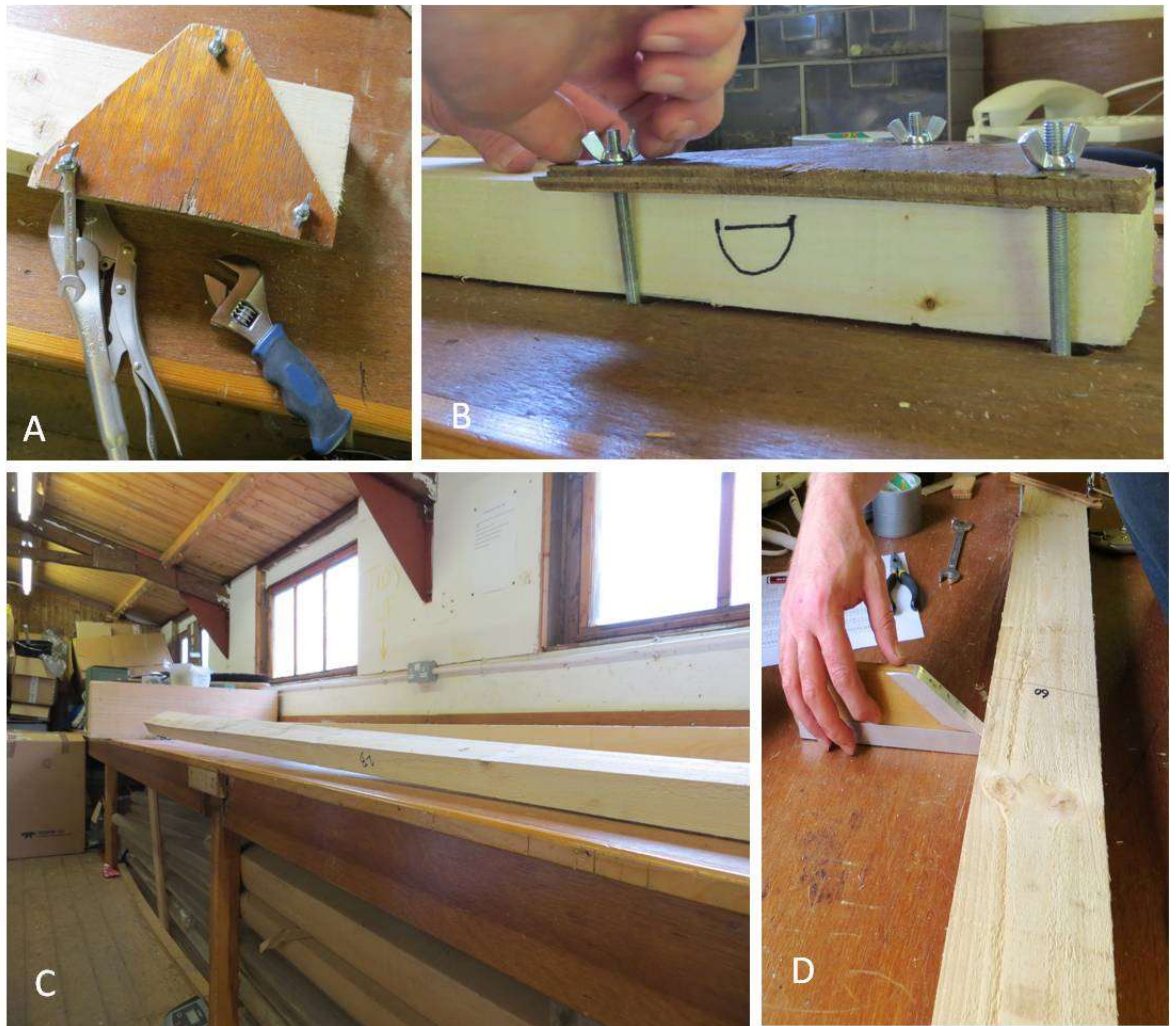


Figure 2.8. Batten showing the dimensions used to calculate degree of twist. Red lines A1 and A2 are the line of movement of the laser from end to end, the path gap (pg) is the distance between these two lines. The degree of twist is calculated from the vertical height difference between A1 and A2.

### 2.2.5 Measurement of twist: calibrated wedge

After some preliminary experimentation to assess the viability of using calibrated wedges to measure twist, a suitable method was developed. The use of wedges as a method to measure twist complies with the current European standard EN 1310:1997 (CEN). The basic concept is similar to that of the FRITS Frame in that the measurement of the extent of distortion along the two edges of each face are recorded and from this data the degree of twist can be calculated.

The sample batten was secured at one end to the surface of a flat workbench. To achieve this, a three sided piece of rigid plywood was attached to the surface of the bench by three bolts. The bolts were fed through three holes in the bench, the bolt heads secured beneath. With the sample positioned between the bench and the plywood shape, it was held in place by tightening the bolts from above with wing nuts (Figure 2.9A and 2.9B).



**Figure 2.9. Securing a batten to the bench for wedge measurements. A: Three sided plywood shape secured to workbench by three bolts. The shape allows for the minimum number of bolts to secure the batten. B: Securing a batten to the bench, C: A secured sample batten showing considerable elevation from the bench due to distortion, D: Taking measurements with a calibrated wedge.**

When firmly held in place the gaps between the sample batten and the bench surface could be measured with a calibrated measuring wedge. This was done at 10 cm increments along the length of the sample on both edges (Figure 2.9D). The measuring wedge was constructed from a piece of stiff plywood and two sections of tubular aluminium; one fitted square along the bottom, the other on an angled face which was also marked 0 – 50 mm at 1 mm increments ( Figure 2.10A).

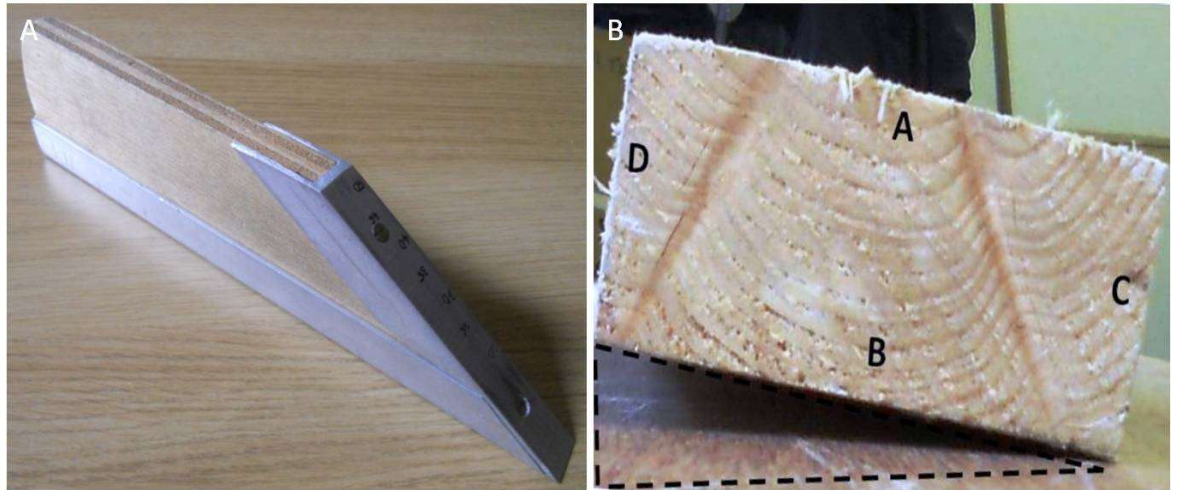


Figure 2.10. A: Measuring wedge, B: End of batten detail with labelled faces and edges. Measurements were taken at 10cm increments along the length of the batten between the bench surface and the base of the sample (B) at either side of the batten (C and D).

### 2.2.6 Calculation of degree of twist: calibrated wedge

Again a simple Pythagorean algorithm is used to calculate the degree of twist. In this case the difference ( $D$ ) between the incremental measurements of height between bench and sample base ( $B$ ) on opposing edges ( $C$  and  $D$ ) is calculated. The degree of twist at each point can then be calculated by applying the width ( $w$ ) at each increment and in this case the inverse sine functions of the right angle triangles (Equation.2.5). The degrees of twist per metre are then calculated in the same manner as with the FRITS Frame data (Eq.2.6). Visual detail of equation elements are shown in Figure 2.10B.

$$\text{Equation 2.5} \quad \text{°Tw} = \sin^{-1} \{D/w\}$$

$$\text{Equation 2.6} \quad \text{°Tw/m} = \text{Corr} (\text{°Tw}, \text{dist}) \left\{ \frac{\text{°Tw}_{SD}}{\text{dist}_{SD}} \right\}$$

## 2.3 Results

### 2.3.1 Measurements

This section reports the degree of twist measured in thirty-six sample battens taken from six trees. The experiment was limited to this number of battens due to the constraints of the time required to carry out measurements. Each set of six battens from each tree are divided into two sets; three from a butt log and three from a crown log. Calculation of degrees of twist per metre for each batten are used to analyse; between tree variation, within tree variation (between butt and crown logs) and within log variation (between individual battens) with particular reference to position within the log in relation to the pith.

### 2.3.2 Method choice; FRITS Frame and wedge method

The results presented in this section are taken from calculations of twist recorded by the FRITS frame method and do not include any measurements using the wedge method. With the exception of measurements taken in green condition and those with very high values of twist, the correlation between methods can be considered reasonable (Figure 2.11). The collective values of twist recorded from the wedge method were on average 18% lower than those from the FRITS frame method. This may have been due to some operational issues. As the batten is effectively being elevated from the measuring surface by being anchored at one end, there may have been a gravitational effect the more the batten was raised from the bench surface at distance from the anchoring point. There is also the possibility that movement caused by the insertion of the wedge or damage to the edges of battens could impact upon the accuracy of the measurements. Some values were missing from the wedge method data due to the degree of twist being greater than the upper limits of the wedge scale. There were similar problems with green samples where the measurement was too small. To this end it can be concluded that the wedge method is not particularly useful where high resolution is required. However, in a

commercial setting it may be of use as a quick and inexpensive way of filtering out sawn timber which exceeds the upper limits for twist.

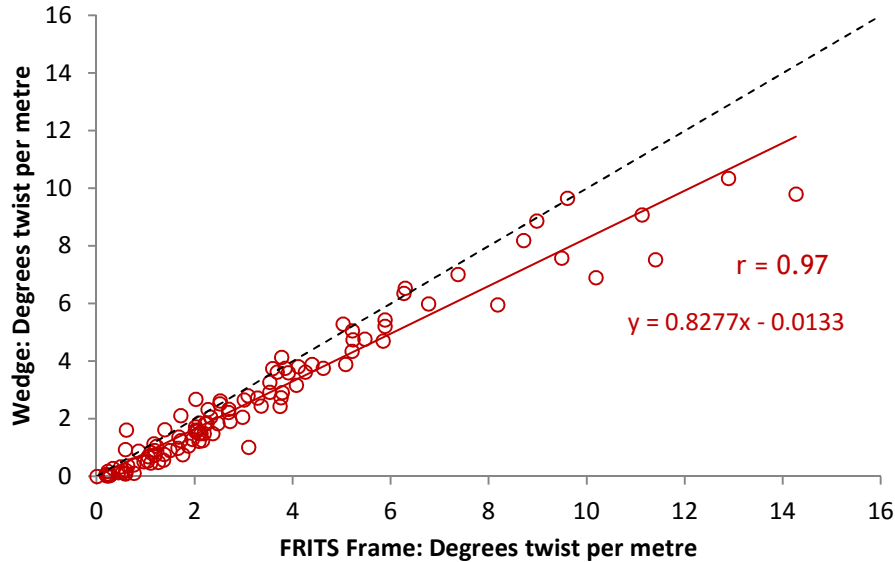


Figure 2.11. Scatter plot of FRITS Frame results against wedge method results showing 1:1 fitted line (dotted line) and line of best fit (red line). The collated results from all three drying targets at 20, 15 and 8% moisture content are represented for both methods. Green results are excluded as wedge measurements were not comparable at this moisture content. Results between methods differ by 18% on average (lower values from the wedge method) with discrepancies more notable at low and high values of twist. Comparison of the data returns a strong correlation ( $r = 0.97$ ).

### 2.3.3 Drying Cycles

The first drying cycle target moisture content of 20% was chosen to reflect the average moisture content for commercially dried Sitka spruce. The second drying cycle was intended to dry down to approximately 12% moisture content. However, this cycle was stopped early due to problems with the air flow system in the kiln. Given the potentially lengthy time lapse to carry out repairs, it was decided to measure the samples at the 15% moisture content which had been achieved. The target of 12% would have been preferred as this is a potential drying target for material requested for cross laminate or glue laminate procedures. The final target of 8% was chosen to evaluate to what extent twist continues to develop at lower moisture content, not normally required for construction timber. Drying to low moisture content was carried out in stages, i.e. not dried directly from green to targets below 20%. This was done to assess the variation in twist development when dried

incrementally compared to drying directly to target. Results from this method are compared later in this chapter with a subsequent experiment where samples were dried directly from green condition to 12%, under restraint. Kiln drying was scheduled to minimise any delay between each drying target. This was dependent on kiln availability and reliability. The experiment was carried out between the 26<sup>th</sup> May and 29<sup>th</sup> August 2012. The thirty six green sample battens had an estimated average moisture content of 60% directly after processing and were held in cold storage at 3°C ( $\pm 1^\circ$ ) for eleven days before kiln drying. When loaded into the kiln the moisture content had fallen to an average of 52%. Due to a misunderstanding of the drying schedule programming, this first drying cycle progressed very slowly and it took thirteen days to achieve the target moisture content. This was not thought to have affected the resulting condition of the samples. Having overcome the programming issues, the second drying cycle, from 20% to 12% was commenced immediately after the required measurements were taken. This cycle was aborted after three days due to a malfunction of the air flow system. The prognosis of this fault suggested a significant period before repairs could be carried out. It was decided to measure the samples at the 15% moisture content which had been achieved and thereafter, to put the samples into suitable storage until further use of the kiln was possible. The samples were stored at Edinburgh Napier University under climate controlled conditions (constant temperature; 21°C, relative humidity; 50 %) for six weeks until the kiln was operational. Given these unexpected circumstances, it was decided that further measurement of the samples should be carried out prior to the final drying cycle. This would not only provide an accurate reference of dimensions prior to drying but also a insight into what may or may not have changed in the intervening period. The final drying cycle, to 8% moisture content, was completed in six days.

### **2.3.4 Between tree variation**

Statistical analysis of the mean values for twist per tree (the average of mean twist per metre taken from all six sample battens within each individual) shows highly significant between tree variation in accrued twist over the three drying cycles (ANOVA two-way tree: target MC.  $p = 0.001$ ) but not specifically between all trees. Values are shown in Table 2.1 with the value for the standard error between battens included. Table 2.2 shows the groupings for trees based on significant differences

using Fisher post hoc analysis based on a least significant difference of 5% (LSD 5%).

**Table 2.1.** Total mean twist per metre calculated for all six battens contained within both logs of each tree are reported in degrees of twist per metre for all six sample trees. Analysis of variance (ANOVA two-way; tree, target MC) shows a significant between tree difference ( $p = 0.001$ ) in twist accrued between the six sample trees over the course of the experiment; from green condition through the three moisture content targets. Standard error between the six battens in each tree is given in parentheses. Not all trees are significantly different (see Table 2.2).

°Tw/m (standard error) at target moisture content

Tree	Green (52%)	20%	15%	8%
1	0.09 (0.03)	1.21 (0.31)	1.91 (0.61)	2.80 (0.92)
2	0.35 (0.10)	4.18 (1.25)	5.53 (1.45)	7.83 (1.84)
3	0.17 (0.05)	1.37 (0.34)	1.93 (0.55)	4.06 (1.18)
4	0.12 (0.04)	2.34 (0.47)	3.42 (0.60)	6.08 (1.53)
5	0.15 (0.06)	0.85 (0.41)	1.08 (0.61)	2.25 (1.07)
6	0.21 (0.07)	2.54 (0.67)	3.22 (0.83)	5.27 (1.31)

**Table 2.2.** Between tree differences in mean twist shown as groupings for significant differences after Fisher post hoc analysis has been applied. Least significant differences are calculated at 5% which returned a value of 1.01 °Tw/m. Trees are displayed from left to right from lowest mean value to highest. Trees with the same grouping are not significantly different.

Tree	5	1	3	6	4	2
Mean °Tw/m	1.08	1.50	1.88	2.81	2.99	4.47
Grouping	a	a	a	b	b	c

Table 2.2 demonstrates the considerable variation in mean accrued twist between the six trees based on the mean twist per metre from all six battens in each tree.

Between tree variation was also examined by looking at the percentage increases in accrued twist between drying stages (Figure 2.12). The data shows that most of the

twist develops in the initial green to 20% stage and the 15% to 8% stage. This is confirmed by testing with ANOVA two-way (tree: drying target) which returned significant  $p$  values of  $<0.01$  and  $0.012$  respectively. Although this is consistent with all six samples, there is some variation between individuals regarding at which stage the majority of the total twist is added.

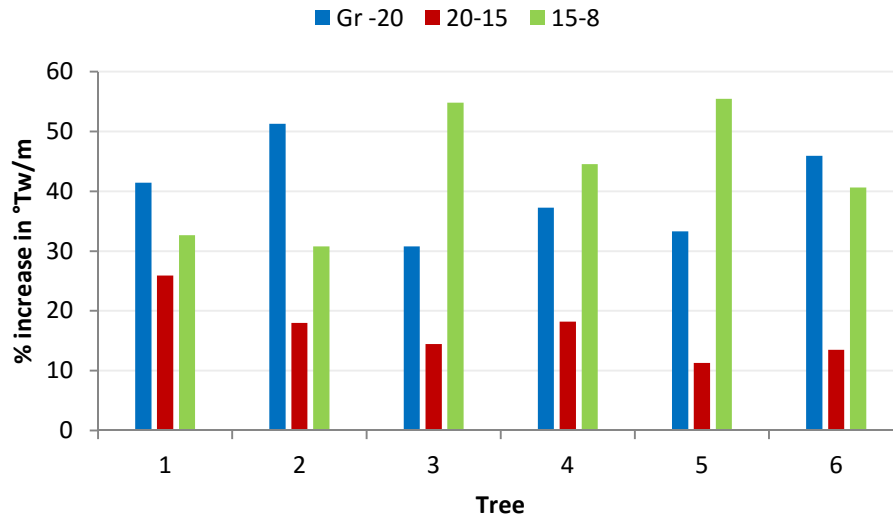


Figure 2.12. Comparing the percentage accrued twist at different drying targets. Blue bars: green - 20% MC, red bars: 20 - 15% MC, green bars: 15 - 8% MC. Statistical analysis (ANOVA two-way, tree: drying target) shows a significant difference between trees at drying stage green to 20% ( $p < 0.01$ ) and at 15% to 8% ( $p = 0.012$ ).

The variation between trees was analysed with a Fisher post hoc test to establish the differences in accrued twist at each drying target. The results are shown in Table 2.3.

Table 2.3. Fisher post hoc analysis of accrued twist at each of the drying targets. The order of magnitude of accrued twist is shown from lowest to highest, left to right. The LSD 5% is given for each drying target. Individuals with the same category grouping (a-d) are not regarded as being significantly different.

Target MC	LSD 5% (°Tw/m)	Accrued twist ordered by tree					
Green-20%	1.10	5 a	1 a	3 a	4 b	6 b	2 c
20%-15%	0.38	5 a	3 b	6 b	1 b	4 c	2 d
15%-8%	0.67	1 a	5 a	6 b	3 b	2 b	4 c

The between tree, log and position variation shown in Figure 2.13 demonstrates the dominance of shrinkage in battens cut close to or containing the pith (B battens) at 20% moisture content. It is evident when viewed in conjunction with Table 2.1 that the between tree variation in twist is relatively established at this moisture content.

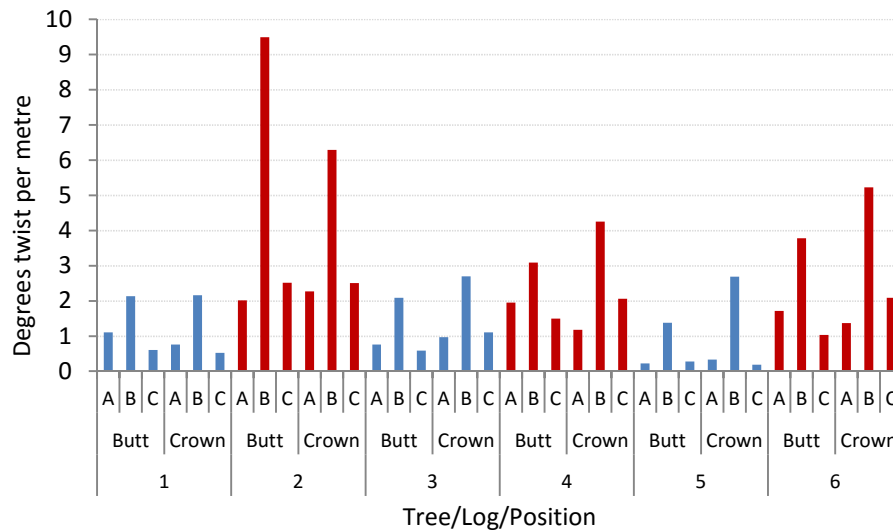


Figure 2.13. Accrued twist in thirty-six battens after drying to 20% moisture content. Tree (numbers 1-6); log (crown or butt) and position within log (ABC) are detailed on the x axis. Blue bars are used for the odd numbered trees and red for the even numbered.

### 2.3.5 Between log variation

Analysis of the average values of twist per metre for all three battens taken from each log were used to compare the results obtained from butt end logs and crown end logs. Butt logs were taken from the area directly above where it was considered that the basal flare of the tree ended and were approximately four metres in length. Crown logs were taken around 5cm above the upper cut of the butt log, allowing for one disc to be removed for grain angle analysis, and were also approximately four metres in length. The upper limit of the crown log was determined not to feature any of what may be considered the true crown in all six trees. Comparison of average values of twist per metre obtained from battens A, B and C for butt and crown logs is shown in

Figure 2.14. These are also displayed as scatter plots; all data in Figure 2.15 and individually for each drying target in Figure 2.16. The twist accrued in crown logs was 10.7% greater than in butt logs. However this is not statistically significant. The differences between butt and crown logs can be said to be small and inconsistent in direction.

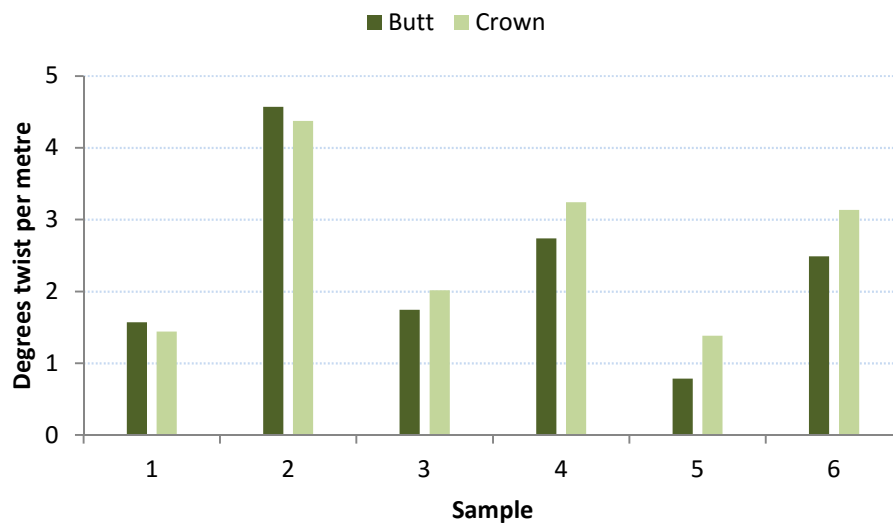


Figure 2.14. Mean twist per metre values showing the butt and crown variation for all six sample trees. Between tree variation is irregular. Averages of all data shows twist accrued in all crown battens to be 10.7% greater than in butt battens although this difference is not significant or consistent with all trees.

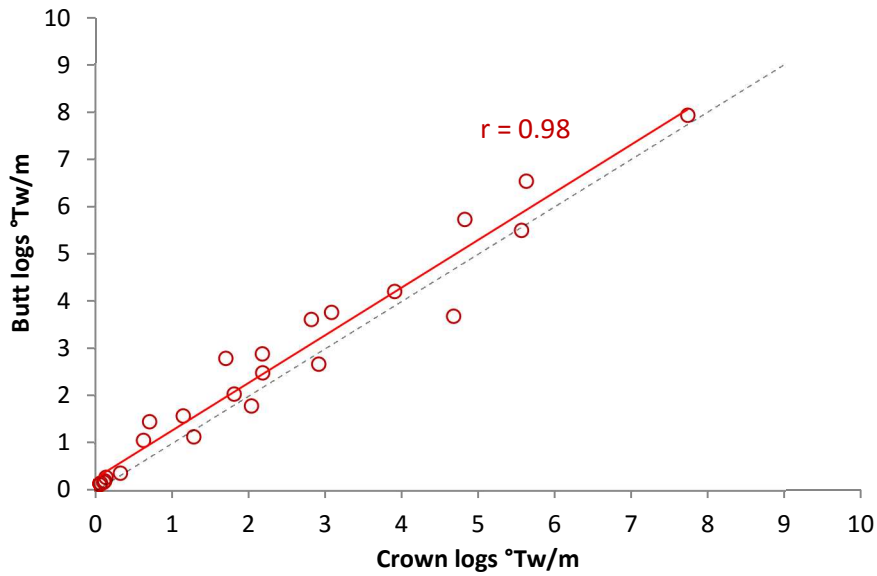


Figure 2.15. Scatter plot of mean twist per metre for butt logs against crown logs. Relationship between measured values is shown by the red trendline with 1:1 relationship shown as dotted line. The relationship is strong. This is shown by the correlation co-efficient ( $r = 0.98$ ). Statistical tests show no significant difference in the accrued twist with height.

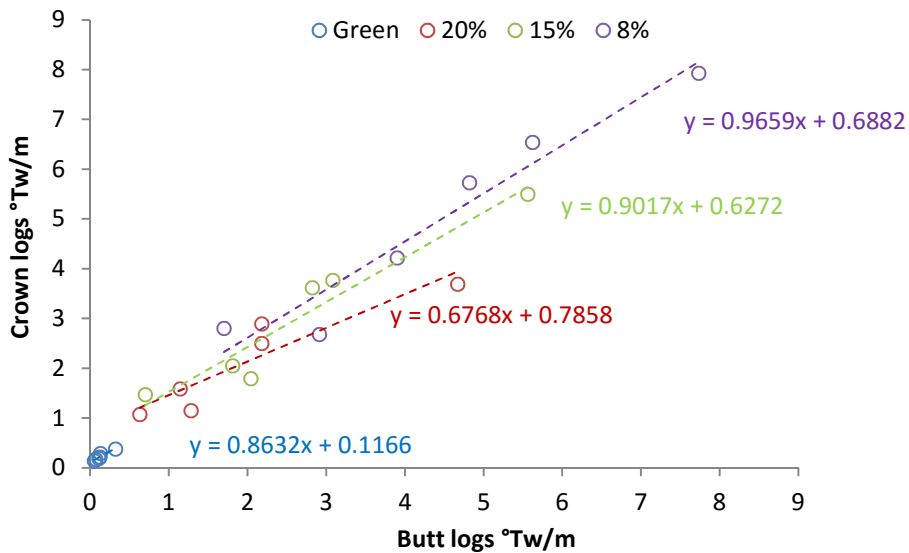


Figure 2.16. Individual scatter plots of average twist per metre for butt log against crown log at each of the measured targets with equation for the slope of each displayed.

To assess if the rate of change in accrued twist is consistent over all drying targets testing for covariance between the slopes was carried out.

**Table 2.4. Covariance matrix comparing slopes between accrued twist in butt and crown logs at four stages of different moisture content.**

	Green	20%	15%	8%
Green	1	0.73	0.54	0.37
20%		1	0.74	0.61
15%			1	0.98
8%				1

To test if the slopes were significantly different, analysis of covariance (ANCOVA) was carried out. The results are shown in Table 2.5.

**Table 2.5 Results of ANCOVA (analysis of covariance) test to establish the difference in slope between accrued twist in butt and crown at four different stages of moisture content.**

Aggregate correlation within samples	$r = 0.95$	$r^2 = 0.91$			
	SS	df	MS	F value	P value
ANCOVA summary	1.4	3	0.47	2.44	0.096
Test for homogeneity of regressions	0.6	3	0.2	1.06	0.394

The results in Table 2.5 show that there is no significant difference between the slopes and that the rate of accrued twist between butt and crown logs does not significantly change with decreasing moisture content.

### 2.3.6 Between position variation

Much of the between batten variation in twist arises from position within the log. Specifically, battens that wholly or partially contain the pith along their length are more likely to distort and exhibit higher degrees of twist.

In this experiment, three battens were sawn from each of the twelve logs. A sawing pattern was selected to deliver two battens from the annual rings free of the pith and one containing or partially containing the pith (Figure 2.17). The battens all contain a considerable percentage of juvenile wood.

Testing with a Balanced ANOVA (position: tree: target MC) shows a highly significant difference in the collective positions (ABC) between trees ( $p < 0.001$ ) and between drying targets ( $p < 0.001$ ). A one-way ANOVA shows a significant difference between the A, B and C positions for all measured data ( $p = < 0.001$ ). In all cases this can be attributed to the high values of twist in the B battens.

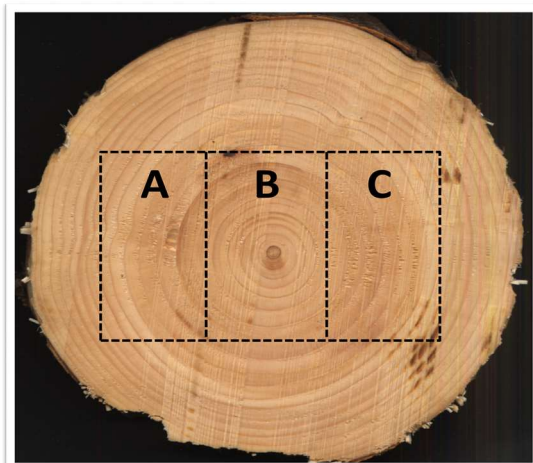


Figure 2.17. Sawing pattern selected to deliver three battens from each log; one (B) wholly or partially containing the pith through some or all of its length and two others (A and C) outside the area of the pith but containing a percentage of juvenile wood.

The B position battens, containing the pith, developed considerably higher degrees of twist when all A, B and C battens from all six trees are compared. Results given in degrees of twist per metre are shown in Figure 2.18.

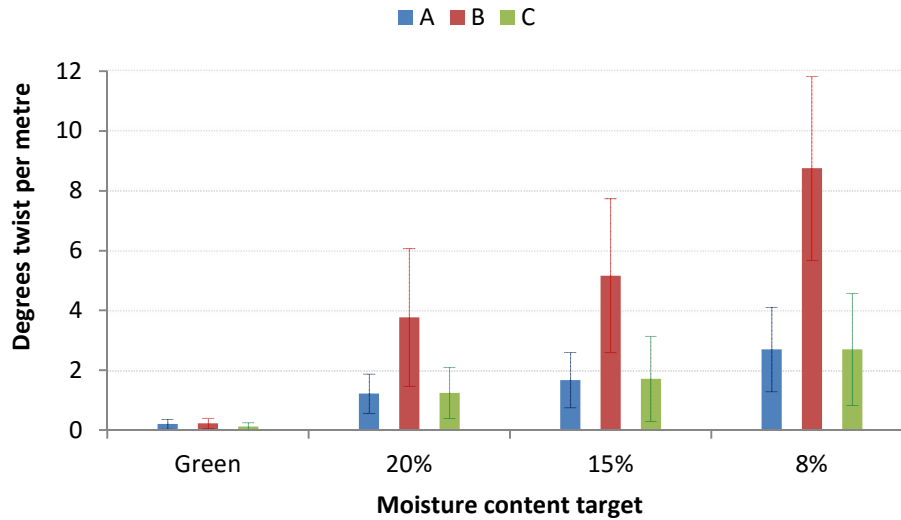


Figure 2.18. Columns show means for degrees twist per metre for all A, B and C battens at each drying targets with error bars displaying one standard deviation around the mean. This demonstrates the disparity in accrued twist between the B series and the A and C series' over the three drying stages. This is accentuated by the close relationship between the A and C series'.

Increases in twist proceed at a relatively constant rate for all positions within the log as moisture content decreases. Between the 20 and 15% target the twist accrued in the A, B and C battens rises by 37% for all three positions. Between the 15 and 8% target, twist increases by 61% for the A position, 70% for B and 57% for C. When compared with total twist, the percentage accrued twist is very consistent across the positional categories. The trends are shown in Figure 2.19.

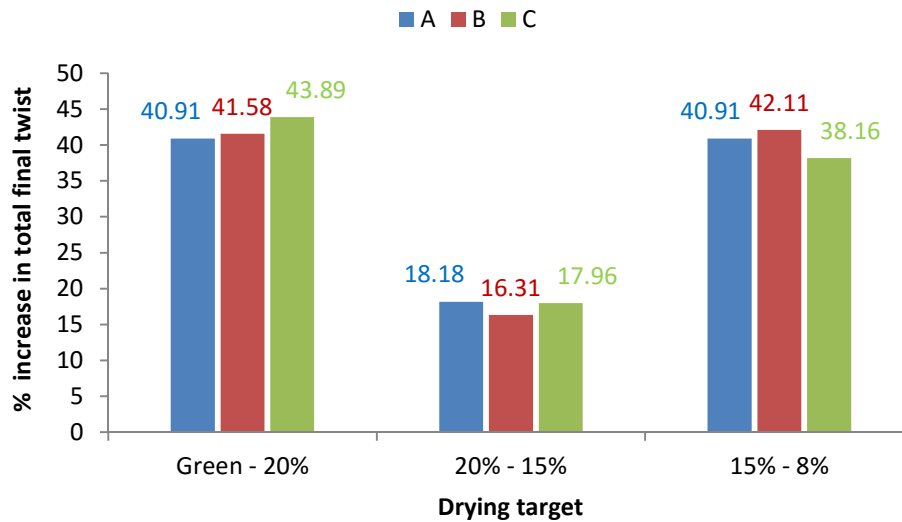


Figure 2.19. Percentage increase in twist for batten position at each drying target relative to final total twist (i.e. 100% for each position over the three drying cycles). The percentage increase between A, B and C battens at each target are not significantly different.

These increases for each radial position agree with the between tree increases in Figure 2.12; that most of the twist develops over two of the drying stages. This goes further by showing that the increases as a percentage of total twist accrued by position are proportionate across all positions within the log. The same data is reworked in Figure 2.20 to show the percentage of total twist accrued for each position.

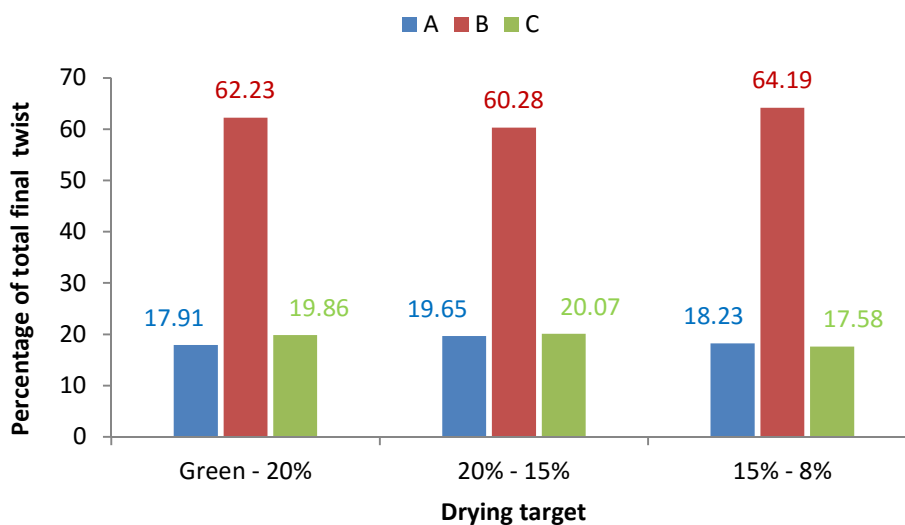


Figure 2.20. Percentage of total twist at each drying target by batten position based on 100% twist at each target. Differences between the A and B positions and between the C and B at each target are significantly different (ANOVA:  $p < 0.001$ )

This highlights the considerable difference in the B battens but again demonstrates the proportionality of the increases with position.

### 2.3.7 Storage period

When the samples had been dried to a mean moisture content of 15%, repairs to the kiln were required before the next drying cycle could commence. During this six week period the samples were stored at Edinburgh Napier University under climate controlled conditions (constant temperature; 21°C, relative humidity; 50%). The stack, which was separated by stickers to allow for even aeration, was rotated on two occasions during this period. Before drying to 8% moisture content was carried out, the samples were fully measured to compare with the data recorded at 15% moisture content. This showed that some resettlement of twist had occurred in the samples. The mean post conditioning moisture content was 14.7%. The measured mean post conditioning twist per metre for each tree is shown in Figure 2.21 beside the values measured at 15% moisture content.

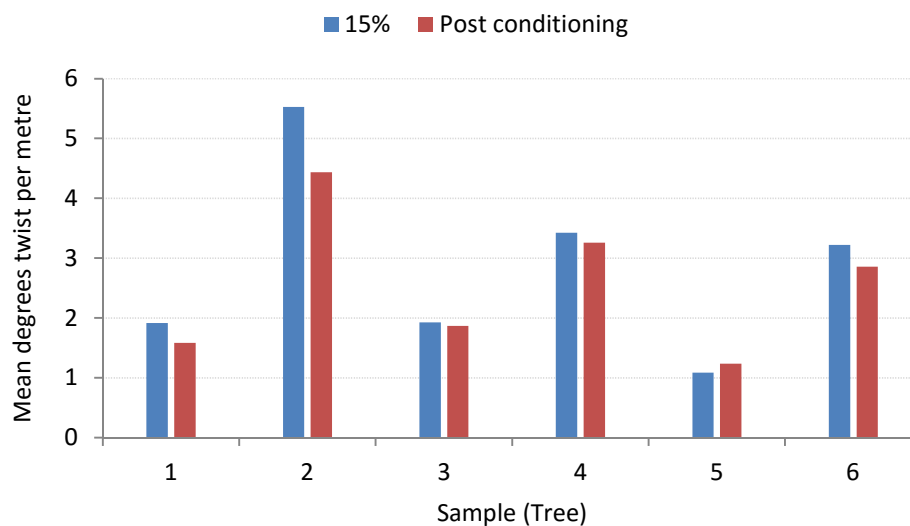


Figure 2.21. Change in mean degrees twist per metre from 15% moisture content measurements to post conditioning measurements after six weeks storage in a controlled environment (T = 21 °C, RH% = 50). Mean post conditioning moisture content was 14.7%.

The conditioning period caused a drop in the mean degrees twist per metre in all but one tree (Tree 5). The percentage change in twist for trees 1-6 over the storage period is shown in Table 2.6. It may have been assumed that any drop in moisture content should have led to an increase in twist. The post conditioning results show a small but measurable decrease. However, the performance of a t-test does not suggest a significant difference from zero in this change. A similar effect has been shown in a study by Rice (2000) where a percentage of studs of eastern spruce (*Picea rubens*) were found to have decreased in twist over a two week period with a drop in moisture content of 1.6%. The same study also found increases in twist among the sample population although the sample size used was far larger than in this work.

**Table 2.6. Percentage change in degrees of twist per metre after a conditioning period of six weeks at temperature; 21 °C and relative humidity; 50%.**

	Tree					
	1	2	3	4	5	6
Mean change °Tw/m	-20.72	-24.61	-3.27	-5.05	12.21	-12.67

The change in twist is variable between trees and there is no apparent pattern. Trees 1 and 3 have very similar values for twist at 15% moisture content yet the change after conditioning is very different.

## **2.4 Kiln Drying of Sitka spruce under restraint**

### **2.4.1 Introduction**

Producers will often make use of restraint (top load) upon a stack during the drying process. This can involve the direct placement of weight atop the stack, often in the form of concrete blocks. The stack may also be strategically strapped down prior to drying.

In this experiment an attempt is made to assess the potential impact of restraining the load while drying. As with the previous experiment, the sample size is small and will not be representative of a commercial operation in terms of scale. In particular, the experiment is designed to consider the difference between drying to low moisture content (in this case a target moisture content of 12%) with battens close to green moisture content and with battens which have been pre dried to the average commercial value of approximately 18-20%. The value of 12% moisture content was chosen as this is the suggested maximum moisture content appropriate for use in cross laminated or glue laminated timber products which may increase in demand in the future.

In making these comparisons, this experiment, in conjunction with the unrestrained experiment, aims to explore relationships between twist at different drying targets to ascertain the potential for a model to predict the development of twist.

### **2.4.2 Materials and methods**

#### **2.4.2.1 Sampling**

Sixty battens of Sitka spruce (approximate dimensions; 3000 x 148.5 x 102 mm) were acquired from James Jones & Sons Ltd, Lockerbie. Thirty of these battens were in green condition and had been rejected prior to drying as being unsuitable for construction timber. The remaining battens had been dried at James Jones to a moisture content of around 18-20% and had been rejected by visual grading, post drying, as unsuitable for construction timber. In all cases, the samples had been sawn with either the whole pith contained within the batten or had been sawn through or within a few annual rings of the pith (Figure 2.22). In either case, this would raise the probability of the material being prone to twist.

Prior to drying the average moisture content of the green samples was 53% and the pre-dried samples 17.5%.

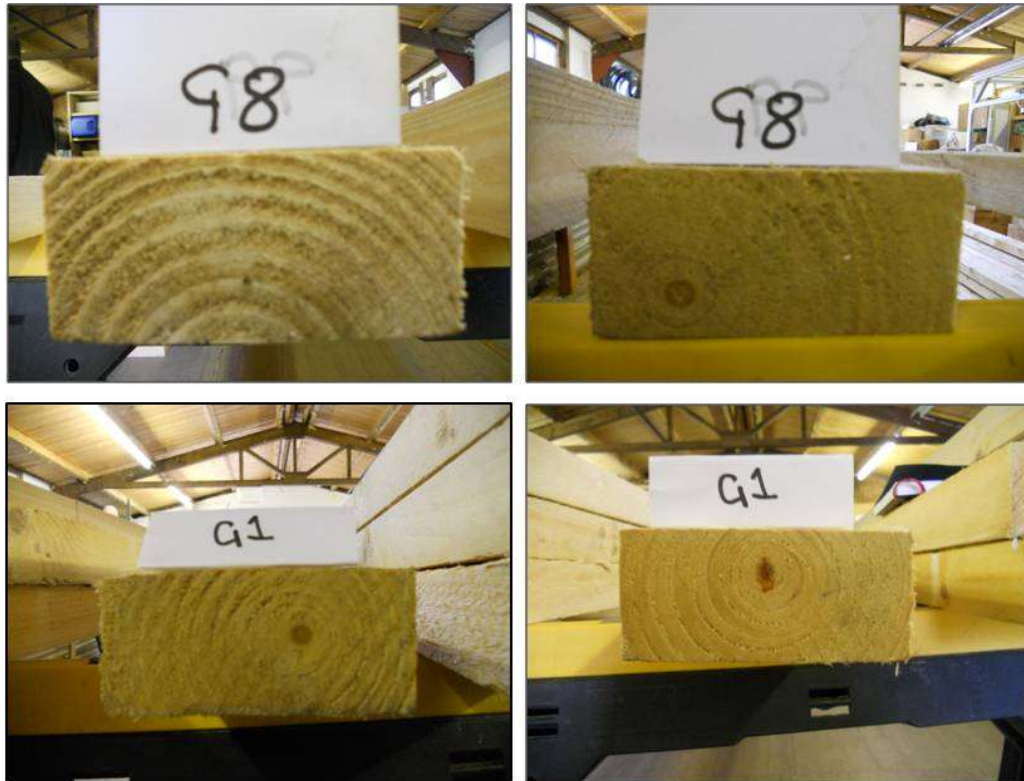


Figure 2.22. Two samples from the green batch used in the restrained drying experiment. Images show either end of the batten and the resulting positioning of the pith through the batten after sawing. In G8 the pith is wholly present at one end of the batten. The log has been sawn through with the pith visible on the face to exclude the pith at the other end. In G1 the pith is present at both ends and contained through the length of the batten.

#### 2.4.2.2 Kiln drying under restraint

Drying was carried out at the same facility and in the same kiln as was used for the unrestrained drying experiment. Correspondingly, the same default kiln schedule for Sitka spruce was applied. Refer to section 2.2.2 of this chapter for further detail of kiln specifications and drying schedule information.

The kiln loading and arrangement of the samples differed from the unrestrained experiment. In order that the restraint could be applied the samples were stacked in five rows and separated by stickers placed at 75cm intervals along the 3m length. Position of

the stack in the kiln was chosen to allow for optimum air flow through the stack. To this end the stack was placed in the centre of the kiln around 10 cm from the kiln floor and a baffle was introduced to regulate air flow (Figure 2.23). Two simple frames were assembled to hold the samples in place at either end of the stack. Each frame consisted of two battens joined by three threaded rods with retaining nuts at each end. With the stack in place, the nuts on the three threaded rods were tightened to secure the load. The pressure applied was not measured. The nuts were tightened until it was felt that the load was secure enough to prevent any movement at either end of the stack.



**Figure 2.23. Stack arranged in frame for restrained drying. Frame was secured by tightening of nuts on top side of the frame. A baffle was positioned to ensure optimum capture of air flow.**

A heavy duty polythene baffle was laid lengthwise over the top of the load to enable even air flow through the stack. This was secured on top of the load with three concrete slabs weighing approximately 25 kg each. This also added additional restraint to the unrestrained areas of the stack.

The two loads of samples; green and 18-20%, were dried independently (i.e. not in the kiln at the same time) but under the same conditions and with the same drying cycle. Post drying, the restraining boards in the frame were inspected for any shrinkage deformation that may have affected the sample battens. There was no evidence that any significant

movement had occurred. It should be considered that this method of restraint does not restrict lateral shrinkage and twist may also develop within the frame due to shrinkage in this direction. In this respect the experiment replicates the situation in a commercial kiln where there is no lateral restraint.

### 2.4.3 Results

The samples used in this experiment were obtained on the basis that they were not of construction timber quality. As all samples contained a significant section of the pith area along their length, the probability of significant measures of twist developing was more predictable. Even so, it is useful to compare the effects of drying from the two differing start points; green and 18% moisture content (Figures 2.24 and 2.25). Comparison can also be made to a selection of the results from the former experiment, namely those that also contained a significant section of the pith area. In this respect, the effect of restraint can be compared with no restraint (Figures 2.26 and 2.27).

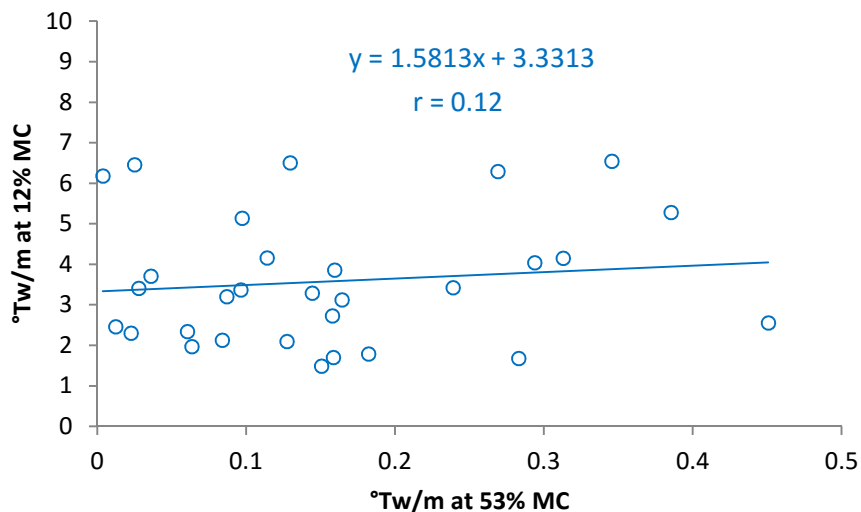


Figure 2.24. Scatter plot of the relationship between twist in green samples, at 53% moisture content, and accrued twist at 12% moisture content after drying. The poor relationship depicted (correlation coefficient;  $r = 0.12$ ) suggests that the small amount of twist measured by this method at green moisture content would not be satisfactory as a predictor for twist development in individual battens or logs post drying. The results are significantly different (ANOVA one-way;  $p < 0.001$ ).

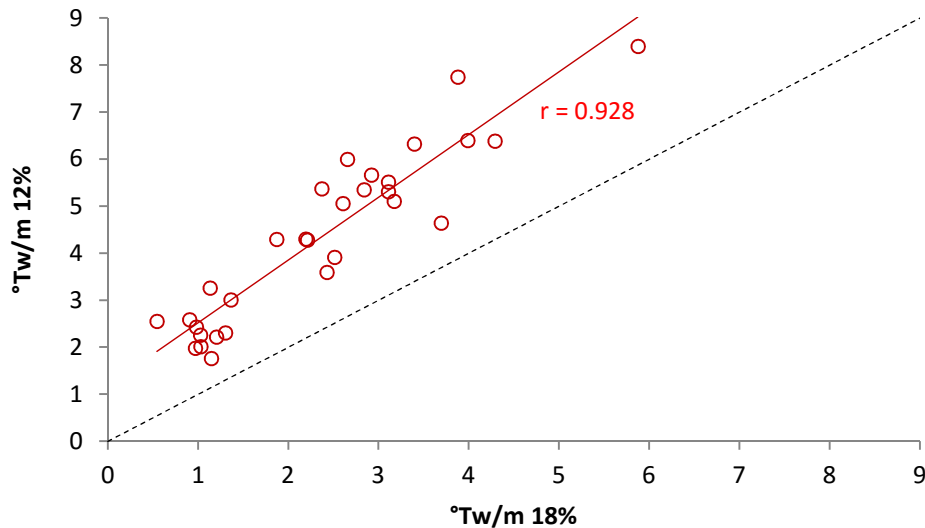


Figure 2.25. Scatter plot of the relationship between samples with an initial moisture content of 18% prior to drying against the final moisture content of 12%. A discernible relationship between the measured twist at 18% MC and the accrued twist at the 12% MC target moisture content is apparent (correlation co-efficient;  $r = 0.928$ ). The 1:1 line shows the increase in twist at 12% MC. The difference between the values at 18% MC and 12% MC is significant (ANOVA one-way;  $p < 0.001$ )

#### 2.4.3.1 Comparing restrained and unrestrained drying

The results from the two experiments: unrestrained drying and restrained drying are compared in Figures 2.26 and 2.27. The range of moisture content differs in the three examples shown; Restrained 1: green MC – 12% MC, Restrained 2: 18% MC – 12% MC and Unrestrained: green MC → 20% MC → 15% MC → 8% MC. The battens used in both restrained experiments had been previously rejected as unsuitable for construction grade timber. Those in the unrestrained experiment were sawn from selected trees and their suitability for construction grade timber was unknown. The charts show that the twist developed at around 18-20% MC appears to determine the pattern of continuing twist development at lower moisture content. This is shown best in Figure 2.27 where lines for the passing grades have been superimposed. It could be suggested from this that degrees of twist unsuited to construction grade timber could be predicted from twist that has been established by the 18-20% MC level.



Figure 2.26. The column chart displays the before and after results from five drying cycles, two from the restrained experiment and three from the unrestrained. Mean degrees of twist per metre (all samples) are shown for; Restrained 1 (green to 12%), Restrained 2 (18-12 %) and Unrestrained, (showing values for only the battens containing the pith for more direct comparison) at the three drying targets (green -20%, 20-15% and 15-8%).



Figure 2.27. Column chart displaying the values from Figure 2.22 after conversion to values fitting with the BS EN 14081 and EN 338 grading standards; twist per 25 metres width over 2 metres length. The line at 2mm is the passing grade for C16 and above GS (General Structural). Line at 1mm is the passing grade for C18 or above SS (Special Structural). The results suggest that drying battens of this kind beyond 18% moisture content may exceed the current classification limits.

## 2.5 Predicting twist

The results from both experiments suggest a strong relationship between battens dried to moisture content of 20% and battens dried below this figure; to as low as 12% in this case, and the degree of twist developed. To this end it would be possible to make reasonable predictions of twist at lower moisture content from material dried to the commercial standard of 18-22%MC. Figure 2.28 shows this relationship between the data from the 20% and 8% and 20% and 15% unrestrained drying targets.

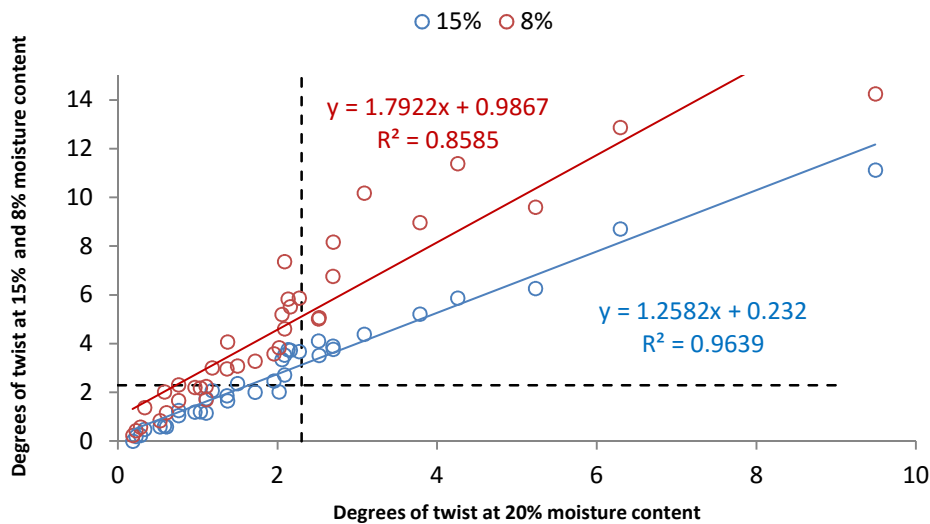


Figure 2.28. Scatter plots of measured twist at 20% against 15% (blue circles) and 20% against 8% (red circles). All values are from the unrestrained experiment. Dotted lines of 2.3 degrees per metre on the x and y axes represent the grading limit for construction timber at C16 or above GS.

This also correlates well with the data obtained from the restrained drying experiment and is compatible with the data at 18% and 12% moisture content shown as a scatter plot in Figure 2.25.

## 2.6 Discussion

Allowing battens of Sitka spruce sawn timber to be kiln dried without restraint enables the development of maximum dimensional change throughout the anatomical structure as water is lost. The anisotropic nature of how cells shrink as water is lost defines how the structure is reshaped by this process. Dimensional change is very much dependent upon the organisation of cell wall components in each individual and the resulting effects can be difficult to predict. However, there are some common defects which occur with regularity. Processors regard twist in Sitka spruce as a significant barrier to improving the marketability of construction timber. Sawn battens that wholly or partially contain the pith have been shown to develop the greatest degree of twist (Kliger et al., 2005; Fruhwald, 2006; Salin, 2007).

### 2.6.1 Measuring twist

Both of the chosen methods; FRITS Frame and wedge, proved capable of returning reliable results. Measuring small values of twist at green moisture content and the large values associated with encouraging maximum twist to develop were limiting factors for the wedge method. The FRITS Frame proved to be very suited to this work, providing an easy to use method which gave good results. It does require being in a fixed location and could not be regarded as easily portable but when accurate results are required for research or study it would be recommended. Where results between methods were available for comparison agreement was good. The wedge method is more suited to the prescribed method in the standard (EN 1310:1997) and for industrial settings where simple and fast methods would be more appropriate and should be capable of providing dependable results given the correct circumstances, i.e. for measuring the upper limits of acceptable twist.

### 2.6.2 Kiln drying

The experimental kiln used for this work was well suited to the requirements of this work in that it provided conditions which closely replicated those of commercial drying. The one disappointment was the malfunction during the 20-12% MC drying cycle which had to be aborted when the samples had reached only 15% MC. This did have consequences for the analysis. Some of the results presented have had to rely to some extent on assumptions due to this missing data.

Drying at conventional commercial temperatures tends to produce a linear relationship between increases in twist and decreasing moisture content (Straze et al, 2011). Disrupting the process by drying in stages did not seem to affect this. There were significant differences in relation to position within the log; battens where the pith was present twisted more but the rate at which twist develops is relatively constant for all samples regardless of position (Figures 2.18 and 2.20). Timber is conventionally dried to around 18-22% MC in the UK. Where material of lower moisture content is desired, drying intermittently may be advantageous. As shown in this work, twist accrued at 20% MC correlates with increases in twist at lower moisture content. Predicting subsequent quality in relation to twist at ~20% MC would allow for segregation and minimise the volume of rejected material after further drying. This would improve final yield at lower moisture content and divert rejected material to other purposes at an early stage before prohibitive levels of twist render it unsuitable as a construction material. Intermittent drying has been shown to have other advantages. Allowing dried wood to re-establish moisture distribution between drying cycles can reduce fissures and cracks (Kowalski and Pawlowski, 2011) and possibly prevent deterioration of other timber properties. This was not explored in this work but it may be useful to investigate these effects in future work.

### 2.6.3 Unrestrained drying

The between tree variation in accrued twist between drying targets was highly significant ( $p = 0.001$ ). Twist was added most significantly during the green- 20% MC and 15 – 8% MC drying cycles. This was true for all samples; however, the stage at which the greater degree of twist was added in individuals differed between the two drying cycles. Indeed, the addition of twist between cycles is very disproportionate between trees. This may be a

consequence of differential moisture loss or the effect of moisture gradients in individuals but this effect was not explored in this work.

There was a tendency to higher values of twist in crown logs (+10.7%) but no significant relationship between twist and within tree variation with height could be found. This may in part be due to the relatively small diameter at breast height which would suggest most of the material sawn contained high proportions of juvenile wood and any effect of mature wood in the samples was negligible or undetectable. In more mature trees, the proportions of juvenile wood, heartwood and sapwood would differ and this would undoubtedly have a bearing on twist development.

Positional variation was highly significant (between trees, between targets and between positions  $p < 0.001$ ). Battens containing the pith showed far greater twist than those cut away from the pith. As a percentage of the overall twist accrued between green and 8% moisture content, battens sawn from the centre of the log where the pith was wholly or partially present account for over 60% of the total twist. Taken as a function of total twist accrued, the percentage increase in twist by position is shown to be relatively constant across all three drying targets. Likewise the percentage of total twist at each drying target shows stable values for all three positions.

#### **2.6.4 Restrained drying**

Two batches of rejected samples were obtained to assess the impact of drying under restraint. The batches differed in that one was from green visually rejected material and the other had been dried to around 18% MC and failed mechanical grading tests. Both batches were made up of battens which all either wholly or partially contained the pith. The restraint applied was of a fairly primitive nature and akin to earlier experiments in this area (Mackay, 1973), rather than more recent studies (Erickson and Schmulsky, 2005; Tronstad, 2005; Fruhwald, 2006). For most of the timber produced in the UK for general construction purposes good stacking practice and strategically applied strapping are used to limit distortion. In this respect the method used here may be considered comparable.

The two batches were dried in separate cycles under the same conditions and with the same drying schedule used in the unrestrained drying experiment. Direct comparisons are difficult as there is no tangible relationship between the batches other than the fact that

they are both made up of battens that all come from the centre of logs. Essentially this experiment was designed to provide data which could be compared with the samples that were dried without restraint.

### **2.6.5 Comparing unrestrained and restrained drying**

The lack of data at 12% moisture content in the unrestrained drying experiment limits the conclusions that can be drawn from comparing the data from the two separate experiments. Both experiments do confirm that battens containing the pith that are dried to below 18% moisture content are highly susceptible to develop levels of twist that are likely to exceed the minimum limits for construction grade timber.

### **2.6.6 Storage**

These samples were stored for a period of six weeks between drying cycles under controlled conditions. This was intended to maintain their moisture content as much as possible prior to further drying. Before the next drying cycle was carried out the samples were re-measured to account for any change in properties. It was found that the moisture content had been maintained within reasonable limits. Mean moisture content before storage was 15% and after it had dropped a little to 14.7%. It was not expected that this small change would have made a considerable difference to the amount of twist measured prior to storage. It was found that there had been a decrease in twist in five of the six sample trees. The measured values had changed by 12% on average.

With a drop in moisture content any change, however small, would have been expected to be in the opposite direction. It has been demonstrated that accrued twist can decrease or increase by further treatment or by the climatic conditions it is exposed to. Post drying steam conditioning is known to have a positive effect on twist reduction (Riepen et al, 2004). Johansson et al (2001) found twist to be proportional to moisture content but to some degree reversible through several moisture cycles. A decrease in twist in studs of eastern spruce (*Picea rubens*) was found after a two week settling period with no restraint (Rice, 2000). At cellular level these changes can be attributed to the adsorption/desorption behaviour of individual microfibrils. This effect has been explored in terms of the adsorption/desorption kinetics of wood by Hill et al (2009). These effects highlight the

importance of post drying handling of processed timber. Post drying storage and packaging should be considered as important as the drying process in terms of preventing further distortion and maintaining product quality.

### **2.6.7 Predicting twist**

Predicting twist in samples at green moisture content can only be done by visual means where the battens are obviously unfit for purpose. In this work a distinct relationship between twist in samples that had been dried to around 20% moisture content and twist at lower moisture content in the same samples is shown to exist (Figures 2.25 and 2.28). Segregation of material at any stage of processing is time consuming. The economic advantage of implementing a system of segregation would possibly be dependent on the demand for higher quality timber at lower moisture content. However, none of the above provides solutions for predicting twist in green timber.

## 3. Longitudinal and transverse shrinkage

### 3.1 Introduction

Longitudinal shrinkage as a component of anisotropic shrinkage has been discussed in theoretical studies (Barber and Meylan, 1964; Barber, 1968; Cave 1972) and its relationship with microfibril angle has been observed experimentally (Sadoh and Kingston, 1967; Meylan, 1972; Johansson, 2003). In locations where MFA is expected to be high; close to the pith, in juvenile wood or in compression wood, longitudinal shrinkage is greater (Donaldson, 2007). This relationship might partly contribute to higher levels of twist found in sawn timber removed from areas close to the pith. In addition to this the relationship between longitudinal shrinkage and transverse forms of shrinkage; radial and tangential, are complex (Ylinen and Jumppanen, 1967).

In this chapter longitudinal and transverse shrinkage are measured on previously dried battens used in the unrestrained drying experiment detailed in Chapter 2. The battens were re-saturated to beyond fibre saturation point prior to commencement. Daily measurements of longitudinal shrinkage were taken in a custom built measuring frame as the battens dried to equilibrium moisture content. Transverse shrinkage was also measured concurrently using digital callipers. The aim of this experiment was to measure longitudinal and transverse shrinkage at the macro scale, explore the relationship between them and with the twist data from the experiments in chapter 2.

### 3.2 Materials and methods

#### 3.2.1 Samples

The 36 battens of Sitka spruce obtained from Spadeadam Forest, previously dried to three moisture content targets for examination of twist, were retained for this experiment. Having been dried to 8% moisture content, the samples were stored in a controlled environment ( $T^{\circ}\text{C} = 21$ ,  $\text{RH}\% = 50$ ) at Edinburgh Napier University for

nine months. After this storage period the mean moisture content of the battens measured by moisture meter (GANN Hydromette M2050) was 12.1%.

### **3.2.2 Method validation**

To measure longitudinal shrinkage, a custom-built frame was designed and assembled (see section 3.2.5 for detail). Preliminary trials to investigate the validity of the proposed method were carried out using samples from the restrained drying experiment. These samples had been kiln dried to 12% moisture content and were approximately 3m in length. Due to the presence of significant distortion; twist, bow and spring, a considerable number of the battens were unstable in the frame. Consequently, it was difficult to have confidence in the accuracy of these measurements and particularly, any subsequent repeat measurements.

Further trials were carried out with sample battens cut into three lengths of approximately 1m. At this shorter length the battens were more stable within the frame and it was possible to establish accurate reference points to enable repeat measurements. In addition, this also provided three replicate measurements over each 3m length rather than one at the original length. This does raise questions as to whether the shrinkage in the 3m length is adequately represented by the mean value of shrinkage from the three 1m lengths. Local differences in individual 1m lengths, such as knots or compression wood, will not be replicated in all three pieces with regard to volume or locus. Given the uncertainty of accurately measuring the whole 3m batten, the mean value of the three individual 1m battens must be regarded as a relative measure of shrinkage. As all 3m battens were treated identically, in this respect the comparisons between values for each 3m batten should also be relative but demonstrate adequately the variation between individuals. Replication of shrinkage values between the three 1m battens was generally good. For the whole data set this returned a correlation value of 0.85.

### **3.2.3 Preparation of samples**

Having been allowed to distort freely while being dried to 8% moisture content, the sample battens were not of uniform length. Each batten was marked at 1m and 2m

intervals along its length in the direction butt to crown. They were then sawn with a chop saw at the two marked points to give two sections of approximately 1m in length (battens 1 and 2) and a third, shorter section (batten 3). The mean length of battens in the 1 and 2 category was 997mm and battens in category 3 were 979mm. To facilitate explanation, these are referred to as the 1m battens for the remainder of the text.

### **3.2.4 Saturation of battens and moisture content**

Moisture content of around 30% is generally acknowledged as the estimated value of fibre saturation point for many conifers including Sitka spruce and it can be assumed that this is a reasonable estimate (Walker, 2006c). Drying of wood is dependent on a number of variables however and the size of the timber, position in the log and rate of drying amongst other influences will have an effect on the actual FSP. Feist and Tarkow (1967) found ranges of 20-50% MC for Sitka spruce and other species dried under different conditions.

There was no practicable way to assess the equivalence of the re-distribution of moisture in the battens after re-saturation and this variation would have been continuous throughout the drying period. The measured moisture content and shrinkage presented in the results section should therefore be regarded as averaged for the whole batten and the visual material presented in this section should be viewed as practical estimates of FSP.

Moisture content was measured by weighing individual battens before each set of measurements were taken. Weights were related to the oven dried weights of sample pieces from each batten.

To measure shrinkage in the longitudinal direction it was necessary to re-saturate the battens to beyond fibre saturation point. To facilitate this, the battens were immersed in water in an inflatable pool (Bestway Pools UK, Newton Abbot, Devon, pool dimensions; 262 x 175 x 51cm). Re-saturation was carried out on batches of 27 battens at a time. This number was chosen as it allowed for all the required measurements to be completed in one day and also provided for four even batches. The four batches in order were; butt log battens, trees 1-3 followed by 4-6, crown log

battens, trees 1-3 followed by 4-6. Weights (concrete slabs dimensions; 50cm x 50cm, approximate weight 25 kg) were applied on top of the load but separated by stickers to ensure complete immersion throughout the re-saturation period. Battens were soaked in the pool for a minimum of seven days to ensure re-saturation beyond fibre saturation point (Figure 3.1). The implications of re-saturating battens are addressed in the discussion section of this chapter.



**Figure 3.1.** Re-saturation of samples. The samples were arranged in batches of 27 and weighed down with slabs to ensure total immersion at all times. Samples were soaked for a minimum of seven days. The water level was checked daily and topped up as required to ensure complete coverage of the samples.

### 3.2.5 Measuring frame

Battens were measured in a frame designed and built for this purpose (Figure 3.2). This was constructed from two lengths of right angled, slotted steel (Handy Angle©) measuring 40 x 40 x 1500 mm. The two lengths were bolted together with two slotted, right angled connector strips leaving a gap of approximately 60 mm width between the two lengths. The structure was then secured to a stable workbench with two heavy-duty, cast iron G clamps. To enable measurement a 50mm round headed bolt was attached to the right angled connector at one end (positioning end) with the

round head facing towards the opposing end (measurement end). At the measurement end, a digital indicator (Mitutoyo Absolute, model IDS1012B, Mitutoyo Corporation, Japan; step-0.01mm, accurate to 0.02mm) mounted on a wood block was securely attached to both strips of the frame with the contact plunger facing towards the positioning end. The distance between the tip of the plunger of the digital indicator and the centre point of the round headed bolt was then set to the appropriate distance for measurement by adjusting the protrusion of the bolt. Although the tip of the plunger attached to the digital indicator has a rounded head, a removable spacer of firm plastic with dimensions 120 x 20 x 5 mm was used as a separator between the plunger and the batten surface to ensure that any point sources of indentation or deterioration on the batten surface did not impact the consistency of repeat measurements. A second spacer, an aluminium block of dimensions 120 x 20 x 20 mm was inserted between the plunger tip and the plastic spacer to measure the shorter battens. For consistency, spacers were marked on one surface to identify a regular top side and when placed on the frame the spacer was positioned to be flush with the far side of the frame before measurement was recorded.

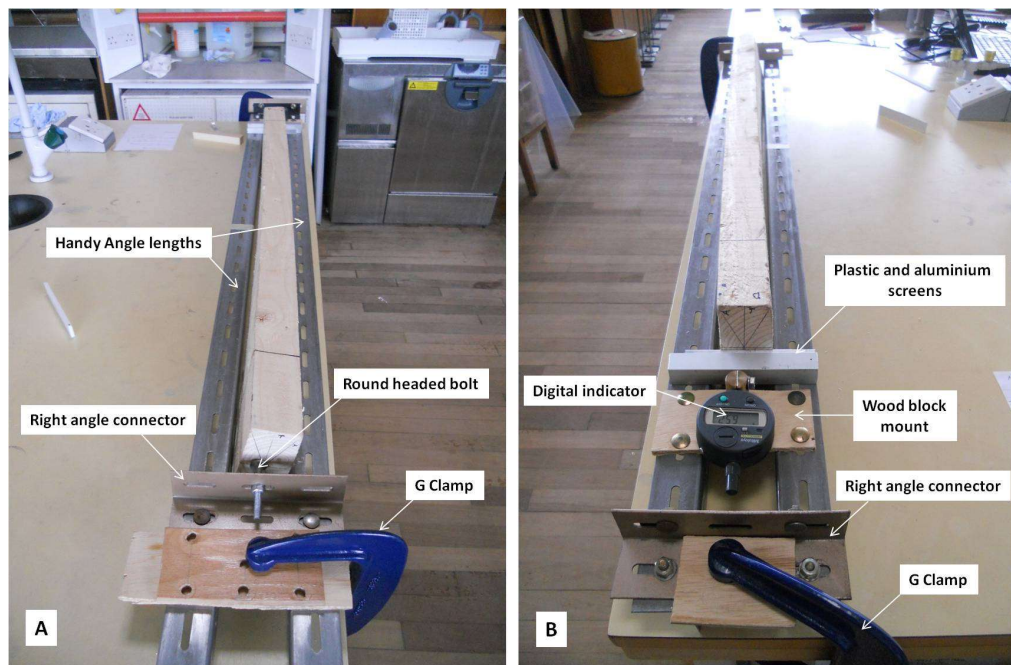


**Figure 3.2. Overview of longitudinal shrinkage measurement frame. Image A, on the left, shows detail of the arrangement at the positioning end. Image B, on the right, shows the arrangement and apparatus at the measurement end.**

### 3.2.6 Timescale of recorded measurements

The samples were measured prior to re-saturation for reference purposes. Initial measurements of re-saturated samples were taken on the day of removal from immersion and at 24 hour intervals thereafter. Measurements were stopped when it was considered that equilibrium moisture content had been reached in the sample. This was regarded as when the weight of the sample had decreased by less than 2% of the last measurement days' recorded weight loss.

### 3.2.7 Longitudinal shrinkage measurements

Battens were placed in the frame with the edge face down and the appropriate spacer or spacers inserted and positioned to accommodate the length. When stable it was allowed to rest against the round headed bolt at the positioning end. Prior to the initial measurement being recorded, a semi-circular mark (in red ink) was made around the area where the batten end made contact with the round headed bolt to allow for consistent positioning with repeat measurements (Figure 3.3). This was repeated (in green ink) with the batten turned 180° through its width to rest on the opposing edge for a second measurement and further repeated with the batten turned 180° through its length to record measurements three and four. The mean of the four replicate measurements was taken as the value for longitudinal shrinkage on each of the 1m battens. Standard deviations between the four replicates were very small across all samples. The mean value of the three 1m battens that made up each 3m batten was taken as the daily longitudinal shrinkage for each 3m batten.

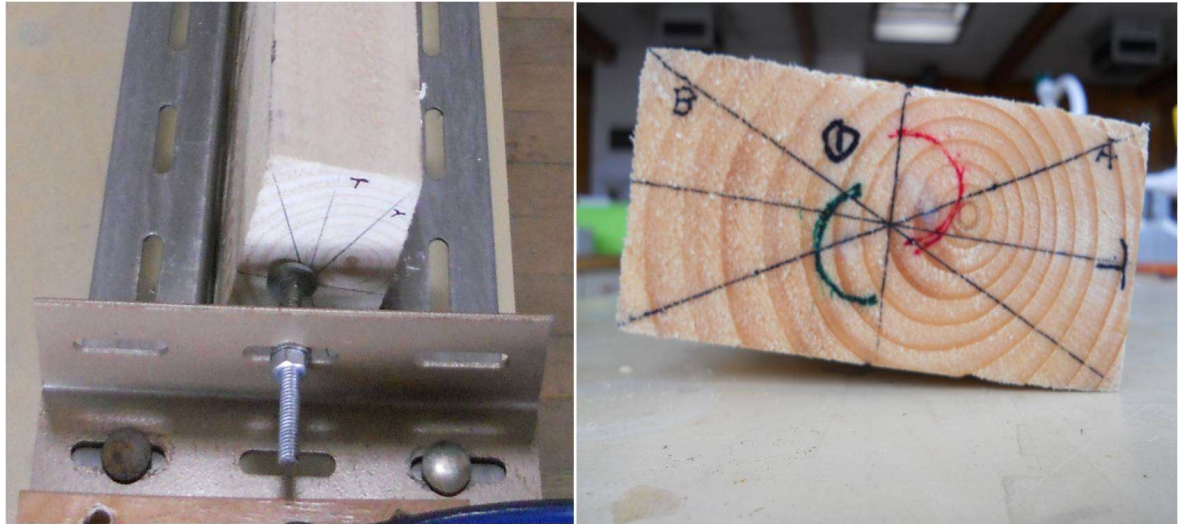


**Figure 3.3. Marking samples for repeat measurement. When stable in the frame, the batten is allowed to rest against the round headed bolt at the positioning end (left). Semi circular marks are then made around the bolt head to show the stable resting position of the initial measurements and to allow for accurate repositioning (right).**

### 3.2.8 Transverse shrinkage measurements

Transverse shrinkage measurements were recorded concurrently with those for longitudinal shrinkage. Measurements were taken using digital callipers (Powerfix Profi+, Milomex Ltd, Bedfordshire, UK), with resolution 0.01 mm and accuracy of 0.02 mm. For each 1m section, two transverse measurements were taken on each face giving a total of 12 measurements for each original 3m batten. Measurements were taken approximately 30cm in from each end at sections where there was minimal presence of knots or other blemishes that may have had an adverse effect on shrinkage. The location of each measurement was marked to ensure replication. The position of each measurement in relation to its original location within the log was noted as outer, inner or pith; outer being the face farthest from the pith, inner being the face closest to the pith and pith being either face of any batten where the pith was wholly or partially present (Figure 3.4).

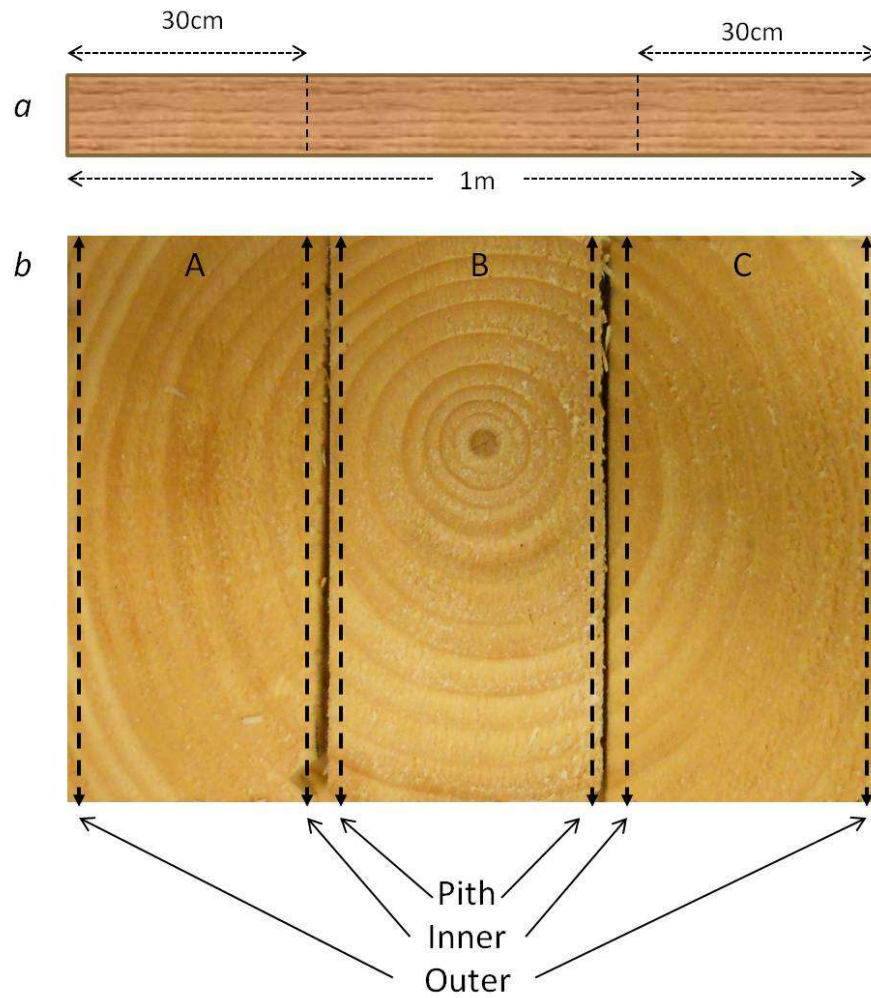


Figure 3.4. Detail of transverse shrinkage measurements.

*a* Transverse measurements were taken across the face of each 1m batten, approximately 30cm in from either end. The dotted lines on the diagram denote potential measurement locations.

*b* Cross section shows location from the pith for three battens; A, B and C, cut from one log. Outer indicates measurements were taken on battens A and C on the face farthest from the pith, inner, measurements on battens A and C on the face closest to the pith and pith for measurements on either face of batten B containing the pith or partial quantity of pith.

### 3.3 Results

#### 3.3.1 Variation in longitudinal shrinkage

In this section the measured longitudinal shrinkage results are presented for each of the six trees with particular reference to; between tree variation, within tree variation; i.e. between butt and crown logs, within log variation; i.e. between battens within a log, and between battens, with particular consideration to position within the log. The effect of decreasing moisture content in relation to each of these categories is also observed and considered. It is assumed that longitudinal shrinkage only occurs beyond fibre saturation point; when bound water is lost. As the battens were initially saturated it is possible to estimate at which point in the drying process fibre saturation point has been reached. The battens are categorised by three distinct positions within each log; A, B and C. These are representative of their relative positions within the log determined by the cutting pattern shown in Figure 3.5. The total longitudinal shrinkage, expressed in millimetres per metre length for each batten (i.e. the mean of the shrinkage recorded in each of the three 1m sections) in this experiment is given in Table 3.1. Mean values of shrinkage for each log and each tree are also given.

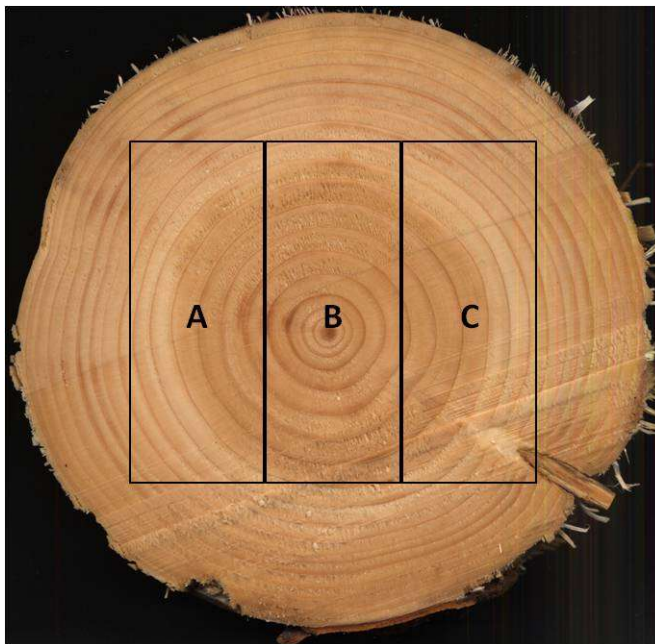


Figure 3.5. Cutting pattern selected to produce three battens from each log. The battens are labelled A, B and C. Battens in the B position are sawn from the centre of the log and wholly or partially contain material from the pith of the tree. The A and C battens are sawn from either side and are free from the pith but all will contain a percentage of juvenile wood.

**Table 3.1.** Values for total longitudinal shrinkage at final equilibrium moisture content (mean final EMC = 13.4% over the range 10.3 – 15.1%) reported in mm per metre length. Measurements were taken over a 20 day period. Temperature (T) and relative humidity (RH%) were subject to laboratory conditions (i.e. uncontrolled) and fluctuated considerably over the period; Mean T = 20.1°C over the range 16.9 – 26.2°C, Mean RH% = 58 over the range 42 – 69. Values are shown for; batten position (A, B and C), log means (butt and crown) and the mean value of shrinkage for each tree.

Tree	1	2	3	4	5	6	
<b>Batten</b>		<b>Total longitudinal shrinkage (mm/m)</b>					
<b>Butt</b>	<b>A</b>	1.13	1.02	0.83	1.04	0.35	1.98
	<b>B</b>	1.19	1.45	0.95	1.70	0.53	1.63
	<b>C</b>	0.86	1.83	0.75	1.96	0.60	0.98
<b>Crown</b>	<b>A</b>	0.53	0.98	0.49	1.19	0.76	1.61
	<b>B</b>	0.67	1.38	0.60	1.05	0.59	1.52
	<b>C</b>	0.57	1.22	0.71	1.07	0.69	1.55
<b>Log mean</b>	<b>Butt</b>	1.06	1.43	0.84	1.57	0.49	1.53
	<b>Crown</b>	0.59	1.19	0.60	1.10	0.68	1.56
<b>Tree mean</b>		0.83	1.31	0.72	1.34	0.59	1.55

Total longitudinal shrinkage represents the final accumulated value in millimetres per metre length of incremental daily measurements from saturated (beyond fibre saturation point) to equilibrium moisture content, when it was considered that no further significant water loss was occurring. Log means are calculated as the mean value of the total shrinkage from the three battens in each log, butt or crown. Tree means are determined as the mean value from all six battens in each tree.

### 3.3.1.2 Between and within tree variation

An individual value plot of the between tree variation in longitudinal shrinkage is shown in Figure 3.6. Analysis of variation; ANOVA one-way, comparing the mean values for total longitudinal shrinkage in each of the six individual battens within each tree, shows a highly significant difference between trees overall ( $p < 0.001$ ). However, shrinkage between all trees is not significant. A breakdown of individual between tree differences is shown in Table 3.2.

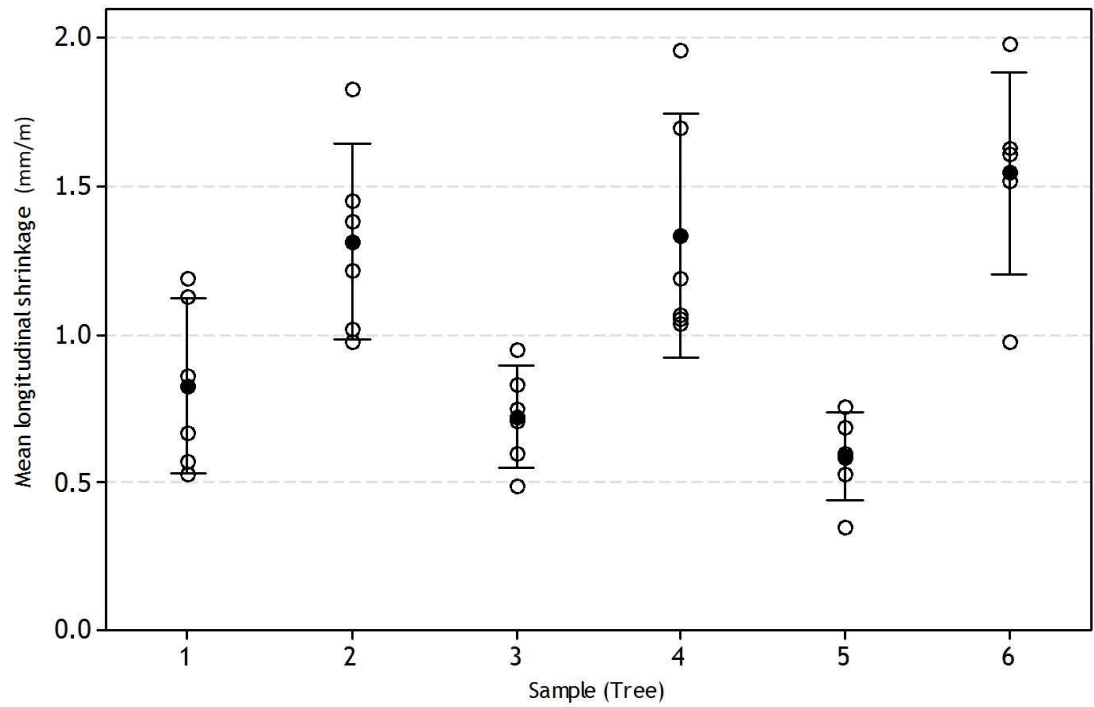


Figure 3.6. Individual value plot showing mean values in mm/m (filled circle) for samples (tree) 1-6. The ranges of values of total shrinkage for each individual batten are shown (hollow circles) with a 95% confidence interval bar. ANOVA one-way test shows significant between tree variation ( $p < 0.001$ ). The between tree variation is more clearly expressed in Table 3.2.

Table 3.2. Results of Fisher post hoc analysis defines the between tree variation for trees 1-6. Means in mm/m are listed from top to bottom as least to greatest mean longitudinal shrinkage. Groupings are based on a calculated 5% LSD (least significant difference) of 0.18. Trees which share the same group ID are not significantly different from one another.

Tree	Mean	Groups
5	0.59	a
3	0.72	a, b
1	0.83	b
2	1.31	c
4	1.34	c
6	1.55	d

### 3.3.1.3 Between log variation

On average longitudinal shrinkage in butt logs was greater than in crown logs by 21% although this does not prove to be statistically significant. The spread of the range of measured values between butt and crown logs is shown in Figure 3.7.

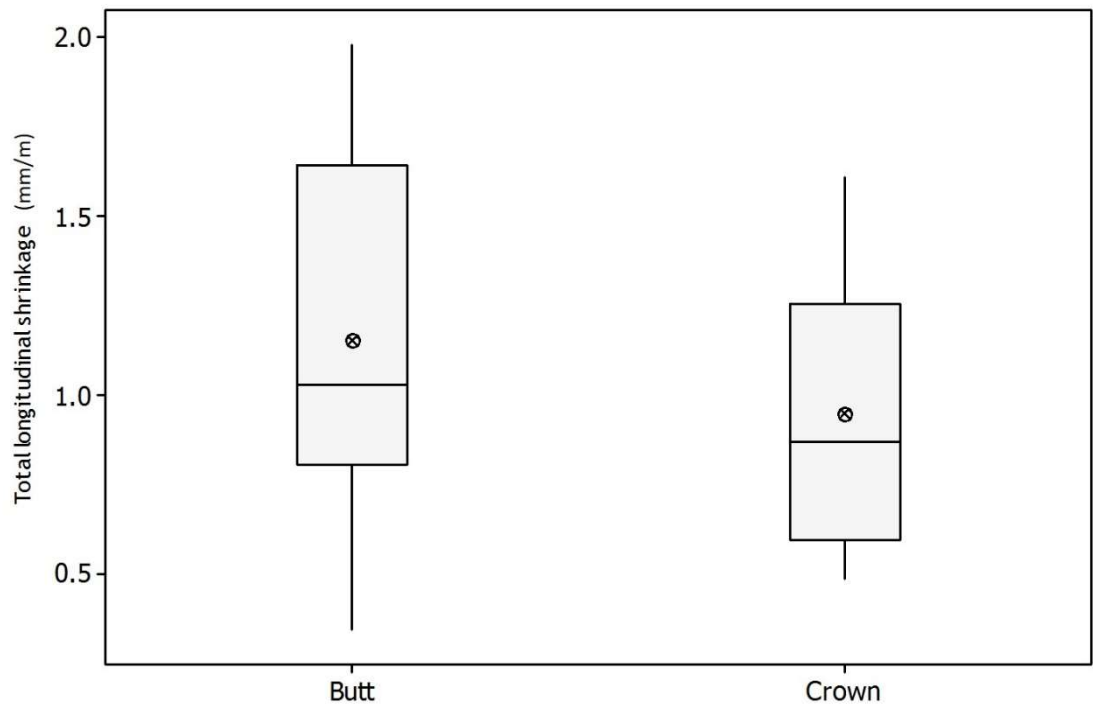
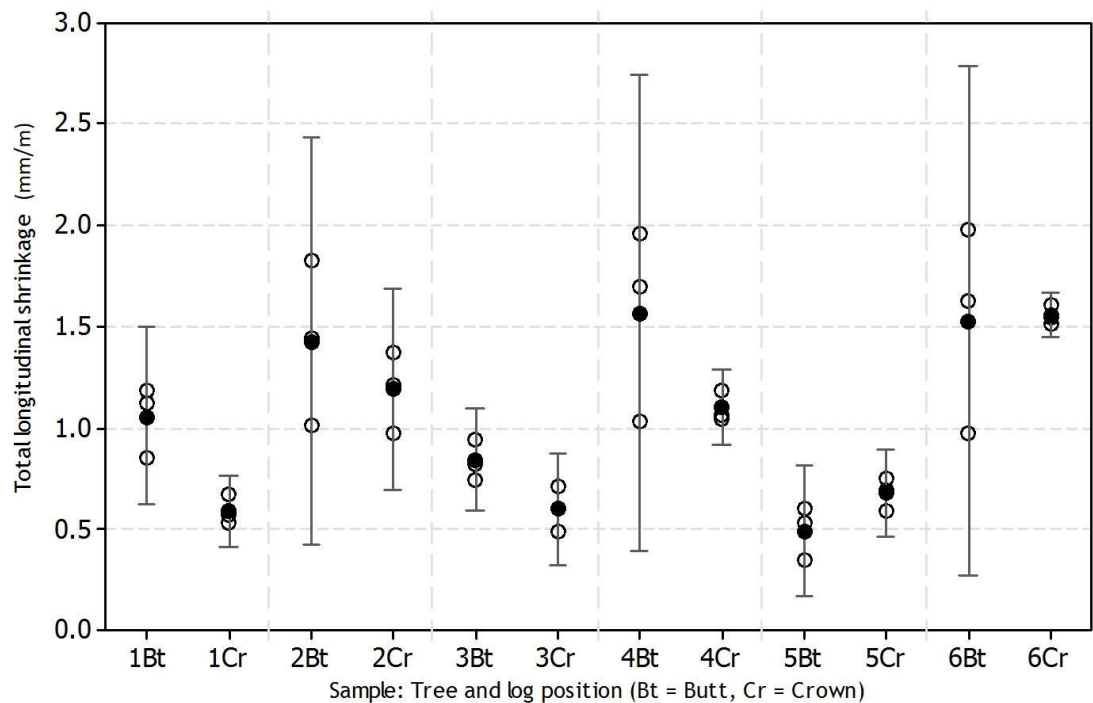


Figure 3.7. Box plots of individual value range in butt and crown logs in mm/m. The total butt log range including outliers is 0.35 - 1.98 with an interquartile range of 0.84 (0.81-1.65). The total crown log range including outliers is 0.49 - 1.61 with an interquartile range of 0.66 (0.60-1.26). Means are shown as circled crosses; butt = 1.15, crown 0.95 and the median is represented by the in box line; butt = 1.03, crown = 0.87.

An illustration of the between log variation in individuals for trees 1-6 is shown in Figure 3.8. This again demonstrates that the mean value for shrinkage is greater in butt logs in the majority of the six trees. There is also a visible trend that shows a wider range of values in butt logs. However, the ratio between butt and crown logs in terms of range is not consistent. The interquartile range for all butt and crown logs and the ratio between the two as a percentage are shown in Table 3.3. ANOVA one-way tests were carried out for butt against crown logs in each individual tree. The results show significant variation in trees 1 and 3 ( $p = 0.013$  and  $0.048$  respectively). Excepting the general trend towards a greater range of values for shrinkage in butt logs, the results suggest that within tree shrinkage follows a more random pattern.

**Table 3.3. Interquartile (IQ) range values for butt (Bt) and crown (Cr) logs in trees 1-6 shown in millimetres per metre length and the butt to crown ratio shown as a percentage.**

Tree	1		2		3		4		5		6	
Log	Bt	Cr	Bt	Cr	Bt	Cr	Bt	Cr	Bt	Cr	Bt	Cr
<b>IQ Range (mm/m)</b>	0.33	0.14	0.81	0.40	0.20	0.22	0.92	0.14	0.25	0.17	1.00	0.09
<b>Bt:Cr (%)</b>	57.8		50.62		-10.00		84.78		32.00		91.00	



**Figure 3.8. Individual value plot showing the mean values in mm/m for each batten (hollow circles) in a butt or crown log (labelled on x axis) and the mean for the log (filled circle). Interval bars show the 95% confidence interval for batten values in each log. Analysis of variation between logs for each tree reveals that only Trees 1 and 3 show significant variance between the mean values of butt and crown logs ( $p = 0.013$  and  $0.048$  respectively).**

Although the mean values only show significant variance in trees 1 and 3, a wide range of values between the three battens in the butt logs of trees 2, 4 and 6 is notable.

### 3.3.1.4 Positional variation

To assess the effect of position within a log, the thirty six sample battens are sorted into three groups of twelve by position: A, B and C. These labels represent the approximate position in the log, determined by the cutting pattern shown in Figure 3.5. The battens cut from the centre of the cant, the B battens, all wholly or partially contain the pith of the tree along their length. The A and C positions contain a percentage of juvenile wood. Positionally, the A and C battens are simply either side of the B battens and the selected position is random rather than directional (i.e. not determined by compass direction). The range of values in millimetres per metre length and the mean for each positional group are shown in Figure 3.9.

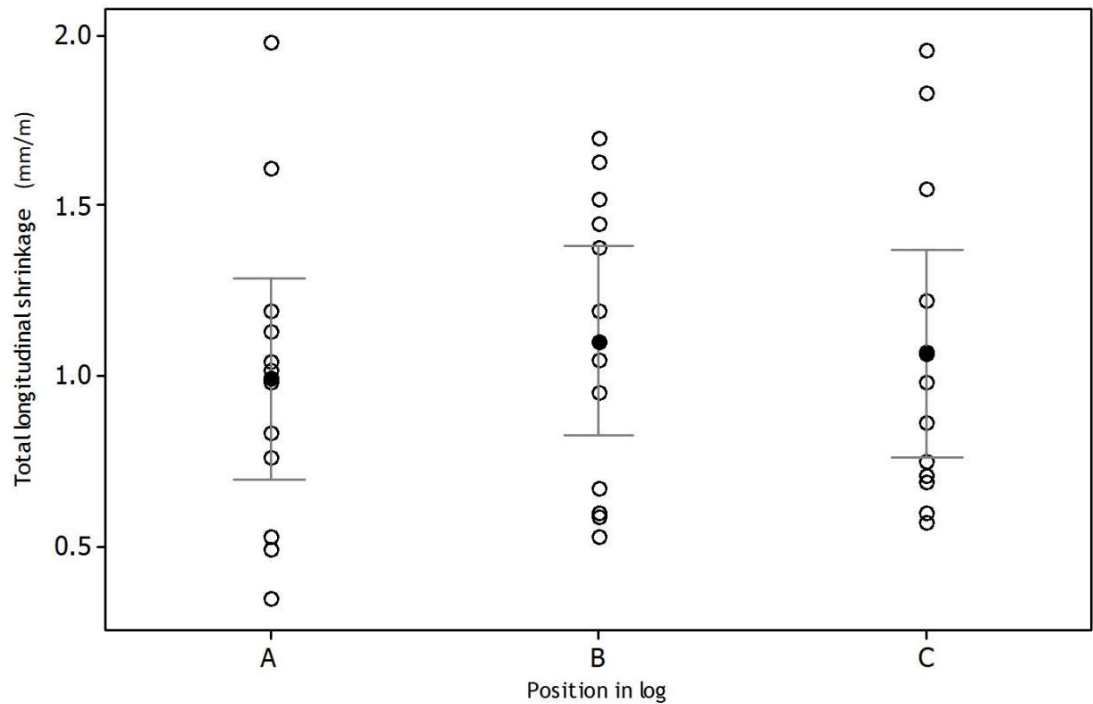


Figure 3.9. Individual value plot of longitudinal shrinkage in millimetres per metre length for all battens from the six sample trees segregated into positional categories; A, B and C. Values for individual battens in each group are shown as hollow circles ( $n = 12$ ) and the mean for each group as a filled circle. Mean values by group are; A, 0.99, B, 1.11 and C, 1.07. Interval bars represent the 95% confidence interval based on the mean for each positional group.

There is a considerable spread of values within and across the three positional groups. Table 3.4 provides the mean value and interquartile range for positional

groups A, B and C. A visual interpretation of the same data, as individual box plots, is shown in Figure 3.10. The groups are further sorted into butt and crown categories.

**Table 3.4. Mean values and interquartile range for positional groups A, B and C in butt and crown logs.**

Log	Butt			Crown		
Position	A	B	C	A	B	C
Mean (mm/m)	1.06	1.24	1.16	0.93	0.97	0.97
IQ range (mm/m)	0.63 (0.71 – 1.34)	0.80 (0.85 – 1.65)	1.15 (0.71 – 1.65)	0.78 (0.52 – 1.30)	0.82 (0.60 – 1.42)	0.64 (0.66 – 1.30)

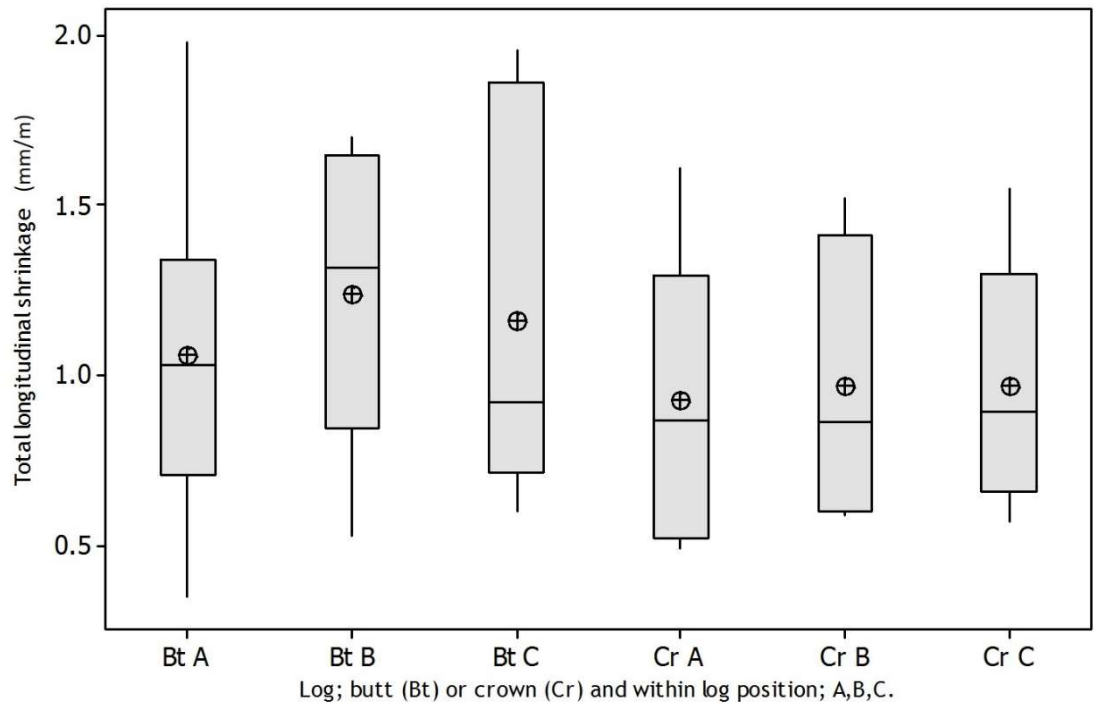


**Figure 3.10. Box plots showing the range of longitudinal shrinkage values for batten groups A, B and C sorted for butt or crown logs. Each box displays whiskers for max and min values, interquartile range box, value for the mean (circled cross) and median (line). Refer to Table 3.3 for values. Butt position values are higher than crown; A: +14%, B: +28%, C: +20%.**

In Figure 3.11 the values for each batten are shown by position and segregated into butt and crown logs within each tree. Testing of within log, positional variation for each individual tree was performed with ANOVA two-way tests.

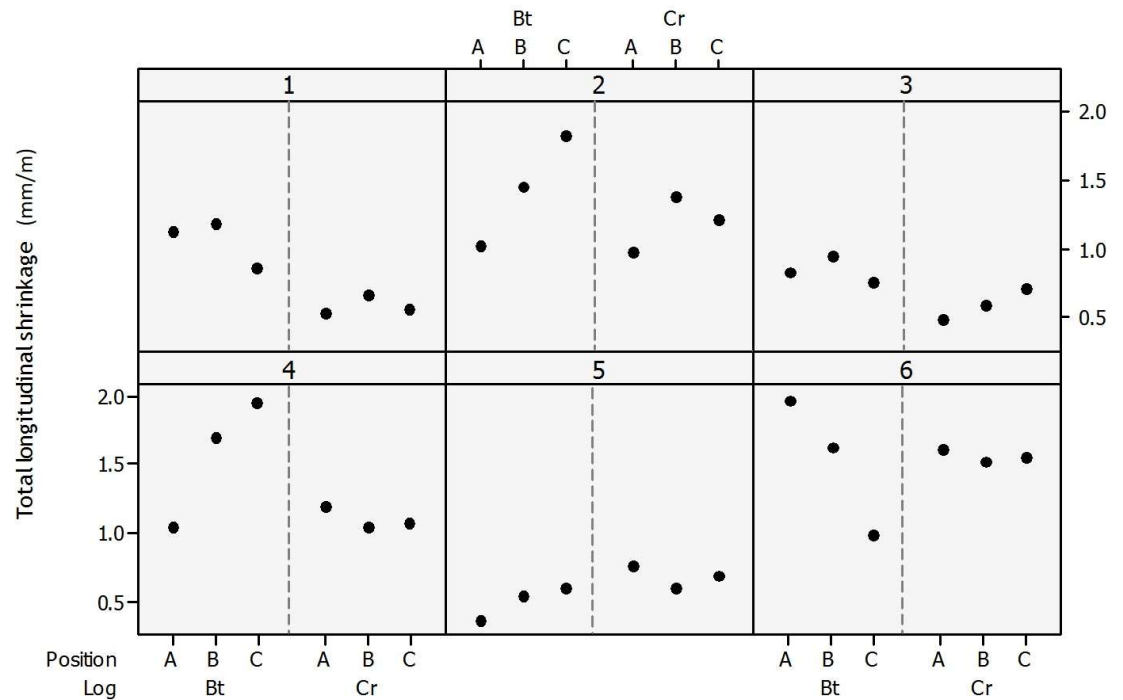


**Figure 3.11.** Individual value plot showing values for total longitudinal shrinkage in millimetres per metre length for each batten by position (A, B or C) within butt and crown logs for trees 1-6 (Tree ID shown at top of panels). Tested with an ANOVA two-way (log: position) the results do not show any significant difference for batten position between butt and crown logs..

### 3.3.2 Longitudinal shrinkage and decreasing moisture content

In this section the relationship between longitudinal shrinkage and decreasing moisture content is considered. The between tree, between log and between position categories are observed in a series of scatter plots (Figures 3.12 – 3.20). In these plots the longitudinal shrinkage values represent the actual daily incremental decrease in length in millimetres. Incremental measurements are used, as opposed to total shrinkage, to evaluate potential shrinkage prior to FSP being reached and to identify the estimated point where FSP is reached. For the between tree category these values are calculated from the means of the daily value of each of the six battens within each tree. The same method is applied for the between log category by

taking the means from all three battens in each of the twelve logs. The between position plots show the actual daily values recorded for each batten; A, B or

C. Moisture content values are presented as percentages which were calculated from daily weighing of the samples with reference to oven dried material from each of the samples. The mean values are calculated in the same manner as longitudinal shrinkage values. In the between position series of plots the scale of the  $x$  and  $y$  axes are consistent for each tree but not consistent between trees. This is done to provide for better resolution in some cases. All plots contain a dashed reference line at 30% moisture content; the generally acknowledged estimated value of fibre saturation point for Sitka spruce.

Note that the number of data points in each plot is not consistent. This is a consequence of drying the samples in separate batches and the ambient conditions in the laboratory over the period of the experiment. In the latter stages of the experiment there was a consistent rise in temperature in the laboratory over several days which increased the rate of drying. This decreased the number of days it took for the samples to achieve equilibrium moisture content. This discrepancy does not seem to have adversely affected the final outcome of the experiment. The final mean equilibrium moisture content was 13.4%, over a range of 10.3 – 15.1%. These values do not necessarily represent the potential for in-service material to dry to lower equilibrium moisture content but was dictated by the prevailing laboratory conditions.

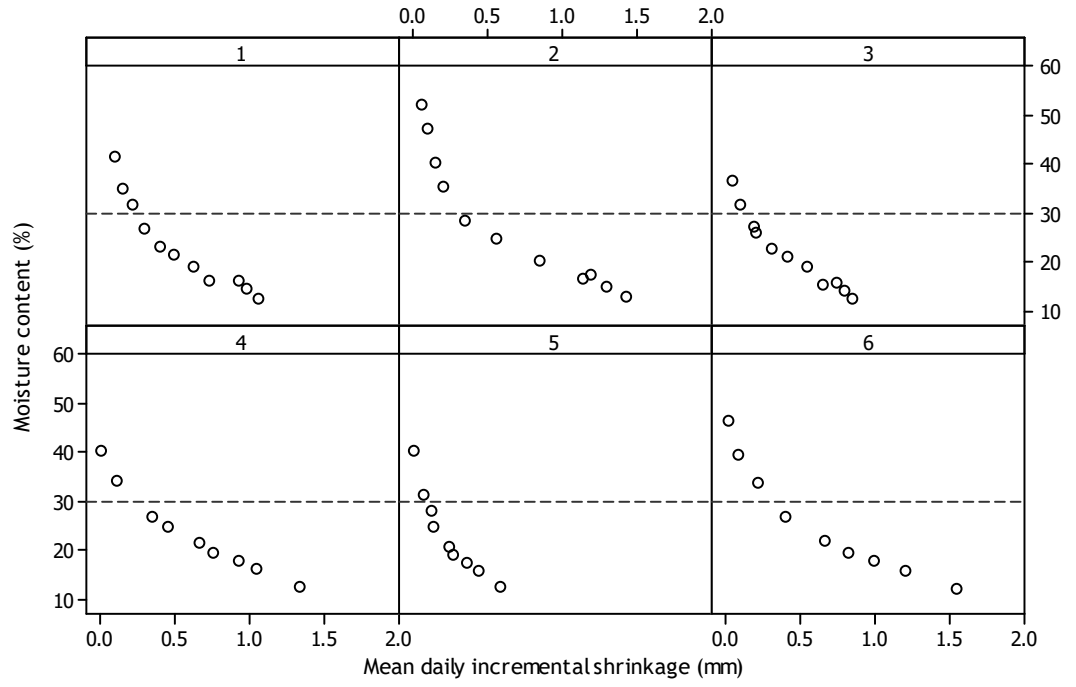


Figure 3.12. Scatter plot of moisture content against mean daily incremental shrinkage for trees 1 – 6.

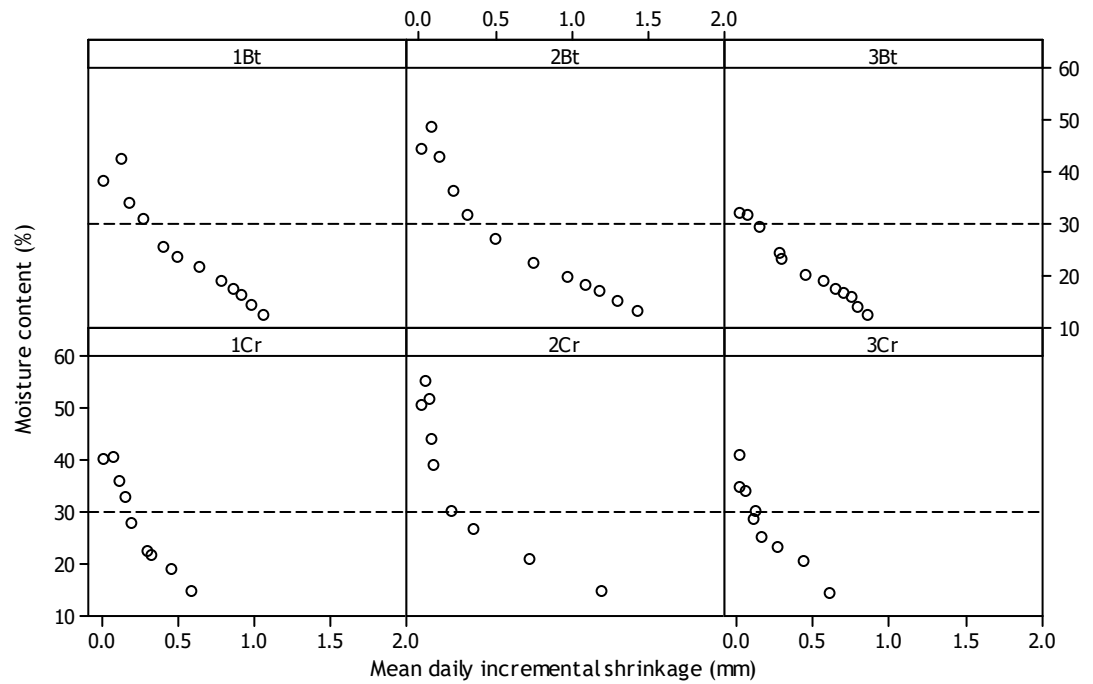


Figure 3.13. Scatter plots of moisture content against mean daily incremental shrinkage for trees 1 – 3 with butt log values in top panels and crown log values in lower panels.

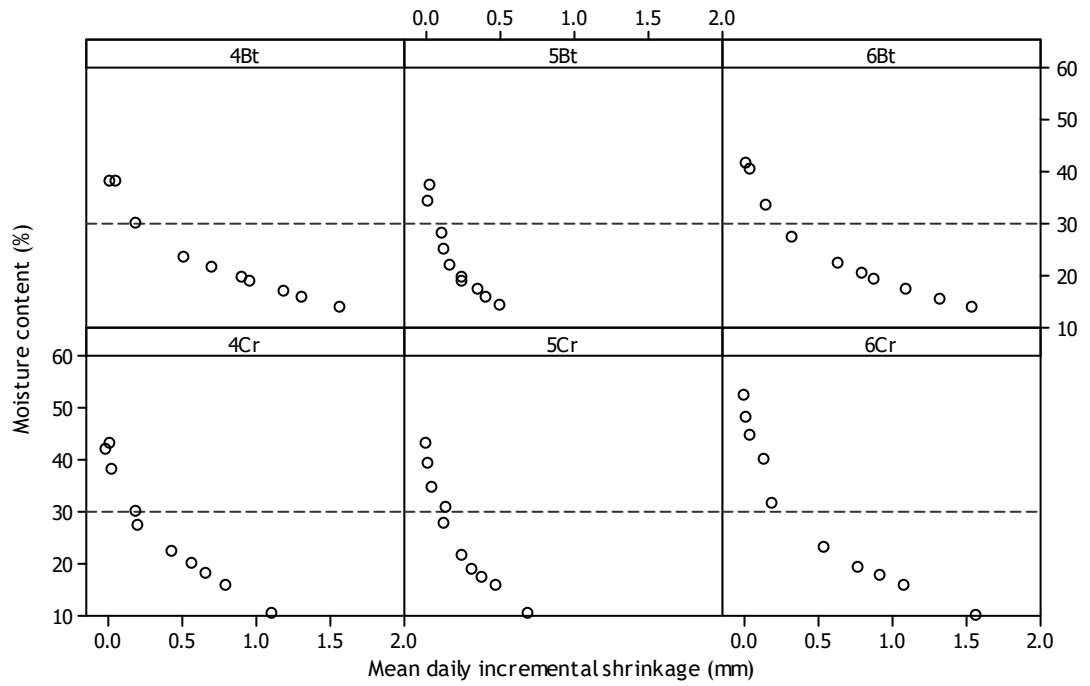


Figure 3.14. Scatter plots of moisture content against mean daily incremental shrinkage for trees 4 – 6 with butt log values in top panels and crown log values in lower panels.

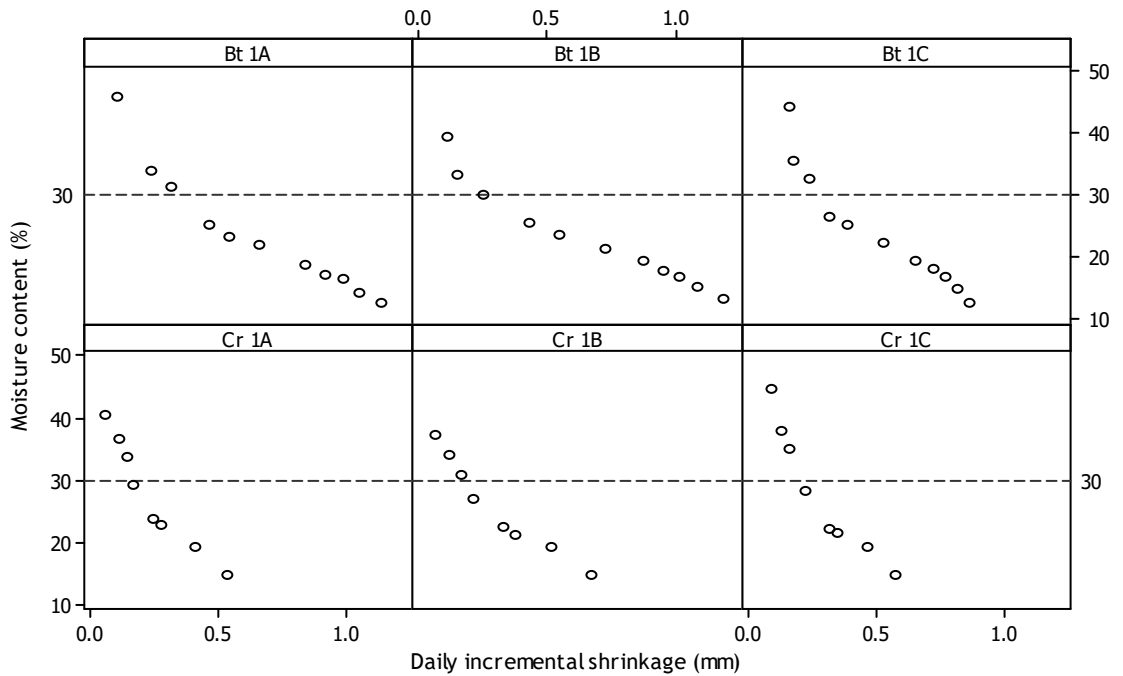


Figure 3.15. Tree 1. Scatter plots of moisture content against mean daily incremental shrinkage in individual battens by within log position. Top panels; butt log, position A – C. Lower panels; crown log, position A – C.

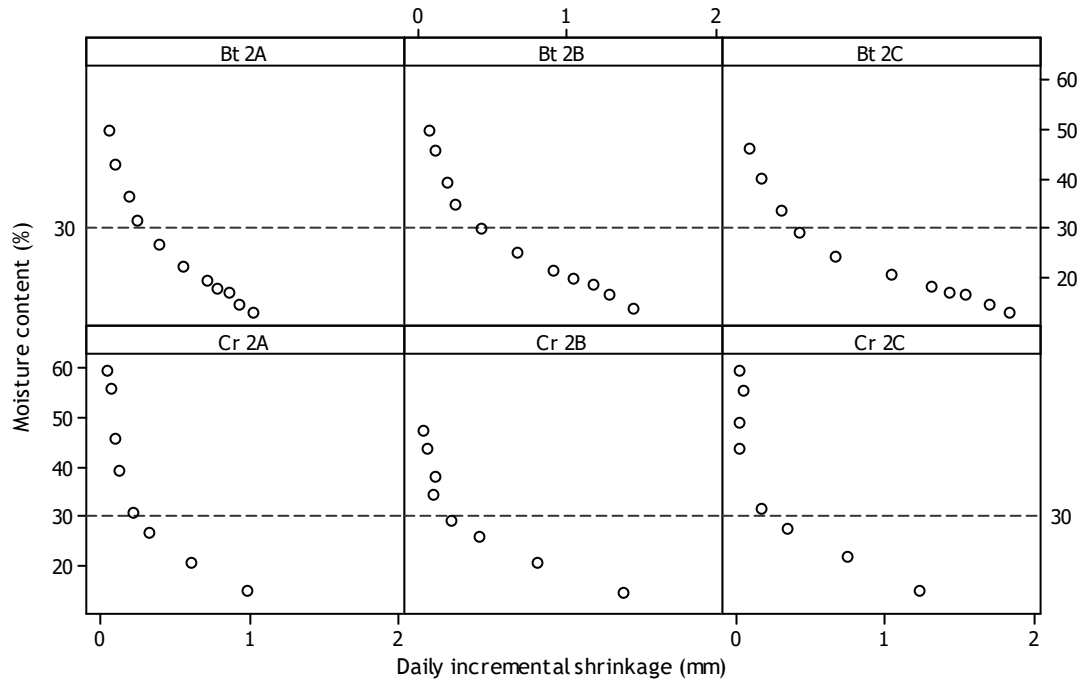


Figure 3.16. Tree 2. Scatter plots of moisture content against mean daily incremental shrinkage in individual battens by within log position. Top panels; butt log, position A – C. Lower panels; crown log, position A – C.

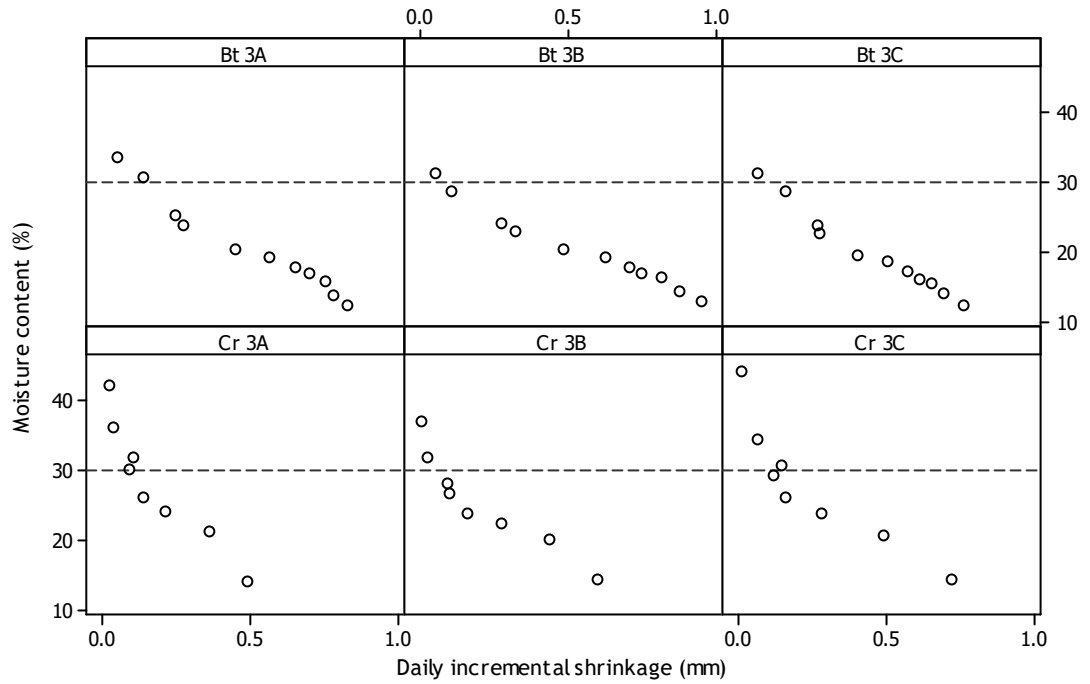


Figure 3.17. Tree 3. Scatter plots of moisture content against mean daily incremental shrinkage in individual battens by within log position. Top panels; butt log, position A – C. Lower panels; crown log, position A – C.

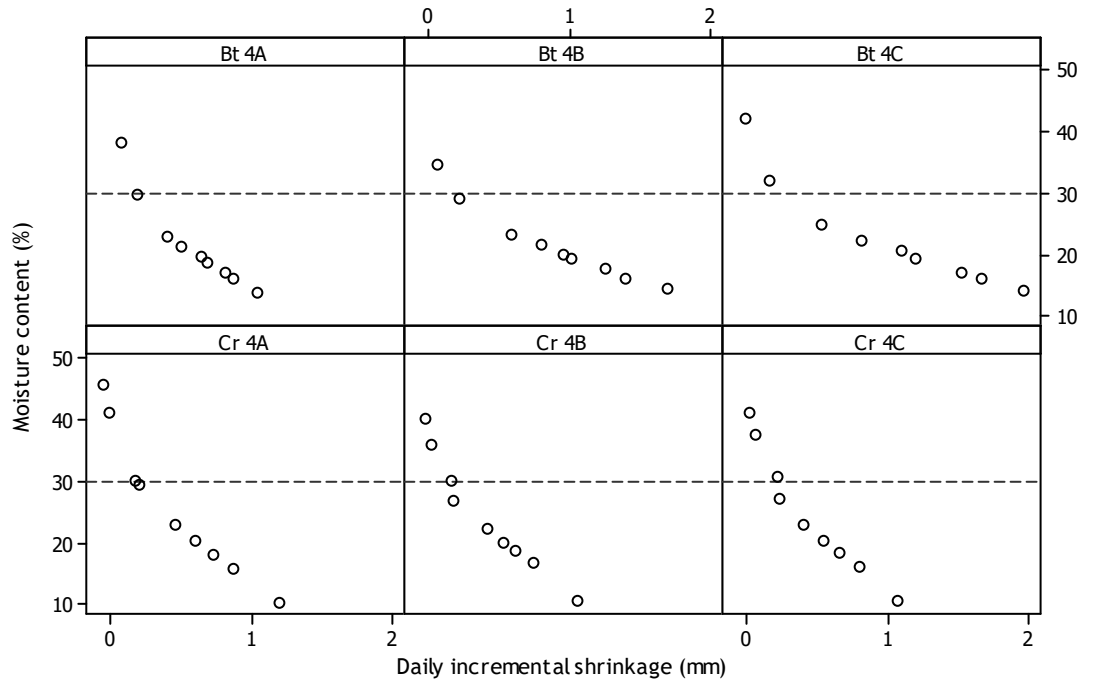


Figure 3.18. Tree 4. Scatter plots of moisture content against mean daily incremental shrinkage in individual battens by within log position. Top panels; butt log, position A – C. Lower panels; crown log, position A – C.

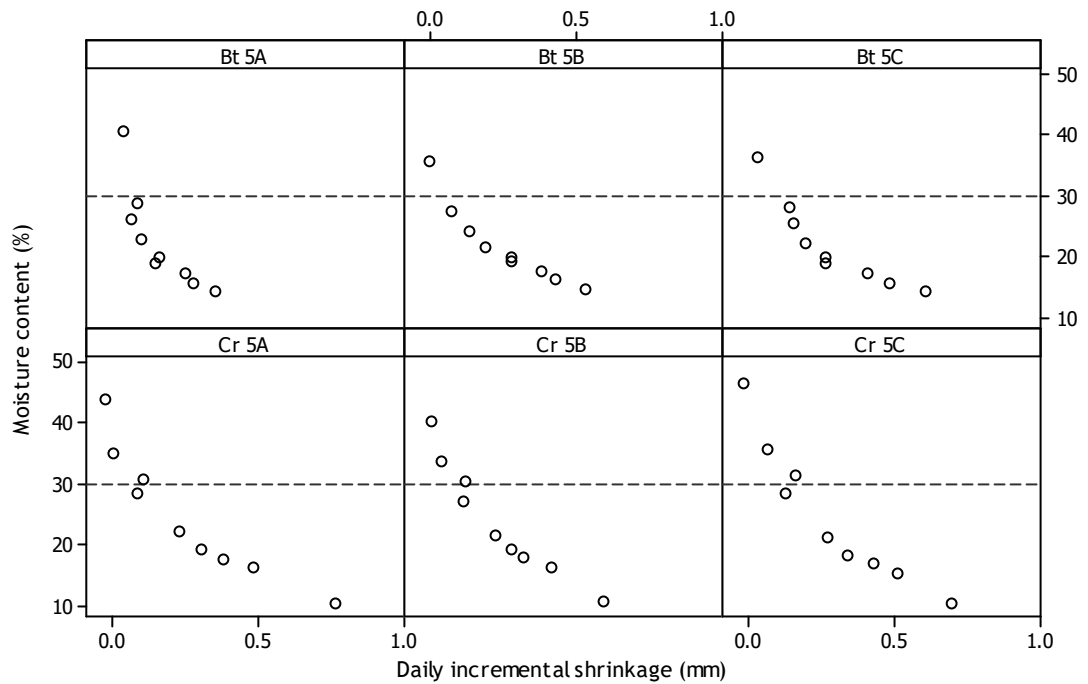


Figure 3.19. Tree 5. Scatter plots of moisture content against mean daily incremental shrinkage in individual battens by within log position. Top panels; butt log, position A – C. Lower panels; crown log, position A – C.

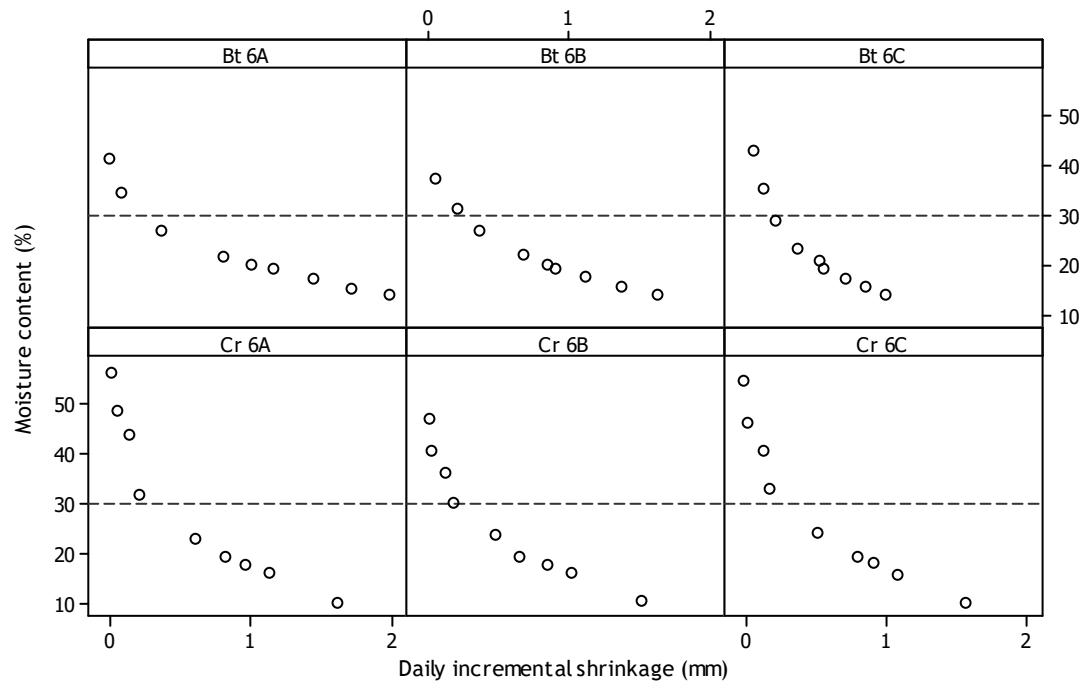


Figure 3.20. Tree 6. Scatter plots of moisture content against mean daily incremental shrinkage in individual battens by within log position. Top panels; butt log, position A – C. Lower panels; crown log, position A – C.

In most of the above charts there appears to be a break in the slope somewhere around the estimated line of fibre saturation point. It is also evident in many cases that some shrinkage is occurring well before the estimated fibre saturation point has been reached. The relationship between moisture content and longitudinal shrinkage is strong. Table 3.5 shows the Pearson correlation values for tree, log and position for trees 1-6.

Table 3.5. All Pearson correlation values for moisture content against longitudinal shrinkage taken from the estimated FSP and below. In all respects, the relationship between moisture content and longitudinal shrinkage is shown to be strong.

Tree #		1	2	3	4	5	6
Butt	A	-0.953	-0.956	-0.98	-0.95	-0.831	-0.935
	B	-0.97	-0.954	-0.986	-0.963	-0.934	-0.952
	C	-0.947	-0.947	-0.983	-0.928	-0.899	-0.93
	Mean	-0.957	-0.952	-0.983	-0.947	-0.888	-0.939
Crown	A	-0.949	-0.855	-0.933	-0.953	-0.92	-0.918
	B	-0.963	-0.889	-0.927	-0.962	-0.949	-0.926
	C	-0.943	-0.855	-0.889	-0.961	-0.936	-0.927
	Mean	-0.952	-0.866	-0.916	-0.959	-0.935	-0.924
Tree	Mean	-0.954	-0.909	-0.950	-0.953	-0.912	-0.931

### 3.3.3. Transverse shrinkage

Transverse shrinkage (i.e. radial and tangential) during drying is known to have an effect on dimensional stability (Barber and Meylan, 1964; Barber, 1968; Cave, 1972; Yamamoto, 1999, 2001). Longitudinal shrinkage is often considered as negligible. The relationship between the two directions of shrinkage is thought to be dependent on the variability of microfibril angle and the influence of compression wood (Skaar, 1988; Leonardon et al, 2010). Measurements of transverse shrinkage were carried out concurrently with those for longitudinal shrinkage to explore this relationship.

The B battens, sawn from the centre of the log, containing the pith, were measured on each face. The battens sawn from either side of the B battens, the A and C battens, were also measured on each face but their faces were differentiated as having annual rings that were closer to the pith or farther from the pith and are classified as inner and outer respectively. Mean values of total transverse shrinkage for trees 1-6 are shown in Figure 3.21.

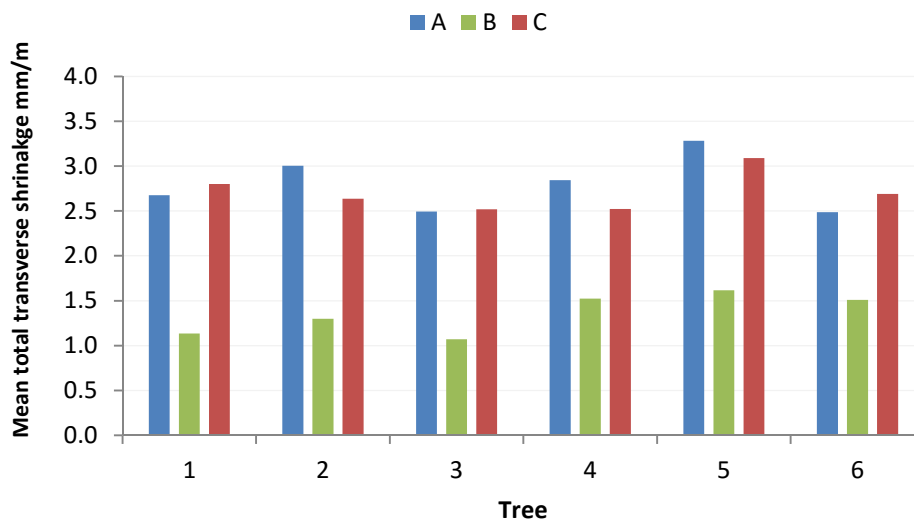


Figure 3.21 Columns show mean total transverse shrinkage for batten positions A, B and C for trees 1-6. Collectively the A and C batten values are on average 49.5% greater than the B battens. This difference is also statistically significant when tested (ANOVA one-way): in both A against B and C against B;  $p < 0.001$ .

Comparison of recorded values for shrinkage on the two faces measured on each batten is shown in Figure 3.22. This shows there was a little more shrinkage in the A and C battens on the inner faces but the differences are not statistically significant when compared with the outer faces. The standard deviation in each (A inner and outer and C inner and outer) is quite similar. The B battens (designated B1 and B2 to differentiate) have identical means and very similar standard deviation values.

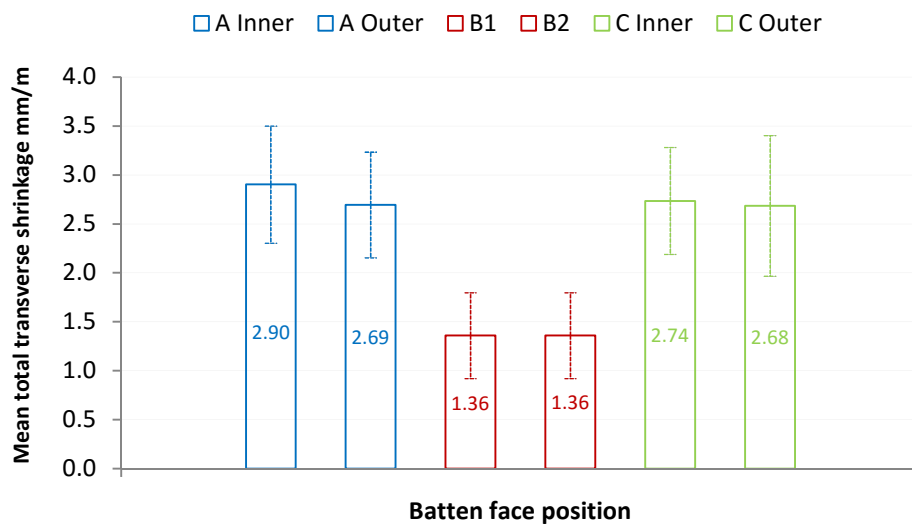


Figure 3.22. Columns show the collective mean values in mm/m for battens A, B and C for transverse shrinkage across the six measured faces with mean values displayed within the bars and error bars for one standard deviation either side of the mean.

### 3.3.4 Longitudinal shrinkage, transverse shrinkage and twist

Comparison of the shrinkage data from this experiment shows that transverse shrinkage is considerably greater than longitudinal in all samples (Moore, 2011). There is no discernible relationship between the two (correlation coefficient;  $r = -0.22$ ). A column chart of the mean values for each tree is shown in Figure 3.23.

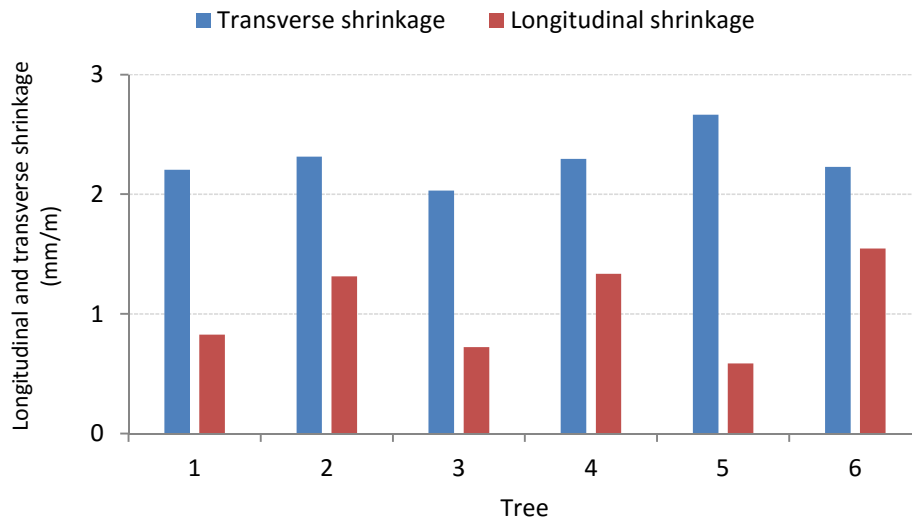


Figure 3.23. Mean values for longitudinal and transverse shrinkage for trees 1-6 in millimetres per metre.

Longitudinal shrinkage can be used as a predictor of between tree variation in twist. A plot of mean longitudinal shrinkage in millimetres per metre against mean degrees twist per metre for mean values of trees 1-6 at 8% moisture content is shown in Figure 3.24.

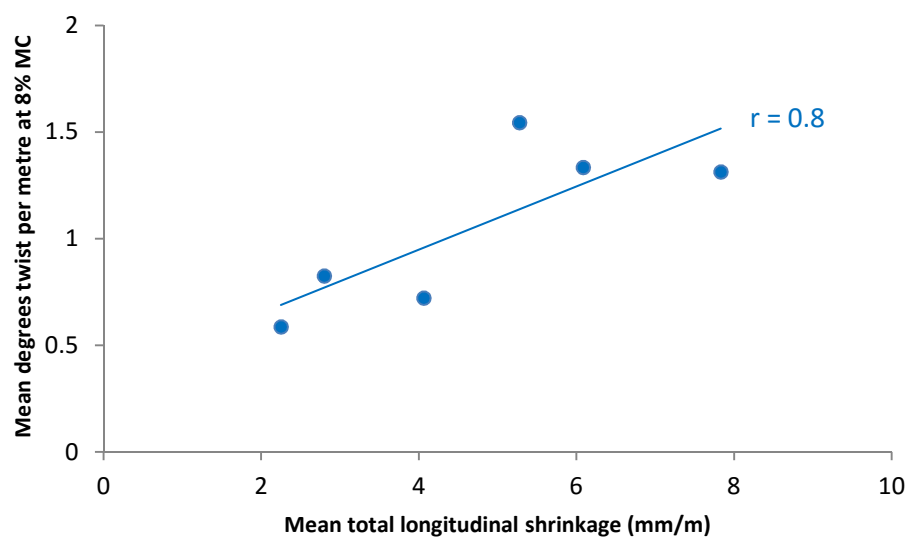


Figure 3.24. Scatterplot of mean total longitudinal shrinkage against mean degrees twist per metre at 8% moisture content for trees 1-6. Correlation coefficient,  $r = 0.8$ . The plot suggests a relatively strong positive relationship between the two of increasing twist with increasing longitudinal shrinkage.

This suggests a relationship exists between longitudinal shrinkage and twist when the mean values for all trees are compared. The correlation is reasonably strong ( $r = 0.8$ ) and shows a generally positive trend of increasing twist with increasing longitudinal shrinkage.

The transverse shrinkage results are similarly used to assess any positional variation between the A, B and C battens when compared with values for twist. In Figure 3.25 mean values for A, B and C battens for trees 1-6 are plotted against values for twist at 8% moisture content.

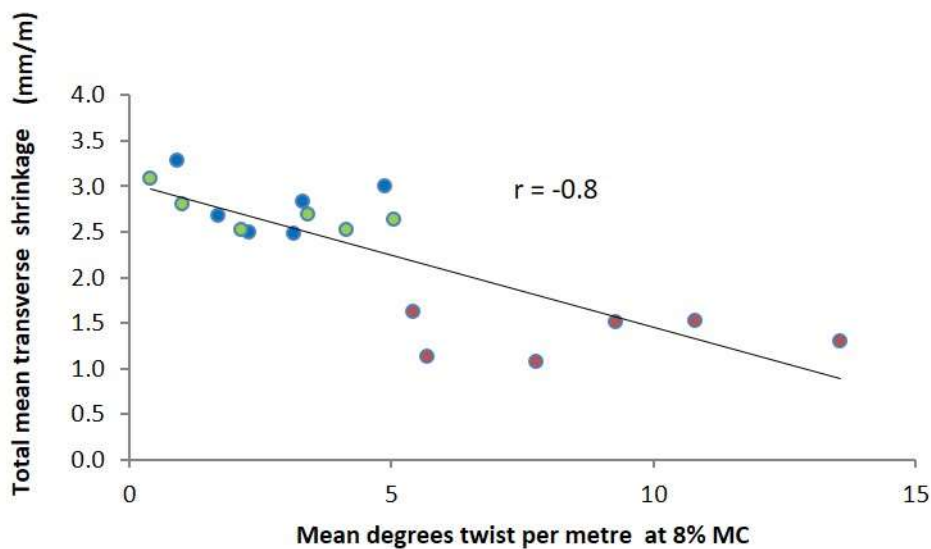


Figure 3.25. Scatterplot of degrees twist per metre at 8% MC against total mean transverse shrinkage across trees 1-6. Data points are segregated in to batten position; A-blue fill, B-red fill and C-green fill. The plot suggests a relatively strong negative relationship but this appears to be driven by the influence of the B battens and is not conclusive.

The general trend shows a reasonably strong negative relationship with an increase in twist at lower transverse shrinkage. However, when the position of the battens is taken into consideration the strength of this relationship appears to be part driven by the higher twist in the B battens. In this respect, any predictions of twist where position was not considered could provide erroneous results.

## 3.4 Discussion

### 3.4.1 Method

Longitudinal shrinkage is not routinely measured, especially on the large samples needed to quantify twist. Here, a method was developed to accommodate this which provided applicable data to suit this purpose. This experiment was carried out nine months after completion of the unrestrained drying experiment. The same samples were used to provide continuity between twist and longitudinal shrinkage. The samples had previously been dried to 8% moisture content. To fit with the method they had to be cut into three 1 m lengths and re-saturated. Re-wetting of previously dried material is complex. Drying will inevitably decrease permeability due to the closure of pits in the cell walls (Comstock et al, 1968). The resulting re-saturation may therefore not replicate the moisture content of the original green wood (Salin, 2011). Battens showed variable uptake of moisture between individuals. The mean re-saturated maximum moisture content was 43% over a range of 32 – 60%. In this respect the experimental results are based on an assumption of relative measured longitudinal shrinkage. Measurement was initially attempted on 3 m long battens but with twist spread over greater lengths it is difficult to differentiate the effect of this on individual measurements and between battens with differing degrees of twist. With the lengths reduced to one metre the effect was calculated to be negligible. This was established in the experimental trials of the method where the discrepancy due to twist was calculated at  $\pm 0.04$  mm and standard deviation between measurements based on this was 0.01mm. The measurement for transverse shrinkage was taken in a straightforward manner as a measurement across the faces of each batten perpendicular to the grain. The battens were divided into three categories; inner rings, outer rings and partially or wholly containing the pith. It does not define radial or tangential shrinkage as would normally be the case but it can be assumed that, due to the nature of the cutting pattern, the shrinkage on the outer face of the A and C battens would be more tangential in nature.

### 3.4.2 Variation in longitudinal shrinkage

Distortion in sawn timber is caused by anisotropic shrinkage of wood cells. This can be quantified in the transverse (radial and tangential) and longitudinal planes.

Transverse shrinkage is greater than longitudinal and perhaps for this reason is considered to have more influence on distortion. The relationship between the two directions of shrinkage is complex due to the anisotropic shrinkage of wood.

Longitudinal shrinkage has been shown to be related to microfibril angle (Donaldson, 2008, Yamashita et al, 2010). Microfibril angle is measureable by X-ray scattering or X-ray diffraction (Buksnowitz et al, 2008; Fernandes et al, 2011). In this work it was hoped that measurement of microfibril angle would be possible but unfortunately this was not achieved.

Longitudinal shrinkage was accurately measured with the aim of finding a relationship with twist. Transverse shrinkage was also measured but not defined in the more traditional radial and tangential context. Sawn timber will provide a variety of batten faces which exhibit both radial and tangential faces. Distinct classification, even with a relatively small sample size, is complex. In this experiment a more relative measure of transverse shrinkage is used. Batten faces were divided into the inner and outer categories detailed in 3.2.8. Measurements of width were then taken at intervals along the batten length.

The method for measuring longitudinal shrinkage produced good results considering the adaptations. Between tree variation in longitudinal shrinkage based on the mean of the six battens in each tree was significant (ANOVA one-way;  $p < 0.001$ ).

Variation between butt and crown logs, based on the mean of all butt log battens against the mean of all crown log battens showed greater shrinkage overall in butt logs (+21%) but did not prove statistically significant. When trees were tested individually two of the six show significant butt to crown variation in mean values; Tree 1 ( $p = 0.013$ ) and Tree 3 ( $p = 0.048$ ). The interquartile range in crown logs is on average smaller than that of butt logs. The interquartile range in butt logs is more varied across the six trees. In trees 4 and 6 this results in a large difference in butt to crown ratio (85% and 91% respectively). It may have been useful to have accurately measured the volume of juvenile wood in samples or to have had microfibril angle information available to explore these results further.

The mean shrinkage (all data) in each of the three positions is very similar, ( $A = 0.99\text{mm/m}$ ,  $B = 1.11\text{mm/m}$ ,  $C = 1.07\text{mm/m}$ ). The B battens show the largest butt to crown difference, 28%, compared with 14% and 20% for A and C respectively. That said and given that a higher microfibril angle would be expected closer to the pith, it may have been expected that the B battens would be shown to dominate the within log positional shrinkage in the butt and crown logs of individuals but this was not the case. In two thirds of the logs either the A or C battens were shown to have the greater shrinkage.

### **3.4.3 Longitudinal shrinkage and decreasing moisture content**

The assumption that fibre saturation point in Sitka spruce is expected to around 30% moisture content is generally verified by this work. In the plotted data to support this, a break in the slope at the marked 30% moisture content line is apparent in most cases. Some individual battens do appear to break at a slightly lower value around 25-30% moisture content. There is some evidence to suggest shrinkage occurring before fibre saturation point has been reached. Average shrinkage of 0.25 mm/m before fibre saturation point is measured across the six trees. This is possibly explained by more rapid drying on the surfaces of the battens which would induce a small amount of measurable shrinkage. It should also be noted that only the average moisture content of the batten is measured. Local differences are not accounted for and it is not considered that the average moisture content will reflect the average shrinkage. The FSP in any individual would always be subject to local variation and perhaps more so in this experiment where pre-dried battens were subjected to re-saturation. It is clear from observing the break of the slope where this effect ends and shrinkage below fibre saturation point begins. The relationship between moisture content and longitudinal shrinkage is strong. The mean Pearson correlation coefficient across the six trees is -0.93 over a range; -0.83 to -0.99.

### **3.4.4 Transverse shrinkage**

Shrinkage in the transverse direction has a direct association with distortion in the form of cup; deviation of a batten across its width on its widest face from edge to

edge. Its relationship with twist is more complex and as this work did not define the transverse shrinkage as specifically radial and tangential, it was uncertain if any meaningful relationship with longitudinal shrinkage would be found. As the cutting pattern used in this work tends to create surfaces that are generally more tangential in nature it could be considered that this is the dominant form of transverse shrinkage being observed. It has been shown that tangential shrinkage can be up to two times greater than radial (Moore, 2011). Both the outer and inner faces, further from the pith, were seen to shrink more than those containing the pith. This may be due to being subject to shrinkage of a more truly tangential nature. Closer to the pith shrinkage would have elements of a more radial or radial/tangential direction. Neither, however, can be defined as such in this situation and only distance from the pith is relevant. Outer shrinkage was greater by 97% and inner 107% when measured against battens containing the pith. Analysis of variance (ANOVA one-way) shows the between position differences to be significant; inner against centre;  $p < 0.001$ , outer against centre;  $p < 0.001$ . When compared with the values for longitudinal shrinkage, the average transverse shrinkage was 117% greater. Between tree differences of longitudinal and transverse shrinkage in this work show no consistent trend and no relationship between them could be found.

### 3.4.5 Shrinkage in relation to twist

When the mean degrees of twist for each tree at 8% moisture content is plotted against the measured values of longitudinal shrinkage in millimetres, they show a positive relationship which returns an correlation coefficient value of 0.8. This result was better than expected and shows a genuine relationship between longitudinal shrinkage and twist.

A plot of all transverse shrinkage against twist at 8% moisture content demonstrates the opposite trend to that of longitudinal shrinkage; a negative relationship with greater twist occurring at lower levels of shrinkage ( $r = 0.8$ ). However, this effect is exaggerated by the lower transverse shrinkage in the B battens when position is viewed in isolation.

A measureable relationship between longitudinal shrinkage and twist could have practical applications for the assessment of timber at the commercial level. The

method used here would not be appropriate therefore a simpler and faster technique would be required. In the following chapter the relationship between longitudinal shrinkage and acoustic velocity measurements is discussed and this could be a suitable application more suited to a commercial environment.

Further exploration of the relationship between longitudinal shrinkage and transverse shrinkage would add to the better understanding of this concept as would additional research into the nature of transverse shrinkage; i.e. the ratios of radial to tangential shrinkage and the influence of microfibril angle.

## **4. Acoustic velocity**

### **4.1 Introduction**

One of the key mechanical properties of wood to be considered when determining grading class is the dynamic modulus of elasticity (MoE) or dynamic stiffness. This value is essentially a measure of the load bearing capacity of the material and can have implications for in-service uses.

MoE and longitudinal shrinkage are both dependant on microfibril angle but in opposite directions. Longitudinal shrinkage is not routinely measured in commercial practice. The possibility that there may be a connection between twist and longitudinal shrinkage is explored in Chapter 3.

Measured acoustic velocity (AV) is more directly related than MoE to microfibril angle as it is not dependent on density. It has been suggested that measurement of AV could serve as a potential predictor of microfibril angle (Fries et al, 2014). It is therefore possible that measured AV or AV calculated from MoE may be used as a predictor of the potential contribution of longitudinal shrinkage to twist in relation to microfibril angle. In this chapter measured values of AV are presented and relationships with other properties are explored.

### **4.2 Methods and materials**

#### **4.2.1 Samples**

Measurements of acoustic velocity, to determine MoE, were taken concurrently with all other dimensional measurements from the 36 samples in the unrestrained kiln drying experiment. Samples were initially measured prior to drying, when the samples were in a near green state. They were subsequently measured immediately after each drying target was reached; at 20%, 15% and 8% moisture content.

### 4.2.2 Equipment

Non-destructive tools used to measure acoustic velocity are becoming an increasingly popular method of quantifying MoE (Auty and Achim, 2008; Chauhan et al, 2013). In this experiment a Hitman HM200, manufactured by fibre-gen, Christchurch, New Zealand was used (Figure 4.1). This is a portable, hand held device which can be used in a variety of settings. It functions as follows. Prior to operation, a measured value for the sample length is entered into the tool keypad and set. The Hitman is then held against one end of the sample, engaging a sensor capable of detecting vibration as a resonant frequency signal. This signal was produced by tapping the opposing longitudinal end of the sample with a hammer. The hammer tap is normally applied at the same end as the tool is held in place and is therefore suited to one person operation, as shown in Figure 4.1. In this work, given the dimensions of the battens, the space taken up by the sensor on application limited the available space to connect fully with the hammer head. Therefore, the method was adapted to employ the opposing end for this purpose. The validity of the results were tested by carrying out both methods on logs and in all cases the same result was returned. The hammer tap causes the batten to resonate, with a plane wave moving back and forth along the batten (Carter et al, 2006). A reading of acoustic velocity in kilometres per second (km/s) is then registered on the unit LED display. The reading is based on the equation;  $\text{acoustic velocity} = \text{length}/\text{travel time}$ . The process is repeated until three corresponding values are registered.



**Figure 4.1.** Hitman HM200. Left; keypad for inputting length data and LED display, right; tool in operation, sensor is held against the log and a tap with a hammer produces the required signal.

### 4.2.3 Calculation of modulus of elasticity

The dynamic modulus of elasticity (MoE) was calculated using the values for acoustic velocity squared ( $AV^2$ ) measured by the Hitman HM 200 ( $\text{km}^2/\text{s}^2$ ) and the sample density ( $\text{kg}/\text{m}^3$ ). Sample density ( $D$ ) was calculated for each sample from the mass in kilograms ( $M$ ) and the means of the measured dimensions (width, ( $w_m$ ), depth ( $d_m$ ) and length ( $l_m$ )) in millimetres as shown in Equation 4.1. As the acoustic velocity results will be affected by the moisture content of the sample, the sample density at green moisture content is conventionally assumed to be  $1000 \text{ kg}/\text{m}^3$ . The calculation for MoE in gigapascals (GPa) is shown in Equation 4.2.

$$\text{Equation 4.1} \quad D = M / (w_m \times d_m \times l_m) * 10^9$$

$$\text{Equation 4.2} \quad \text{MoE} = (D \times AV^2) / 1000$$

## 4.3 Results

### 4.3.1 Modulus of elasticity

The calculated MoE for trees 1-6 are presented in Table 4.1. These are shown as the mean values of all six battens from each of the six trees. Scatterplots for the calculated MoE against  $AV^2$  only are shown in Figure 4.2, for all six trees at each drying target. Correlation coefficients between  $AV^2$  and MoE are strong at all moisture content targets and consistent with changes in density. Therefore, MoE can be used as a proxy to determine  $AV^2$  values at a fixed moisture content.

Table 4.1. Dynamic modulus of elasticity (MoE) values for trees 1-6 at each drying target.

Tree	Green	20%	15%	8%
1	7.20	7.44	7.86	8.31
2	6.09	6.75	7.02	7.48
3	7.95	8.55	8.74	9.57
4	6.00	6.51	6.62	7.26
5	8.76	8.69	9.36	10.49
6	5.11	5.60	5.77	6.22

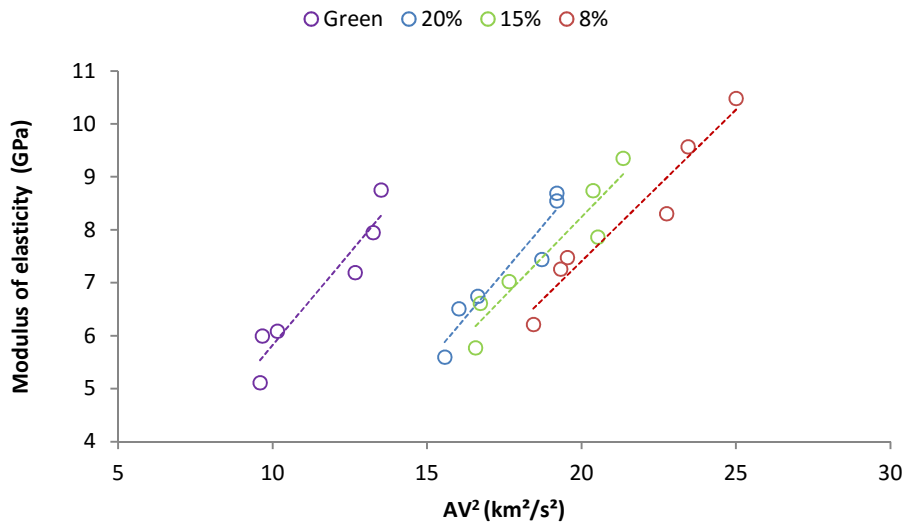


Figure 4.2. Scatterplots of acoustic velocity (AV<sup>2</sup>) from Hitman values against MoE for trees 1-6 at all four drying targets. Relationship between the two categories demonstrates that AV<sup>2</sup> values have a consistent relationship with MoE which correlates consistently with changes in density. MoE: AV<sup>2</sup> Correlation coefficients; r = 0.95 at green, 20% and 15% MC targets and 0.97 at 8% MC.

### 4.3.2 Twist and acoustic velocity

All measurements for twist and AV were taken concurrently at each drying target. It is therefore possible to make direct comparison between the two. The values for twist used in this section are amended to demonstrate their compatibility with European standard EN 1310:1997 (CEN, 1997). Values are reported as twist in mm per 25 mm width over 2 m length, the limits for twist in C16 and above construction grade timber. Given the good correlation between MoE and  $AV^2$  it may be useful to consider either as a relative measure of the other when comparing with twist. This could provide for a simple and fast method for assessing the end use of green timber by processors prior to drying. Figure 4.3 shows the measured values for twist against acoustic velocity at each of the three drying targets with a line drawn at the 2 mm twist/25mm width/2m length limit for C16 and above graded timber.

From the data shown in Figure 4.3 it is possible to construct a basic predictive model based on  $AV^2$  values. This is shown in Figure 4.4. The calculation for the slope is shown in Equation 4.1.

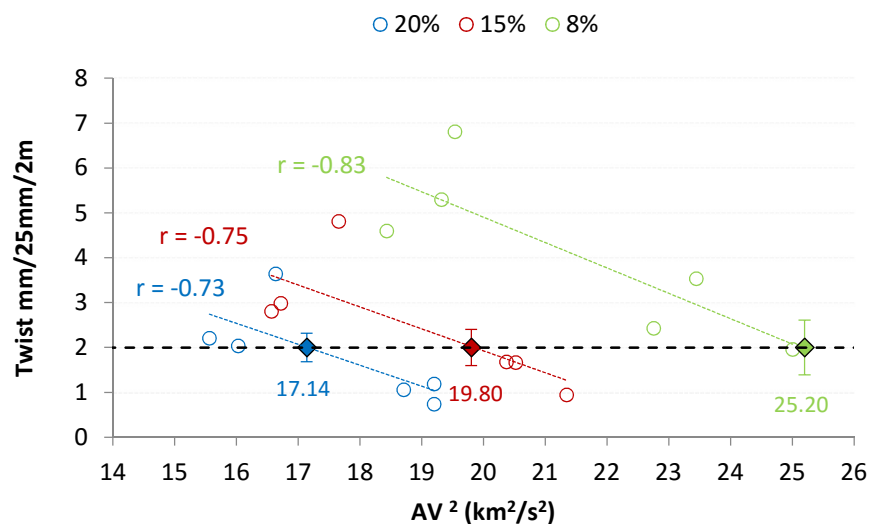


Figure 4.3. Twist against acoustic velocity squared ( $AV^2$ ) at three drying targets. The trend lines are based on the mean values in both categories from six battens in each tree (1-6) at 20%, 15% and 8% moisture content with colour coded correlation coefficient value ( $r$ ) shown for each plot. The dotted line at 2mm on the y axis represents the limit for C16 and above graded timber. The  $AV^2$  threshold value for each drying target is shown by a diamond marker with error bars for the 95% confidence interval and the calculated threshold value shown below.

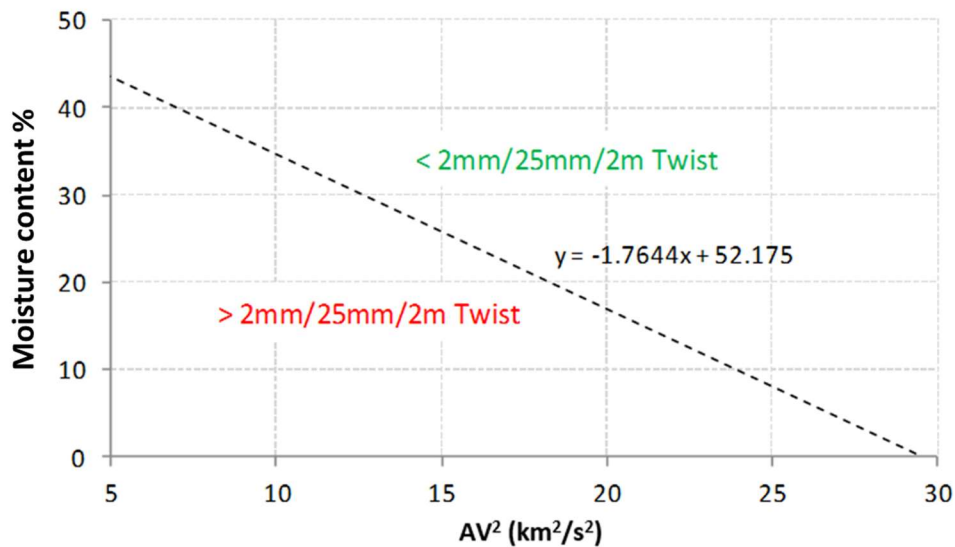


Figure 4.4. Basic predictive model of acoustic velocity values to estimate twist grading of timber by moisture content from measured values in this work and based on twist specifications in BS EN 14081 and EN 338 grading standards. Dotted line represents threshold values of AV<sup>2</sup> at 2mm/25mm/2m of twist with values above the line graded in the C18 or below classification. This line is calculated from the slope of values recorded experimentally at green, 20, 15 and 8% moisture content.

$$\text{Equation 4.1} \quad x = (mc - 52.175) / -1.7664$$

Where;  $mc$  = moisture content

The remaining values are a reworking of the slope of measured values of AV<sup>2</sup> to obtain  $x$

$$\text{Slope } y = -1.7664x + 52.175$$

The values in Figure 4.4 represent an extrapolation of the values measured in this work. To repeat this experiment with a larger sample size may improve the reliability of this example as a potential working model.

### 4.3.3. Longitudinal shrinkage and acoustic velocity

Values of longitudinal shrinkage were obtained from a later experiment, after twist had been established, where the battens were reduced to 1m lengths, re-saturated and then allowed to dry in ambient conditions (see Chapter 3). An exactly concurrent comparison between longitudinal shrinkage and MoE or AV is therefore not possible. However, the same samples were used and to this end the trend in longitudinal shrinkage is presented here and compared to the AV values gathered previously.

Figures 4.5, 4.6 and 4.7 show scatter plots of longitudinal shrinkage against  $AV^2$  ( $\text{km}^2/\text{s}^2$ ) for trees 1-6, the same data segregated into butt and crown logs and a positional comparison of the A, B and C battens for trees 1-6 respectively. The longitudinal shrinkage data presented are the final cumulative values of total longitudinal shrinkage. As the mean final moisture content was 14.84% the AV values recorded at 15% moisture content are used to compare like for like as far as is possible.

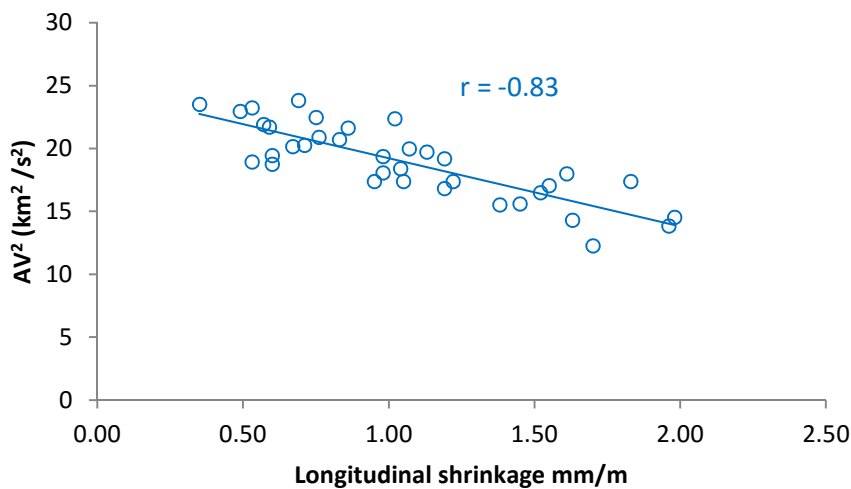


**Figure 4.5.** Scatter plot of all thirty-six battens; longitudinal shrinkage against  $AV^2$  at approximately 15% moisture content shows a strong negative relationship of increasing longitudinal shrinkage with lower values of  $AV^2$ .

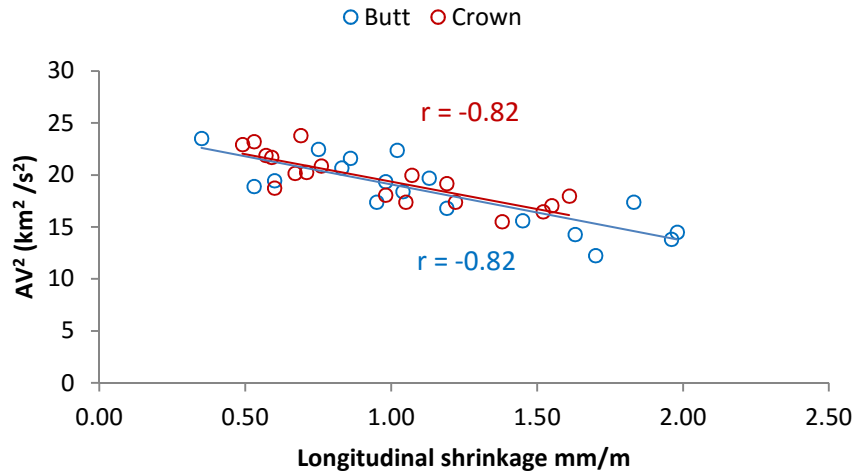


Figure 4.6. Scatter plot of butt log and crown log values for all thirty-six battens; longitudinal shrinkage against AV<sup>2</sup> at approximately 15% moisture content. The plots show a similar relationship and R<sup>2</sup> values to that in Figure 4.5 (all battens). Shrinkage in some butt battens is a little higher at similar AV<sup>2</sup> values as those shown in crown battens.

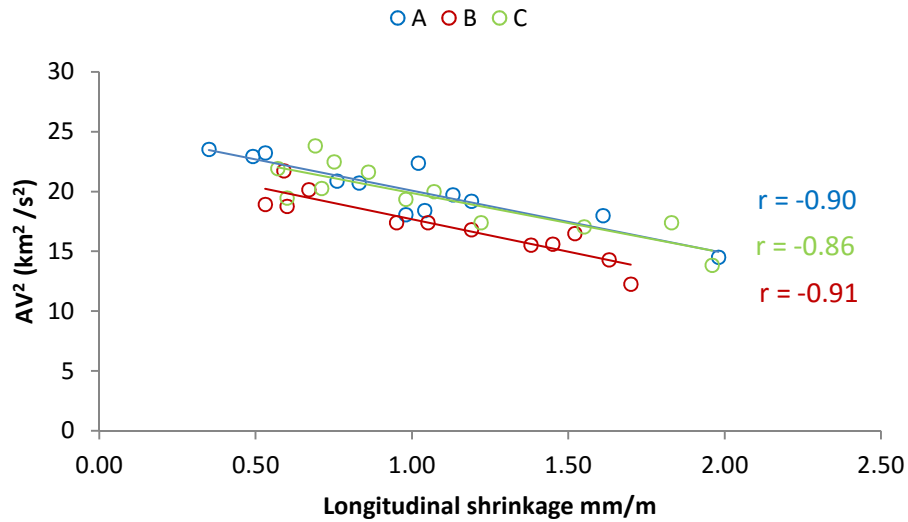


Figure 4.7. Scatter plot of battens by position, A, B and C for all thirty-six battens; longitudinal shrinkage against AV<sup>2</sup> at approximately 15% moisture content. When segregated by position the individual r values suggest a stronger relationship than show in Figure 4.5 for all battens collectively. Greater shrinkage and a larger range is recorded in the outer battens (A and C) than the centre battens (B).

#### 4.4 Discussion

Agreement between the observed readings of acoustic velocity obtained from the Hitman HM 200 and measured MoE shown in Figure 4.2 suggests that values of acoustic velocity could be useful as a predictive tool in a commercial setting (correlation coefficient at 20% MC  $r = 0.95$ ). This compares with other work in this area by Kennedy et al (2013) and Chen et al (2015) who found correlation coefficient values ( $r$ ) between  $AV^2$  and MoE of 0.73 and 0.50 respectively when using similar hand held tools on standing trees. The improved result from the relationship in this work may be attributed to the smaller and more compact volume of each sample and the fact that the battens can be tested from the ends, giving a direct path for the stress wave (Mochan et al, 2009). The decreased moisture content, which was around 15% when the measurements presented were taken, may also be a factor.

The outcome of the relationship between  $AV^2$  and twist was perhaps more surprising (Figure 4.3). Moderate to strong relationships were found with twist at all of the three drying targets 20, 15 and 8% MC ( $r = 0.73, 0.75, 0.83$  respectively). The relationships became stronger with decreasing moisture content; perhaps as a consequence of this, and the effect of microfibril angle. The values either side of the fixed line showing the limit for timber graded at the C18 or below classification show broad agreement with the similar representation in chapter 2 (Figure 2.27). By modelling the values for twist and moisture content from the slope of the measured data it is possible to construct a grading boundary based on values of  $AV^2$  (Figure 4.4). However, given the small sample size used in this work and the lack of applicable grain angle and microfibril angle data further investigation would be required, and it could be suggested that in principle, a successful model based on these properties could be of value to the processing industry.

The plots of  $AV^2$  against longitudinal shrinkage show good agreement and a negative relationship of greater longitudinal shrinkage with decreasing  $AV^2$  values. When the battens are separated into butt and crown categories the  $r$  values are similar in both although shrinkage is seen to be higher in butt logs at lower values of  $AV^2$ . The relationship is a little stronger when battens are separated by radial position. The A and C battens, sawn further from the pith demonstrate a very similar trend. The B battens,

containing the pith, record lower values of  $AV^2$ . This may be an effect of larger microfibril angle closer to the pith but this is not fully understood and this effect would again benefit from further investigation.

If longitudinal shrinkage can be regarded as being closely linked to microfibril angle, it is possible that acoustic velocity data could be a valuable asset in predicting the development of twist. This would involve a model based on a considerable number of measured longitudinal shrinkage values in relation to their  $AV^2$  equivalents and actual data on microfibril angle. Given that  $AV^2$  and MoE have strong relationship at green moisture content ( $r = 0.95$ , Figure 4.2) it may be considered that good estimates could be obtained from freshly sawn timber.

## 5 Grain angle

### 5.1 Introduction

Grain angle, particularly spiral grain angle, can have implications for the quality of sawn timber. The influence of spiral grain is regarded as a fundamental reason for the development of twist in sawn timber (Haslett et al, 1992; Danborg, 1994; Straze et al, 2011). The grain angle is known to change with radial distance from the pith and with height (Northcott, 1957; Harris, 1989). It is also known to change direction; left handed (S) to right handed (Z) or vice versa with distance from the pith and with height. Conifers appear to initially grow in the left hand direction and change to right handed grain angle with age (Kubler, 1991; Gjerdrum et al, 2002). In younger trees this reversal is not always achieved. Genetic heredity has also been shown to have an effect on grain angle (Fonweban et al, 2013) as have environmental factors (Sall, 2002). Grain angle can be difficult to measure as a 'normal' pattern of grain angle is difficult to define (Harris, 1989b).

In this experiment discs were removed from the trees used to produce sawn timber for the unrestrained drying experiment reported in Chapter 2. Grain angle was measured and the results are explored with the aim of establishing the relationship between the nature of the spiral grain and twist. Problems with the chosen methods and samples limited the scope of these aims but the process does highlight the complexity of grain angle measurement.

### 5.2 Methods and Materials

#### 5.2.1 Samples and sample preparation

Six commercially grown Sitka spruce trees were felled at Spadeadam forest North West of Carlisle, Cumbria, UK (55.04.32 N/ 2.36.44 W, Alt 348m). Trees were selected for their straightness and comparable DBH but otherwise randomly. Mean DBH at 1.3m was 32.15cm across the six trees with a standard deviation of 1.74cm. At the time of felling the samples were approximately 37 years old (planted 1975, felled May 2012).

After felling, logs were sawn into two sections (butt end and crown end) of approximately 4m. At this point, three discs were removed; one from the base of the butt end, one from the centre at the area of the divide between logs (~ 4m) and one from the upper section of the crown end but short of the true crown. Mean disc diameters were recorded as 36.2, 23.9 and 21.9cm respectively. Discs were removed by chainsaw at approximately 2-3 cm thickness with their surfaces sawn as flat as possible. The discs were bagged and sealed to preserve green moisture content and transported on the same day to the University of Glasgow and stored in a cold room at 2°C. Before this experiment the discs were air dried in a laboratory for 14 days (temperature;  $21 \pm 2.5^\circ$ , RH%;  $58 \pm 11\%$ ). The mean moisture content prior to measurement was 12.1%.

Discs were split into two sections for the purpose of grain angle measurement. After drying, some of the discs were found to have developed cracks. In these cases the discs were split as a continuation of the crack. Discs that had remained intact were split along areas which were visibly free from knotting, branching or unusual ring patterns. Discs considered knot free with a regular grain pattern were split along a randomly chosen plane (Figure 5.1).

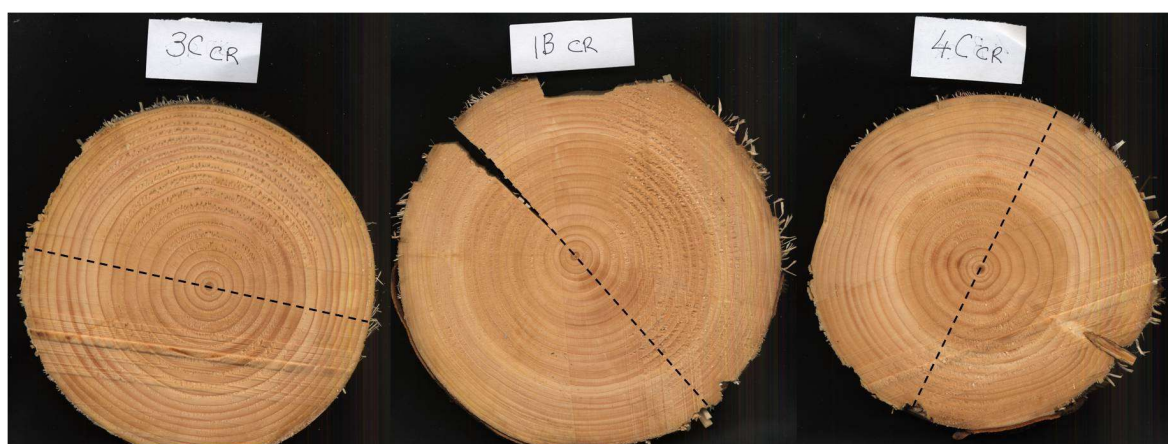


**Figure 5.1.** Splitting of discs based upon post drying condition. Split across diameter shown by dotted line. Disc 3C shows no evidence of cracking and is free from knotting or branching and was split randomly across its diameter. Disc 1B had developed a crack during drying and split was made as a continuation of the crack. Disc 4C has a protruding branch which will influence the regularity of the grain pattern. In this case the split was made away from this area.

To split the discs a line was marked on the surface, through the pith, where the split was required. The disc was then clamped firmly to a stable workbench with a metal bar along the marked line. The protruding side of the disc was then tapped with a rubber mallet until a crack developed along the desired area. The protruding half could then be removed by

pushing gently downwards by hand. After splitting, the crosscut surfaces along the edge were lightly sanded by hand to expose the ring pattern where required and each ring was marked at this edge to ensure repeatability of measurements.

### 5.2.2 Measurement

The method of measurement is based on experiments conducted by Marvou (2007) which was in turn modified from Tranquart (1995). Grain angle was measured using an angle finder. This was set in a pair of retort stands and fixed firmly to a workbench with a series of clamps until no movement of the apparatus was possible. With the section containing the LED measurement display secured, the measuring arm was positioned to be pointing downwards, towards the bench at  $90^\circ$ . A worktop with guide lines was placed on the workbench surface below the measuring arm with enough space for the arm to swing to and fro unrestricted. A desk lamp was placed to the rear of the apparatus to assist with precision of measurement (Figure 5.2).

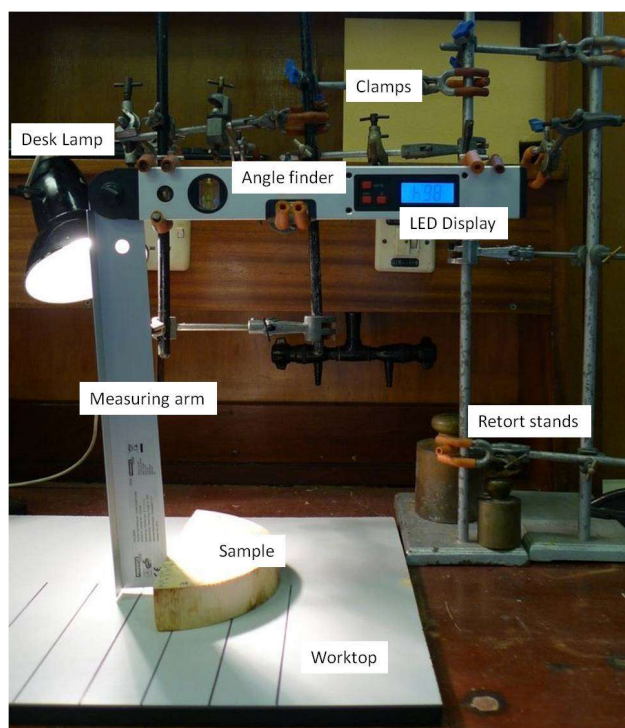


Figure 5.2. Labelled diagram of angle finder and associated apparatus used for grain angle measurement

To measure, the disc was placed on the worktop in line with one of the guide lines. The arm of the angle finder was pushed against the face of the disc until the narrow, flat edge of the angle finder arm was flush against the vertical length of the disc. The light from the desk lamp was positioned to shine towards the area of contact between the sample and angle finder arm. The exclusion or equivalence of the light generated along the line of contact was used to determine accurate positioning. This was repeated three times for each ring and the mean of the three replicates was recorded. The process was repeated for the opposing face of the split on the other half of the disc.

### 5.2.3 Determination of grain angle

An angle was measured for each ring on both halves of the split disc. The angle of the face on either side of the split differed in that the angle on one half was greater than  $90^\circ$  and on the other less than  $90^\circ$  when measured on the angle finder (Figure 5.3). The angle was determined by subtracting 90 from the measured angle on face A and subtracting the measured angle from 90 on face B. The average of these two values was regarded as the mean grain angle for that ring.

The question of the measured grain angle in relation to a regular longitudinal point of axis must be considered. As the location of the pith of the tree tends to be irregular with height (pith wander) it cannot be considered as a consistent point of reference. In this work, where large sections of the tree were missing between discs, this was a particular concern. It was therefore necessary to establish a point of reference. To achieve this, the mean of the grain angles from either side of the pith, normally positive on one side and negative on the other, was assumed as the 'zero point'. Each individual ring value, either side of the pith, was then expressed relative to the 'zero point'. This corrects for any misalignment of the faces of the disc with the plane at right angles to the axis of the tree, without assuming that the pith is in line with the tree's axis. Figure 5.4 shows the original measured values for grain angle and the adjusted values tailored to accommodate the "zero point".

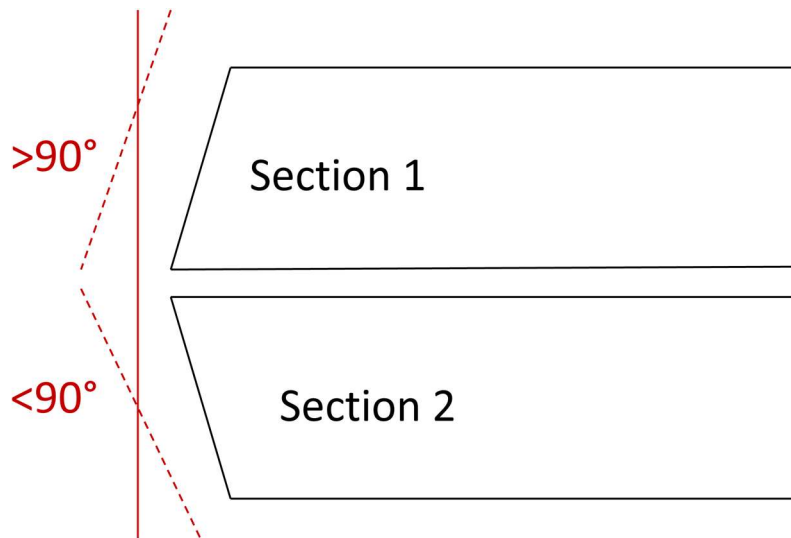


Figure 5.3. Two halves of a split disc; Section 1 and Section 2. Splitting a disc rarely produces two faces with equal angles of  $90^\circ$ . A split would usually create two opposing angles as demonstrated above; one greater than  $90^\circ$  for Section 1 and one less than  $90^\circ$  for Section 2. The solid red line represents the measuring arm of the angle finder at  $90^\circ$  and the dashed red lines, the angle of measurement for each face. The grain angle for each ring is determined as the measured angle minus  $90$  in Section 1 and  $90$  minus the measured angle in Section 2.

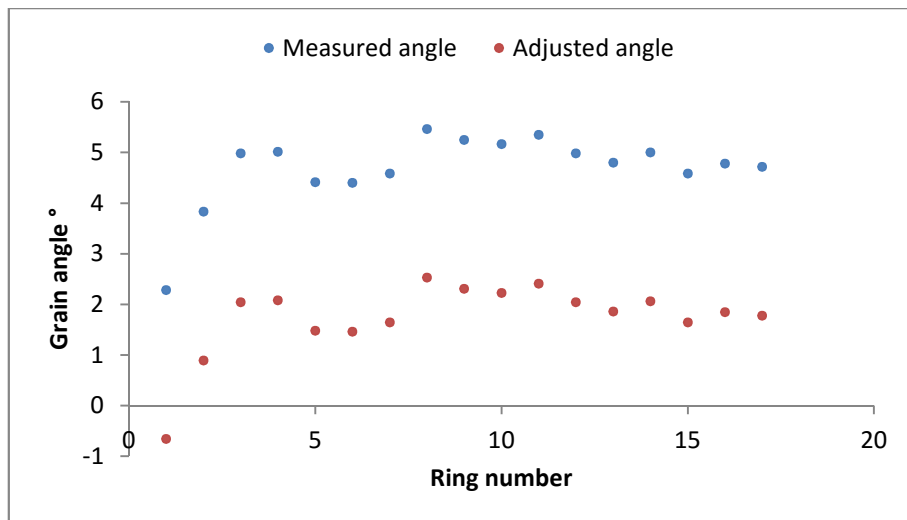


Figure 5.4. Before and after adjustment of measured angle from the butt disc of Tree 1 to create a “zero point”

After adjustment, the reciprocal values for each ring on either side of the pith were averaged to obtain a mean radial value which is considered as representative of the grain angle for the corresponding annual ring.

## 5.3 Results

### 5.3.1 Agreement between measurements

Although three discs from each of the six trees in this experiment were used, the results from tree 6 have been excluded from some sections due to the presence of knots and the general poor condition of two of the three discs. The surfaces of the half discs were often buckled or uneven and this made measurement impossible. For this reason some of the measurements were made on the faces of split battens which reduced the radial profile. For the remainder of the discs, agreement between the reciprocal faces of the opposing half discs was good. The scatter plot in Figure 5.5 shows the relationship between the measurements on the two reciprocal faces of each disc from all the data collected.

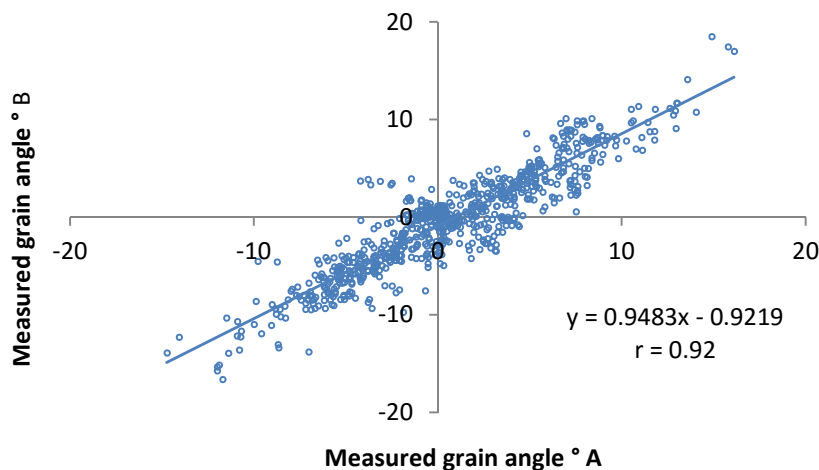


Figure 5.5. Scatter plot of all measurements taken on reciprocal faces of each half disc; Face A and Face B. The relationship is strong; correlation coefficient;  $r = 0.92$ .

It should be noted however, that the within disc variation between values was considerable in some cases, particularly in the butt discs. This may be in part due to the discs being cut from an area where the basal flare was still evident causing the grain angle to be less regular in the radial direction. A column chart of the standard deviation of variation for each disc is shown in Figure 5.6.

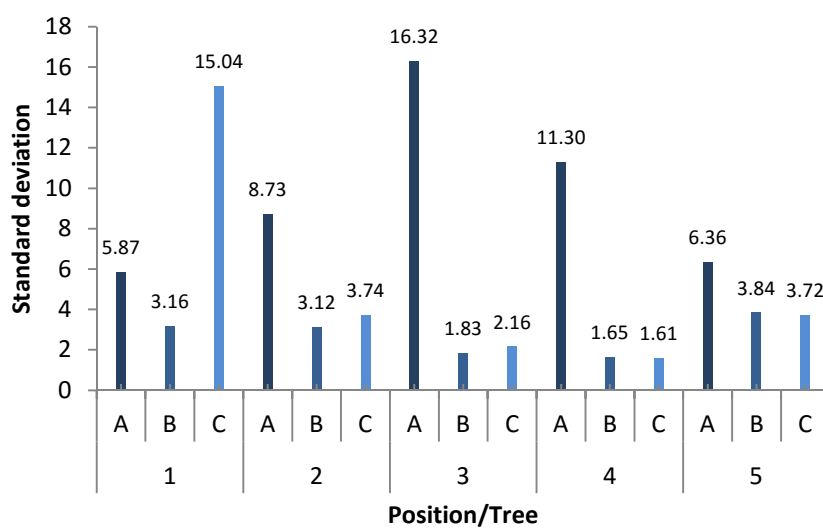


Figure 5.6. Standard deviation of variation between measured opposing angles in each disc. Disc positions; A butt, B centre, C crown. Value for one standard deviation in degrees is shown above column.

Generally the butt discs show the largest standard deviation, perhaps due to the basal flare or the greater number of rings available for comparison. The lower values in the centre and crown discs may suggest this is the case. The pattern in Tree 1 differs significantly from the others. Some minor twisting along the face of the C disc may have been responsible for this.

### 5.3.2 Grain angle values

Values of grain angle are presented for each disc. In some cases the values of the three discs from each tree are averaged and given as the grain angle value for tree. However, the distance between discs prevents any realistic estimation of grain angle for the whole tree. It is also not practicable to consider any defined relationship between the grain angles and the

values for twist obtained from the same samples. This is due to the way the sampling process was conducted; i.e. discs were only taken from either end of each log in order that intact 3m battens were available for the drying experiment. There is however some indication of possible trends between grain angle and twist. Figure 5.7 displays the grain angle values for each of the discs individually.

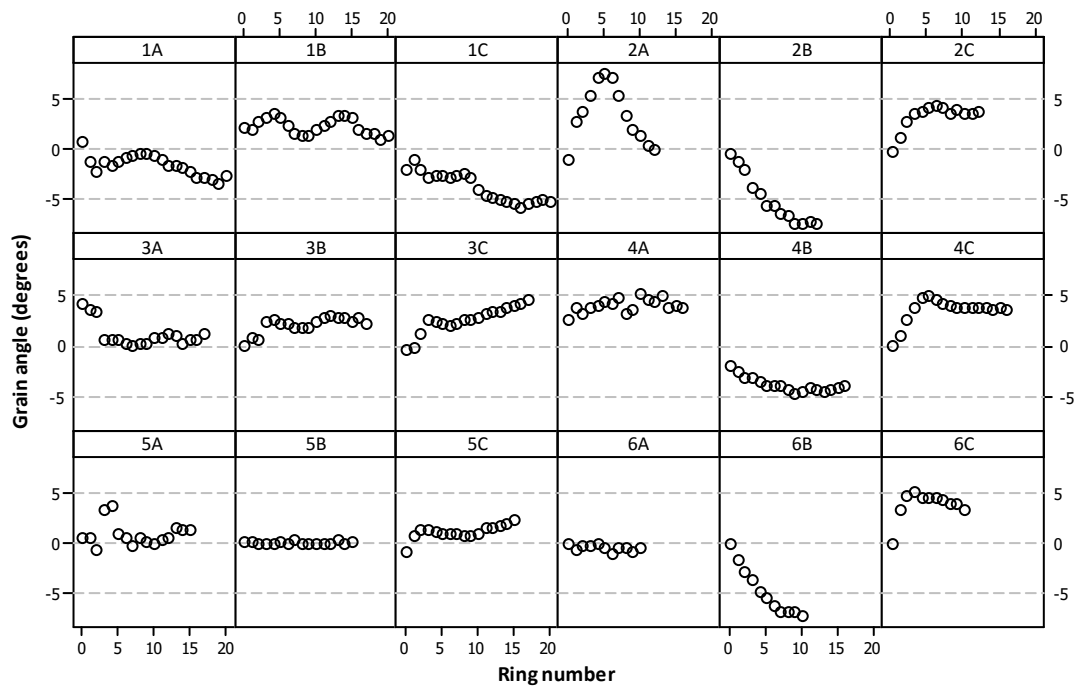


Figure 5.7. Grain angle in degrees for each disc over the core rings for direct comparison (i.e. the number of rings in disc C). Discs are numbered by tree (1-6) and position (A, butt, B, centre, C crown).

Analysis of variance by ANOVA one-way shows a significant difference in average grain angle between trees ( $p < 0.001$ ). This is also the case when the discs are compared by position; butt, centre or crown ( $p < 0.001$ ). The scatter and noise in some discs, particularly butt discs, can possibly be attributed to inaccuracies in measurement caused by uneven surfaces, especially close to knots, or variation in grain angle caused by basal flare. This may also be a consequence of presenting the values for each ring where averaging over several rings may have reduced the scatter and smoothed out the plot. Spiral grain is predominantly positive or in the S direction in butt logs. Shifts in grain angle between discs with height from S to Z direction and back to S are evident in three of the trees. In two of the trees, 3 and 5, there appears to be no change in direction between discs. The three columns to the left of Figure 5.7 display the grain angle values for the three discs of trees 1, 3 and 5. The battens obtained from these trees developed the lowest levels of twist when

they were kiln dried without restraint (mean twist = 1.49 °). The three columns to the right show the mean grain angle for trees 2, 4 and 6. The battens from these trees developed higher degrees of twist when dried without restraint (mean twist = 3.42 °). The mean between disc grain angle trends for both of these groupings over 16 comparable rings is shown in Figure 5.8.

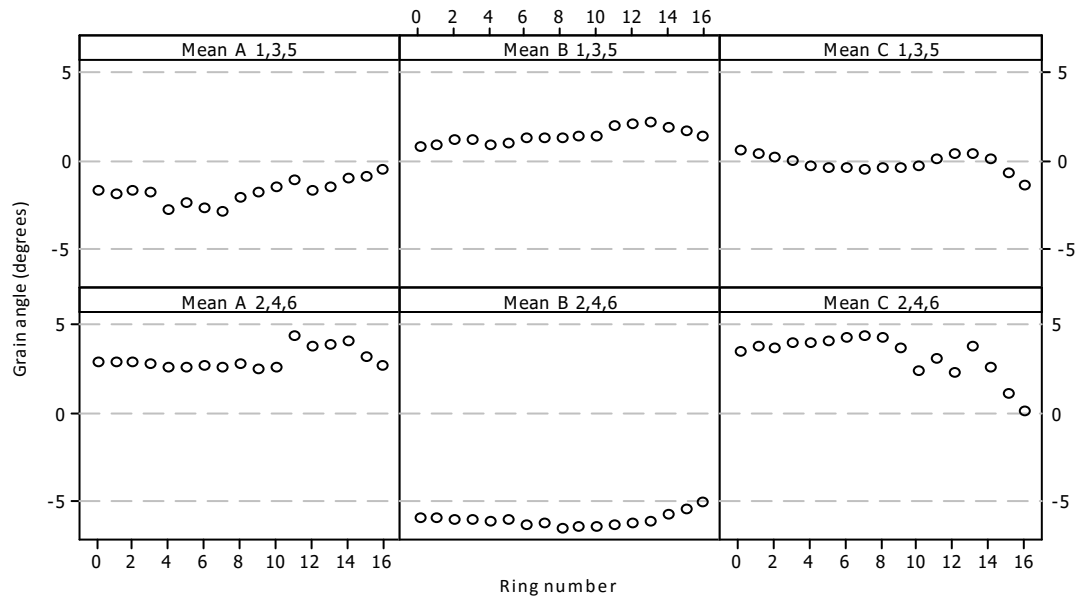


Figure 5.8. Mean grain angle for trees 1, 3 and 5 and trees 2, 4 and 6 by disc position (A, butt, B, centre, C crown).

The trend shown in the mean values derived from the 1,3 and 5 grouping shows a relatively moderate and ordered change in grain angle with height over a balanced range ( $-2.86^{\circ}$  to  $2.28^{\circ}$ ). The trend in the 2, 4, and 6 grouping shows a disorderly trend with the grain angle in the centre discs distinctly different from those of the butt and crown discs over a wide range ( $-6.54^{\circ}$  to  $4.48^{\circ}$ ). This perhaps suggests a sharp reversal of grain angle from left handed to right handed with height which may have an impact on the development of twist as the battens dry. However, nothing is known of what changes in direction may have occurred in the intervening 3m sections which were unavailable for study. Although the data hints at this as a possible explanation, the missing data precludes any solid justification for this.

### 5.3.3 Grain angle and twist

As has been already expressed, the nature of the experimental design unavoidably prohibits any real comparison of the grain angle data in relation to twist in this work. Figure 5.9 shows the relationship between the two with the limited data available.

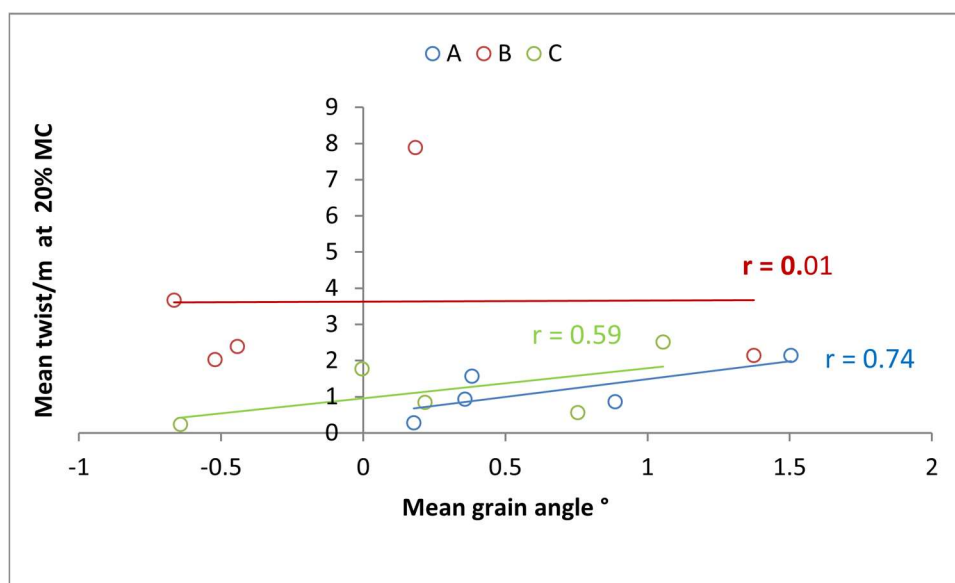


Figure 5.9. Scatter plots of mean grain angle against mean twist per metre at 20% moisture content for trees 1-6.

In this example, a mean value of the grain angle for each tree is calculated as the average of the means of discs A, B and C. This is compared with the mean twist at 20% MC for Trees 1-6. Values are split into the three positional categories representing battens within the log. The comparative mean grain angle values represent the estimated annual rings that would occupy each position.

## 5.4 Discussion

### 5.4.1 Method

The method used to measure grain angle presented in this work was not the method intended when the experiment was designed. The scribing method detailed in the European standard EN 1310:1997 (CEN) was preferred as it appears more compatible with producing comprehensive data directly from samples of sawn timber. When the method was applied it was apparent that it would not be possible to obtain the quantity or quality of required data. The areas of clear wood needed to carry out the procedure were not present in most of the battens. The standard does not prescribe a particular measure of area required but does recommend that several adjacent lines are drawn. This would suggest a minimum area of around 5 x 10cm would be required. In many of the battens this was not possible. Large knots or groups of knots tend to have an influence on grain angle that reaches beyond their visible limits. In some cases, the regularity of knots along the length of the batten made it impossible to determine any area where the grain angle could be defined as free from the influence knots. Knotting in Sitka spruce can be a problem. Annual growth can generate more than ten branches (Achim et al, 2006). Where large volumes of knots are present the prospect of obtaining accurate data on grain angle from the scribing method should be considered limited at best.

In choosing an alternative method various options were explored. There are a variety of methods for measuring grain angle, none of which, as yet appear to be considered as definitive (see Chapter 1; 1.7) . This perhaps highlights the complexity of measuring grain angle.

For the method which was finally chosen, detailed in section 5.2 of this chapter, only three discs from each tree were available. This was not particularly suited to generating the quantity of data required. To this end it is worth commenting on the deficiencies in the method. The agreement between the measurements taken on the opposing faces shown in Figure 5.5 is evidence that the method worked well in principle. However, the small sample size limits the data to a snapshot of the overall grain angle rather than a comprehensive study. The thickness of the discs was also a factor. These were removed with the intention of them possibly being used to measure radial and tangential shrinkage and were cut to approximately 2 cm thickness for this purpose. To replicate the original method (Marvou, 2007; Tranquart, 1995) thicker discs of around 10 cm would have been preferred and would be recommended for any future work with this method. Variability in

sample quality is more pronounced over the shorter face and a longer face in the longitudinal direction may have improved precision. Some of the variability in the results may be accounted for by the fact that measurements were taken at every annual ring. This does not appear to be standard in past work; the mean of every five rings being more common and in some cases, rings close to the pith excluded (Gjerdrum et al, 2002; Fonweban et al, 2013). Taking the increased variability aside, it does provide a comprehensive picture of radial variation. The lack of data from throughout the length of the tree proved to be the limiting factor when trying to find relationships between grain angle and other measured properties, particularly the values for twist. To provide a comprehensive picture of grain angle throughout any individual, a series of regularly removed discs would be appropriate. Harris (1989) recommends one disc for each annual growth increment as being fully representative of the changing pattern of grain angle. This would be most appropriate for trees in which branching was confined to annual whorls with a good length of clear wood between.

#### **5.4.2 Grain angle data**

Grain angle has been shown to have a major influence in the development of twist in sawn timber. This has been demonstrated by a number of studies (Stevens and Johnston, 1960; Brazier, 1965; Balodis, 1972; Harris 1989; Forsberg and Warensjo, 2001). Between and within tree variation can be considerable. Radial variation in grain angle or deviations from left handed grain to right handed with height have been identified as the main drivers of twist in sawn timber (Johansson et al, 2001; Kubojima et al, 2013). In this work, the aim was to establish a link between grain angle and twist in battens of Sitka spruce which had been kiln dried without restraint to promote maximum twist.

The late change of method in this experiment had a detrimental effect on the outcome. The observed results lack conclusive evidence of any substantial relationship between twist and grain angle in this work. However, the data collected is reasonably robust and from this there are some observable trends worthy of some consideration.

As would have been expected the grain angle at the pith is close to zero with a few exceptions. Starting in the butt log, the prevailing trend in conifers according to Walker (2006) is an increase in grain angle to around 5 or 6 ° close to the pith with height to around 6m and a radial increase in grain angle over the first 3-5 rings, decreasing towards

the bark. In Sitka spruce angles of greater than  $6^\circ$  are uncommon (Moore, 2011). The discs used in this experiment were taken from; the butt around the area of basal flare, the centre at around 4 m and the crown at around 8 m. The analysis compares the maximum number of rings in the crown disc with the corresponding rings in the centre and butt discs. In this respect only the crown disc gives a full radial profile of pith to bark. The maximum number of rings in the radial direction in any given set of three discs is twenty. It can then be assumed that the trends presented contain predominantly juvenile wood.

In this sample of six trees, all but Tree 1 has a left handed spiral in their butt disc. Two sets of samples (Trees 3 and 5) behave close to the trend described above. Both do show some scatter around the pith in their butt discs, which may be attributed to noisy data, and both have a slight tendency to an increase in grain angle towards the bark in the crown disc. Neither displays a shift towards a right handed spiral. In all others there is a reversal of the spiral grain angle evident in the centre disc and the centre discs show particular variability. Reports of unpublished data from Forest Research suggest there is no evidence of a decrease in grain angle with height. With the exception of a predominance of left handed grain in the butt there is no distinct trend between the six trees.

#### **5.4.3 Grain angle and twist**

The available data limits comparison of grain angle and twist. In Figure 5.9 mean values of twist at 20% moisture content are plotted against the mean values of grain angle for each tree, taken as the mean values for the butt, centre and crown discs. Both are segregated into the positional categories of the sawn battens. In this respect the grain angle values become a little more diluted as the positional values are estimates of ring number compared to the batten positions. Convolved as this may be, it does return a not entirely implausible effect. The plot suggests higher mean grain angle in battens sawn away from the pith (A and C). These battens would be significantly, if not completely comprised of juvenile wood. The corresponding twist is moderate. This theory is supported by a study of phenotypical correlations of twist in Scots pine (*Pinus sylvestris* L.) by Hallingback et al (2010) which showed better correlations with twist at grain angles between 30-70mm from the pith which would include the A and C plots shown here. This would make the construction of any model from such data very complex.

It is suggested in Chapter 5 that the trends of spiral grain angle shown in the six trees do in some respects mirror the trends in twist from the unrestrained drying experiment. Tree 2 in particular shows very erratic and severe shifts in grain angle over the three discs. This was

unquestionably the most twisted specimen after the three stages of kiln drying. Likewise, Tree 5 barely deviates from the baseline in any of the grain angle plots and was the least twisted of the six trees. These are of course observations of the trends in grain angle, based on limited data, related to more detailed data on twist. To this end they should be viewed as such and not as conclusive results.

## 6. Radial and tangential shrinkage

### 6.1 Introduction

In this chapter the mechanisms of transverse shrinkage are explored in terms of radial and tangential shrinkage. In this respect there is no direct experimental link to the previous chapters, where shrinkage in sawn timber has been the main focus. Transverse shrinkage is seldom quoted as a specific cause of twist. However moisture loss and the resulting anisotropic shrinkage of cells impacts upon the inherent microfibril and grain angle composition. In this respect transverse shrinkage should be regarded as having a major influence on the resulting quality of the material.

Here the results of two experiments carried out to assess radial and tangential shrinkage in discs of Sitka spruce are reported. Between fibre saturation point and equilibrium moisture content, water is lost from the disordered cell-wall matrix between the microfibrils. The resulting shrinkage is therefore greatest at  $90^\circ$  to the microfibril orientation. With a constant microfibril angle shrinkage should be equal in the radial and tangential directions. If microfibril angle is not constant, internal stresses will build up as logs or discs dry. The origins of these stresses are explored here. Attention is given to the effect of decreasing moisture content on shrinkage geometry and the effect of internal stresses on shrinkage when discs crack and tension is released. Around half of the discs used for grain angle measurement in Chapter 5 developed cracks during air drying and a similar result was expected with these samples.

### 6.2 Methods and materials

Two experiments to measure radial and tangential shrinkage were undertaken. Each had slightly different aims but both were concerned with differences in accumulated radial and tangential shrinkage in discs of Sitka spruce due to drying. The first experiment was essentially a small scale preliminary trial to validate the method and used only one disc. This disc was saturated and air dried until a crack developed. Measurements were recorded throughout the drying process and continued after the crack developed until equilibrium moisture content was reached. It was then sawn into quarters to release tension, re-saturated, dried and measured to observe the effects of shrinkage when not constrained by

the circular geometry of the disc. The second experiment applied the same method with some refinements and used a larger sample size. Twelve discs from three trees were used. They were saturated and allowed to dry while measurements were recorded. Tension release was expected to occur through natural cracking as the discs dried.

## **6.2.1 Experiment 1**

### **6.2.1.1 Sample preparation**

Only one disc was used in this preliminary experiment. The disc selected came from a previously unused set of Sitka spruce samples from Coalburn, situated to the east of Kielder Forest in Northern England. It was selected as being relatively free from knotting, branching or other blemishes. Mapping pins were inserted a few millimetres ( $4 \pm 1$ ) into the surface of the disc to represent two radial lines and three tangential lines (Figure 6.1). The disc was allowed to soak in water for 48 hours to re-saturate beyond fibre saturation point. The disc was then measured regularly (see section 6.2.1.2) until equilibrium moisture content was achieved. During this period a large radial, pith to bark crack developed in the disc (Figure 6.2). When the measurement period was concluded, it was decided to split the disc into four approximate quarters, organised around the alignment of the naturally developed crack. The mapping pins were removed and the disc was split and re-pinned with stiffer pins to provide for better stability along the radial edges. The quarters were pinned in a similar but not identical manner to provide eight radial sections and six tangential (Figure 6.3). The quarters were re-saturated and measured in the same manner as before.

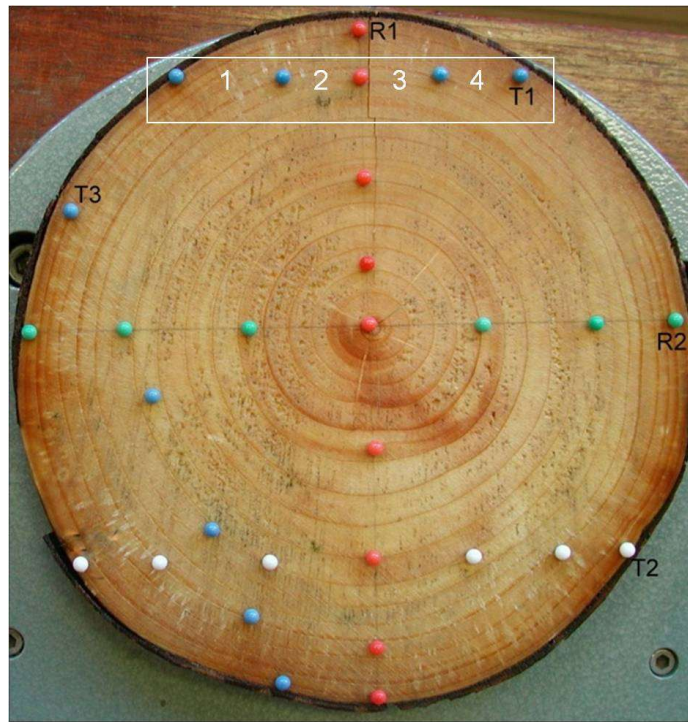


Figure 6.1. A disc of Sitka spruce, pinned to measure radial and tangential shrinkage. Five sections of pins were set; two radial (R) and three tangential (T); R1, red pins, R2, green/red pins, T1, blue/red pins, T2, white/red pins, T3, blue/green pins. Measurements were taken as the distance between pairs of pins in each section, i.e. four measurements in total for section T1 as highlighted in white text.

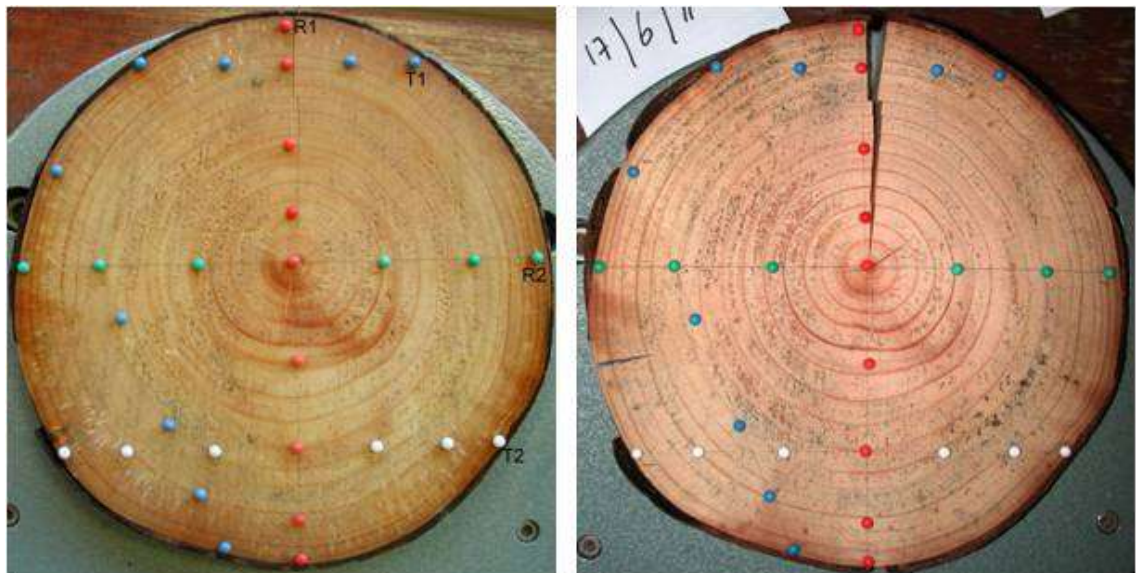


Figure 6.2. Same disc as shown in Figure 6.1 before (left) and after (right) the development of radial crack.

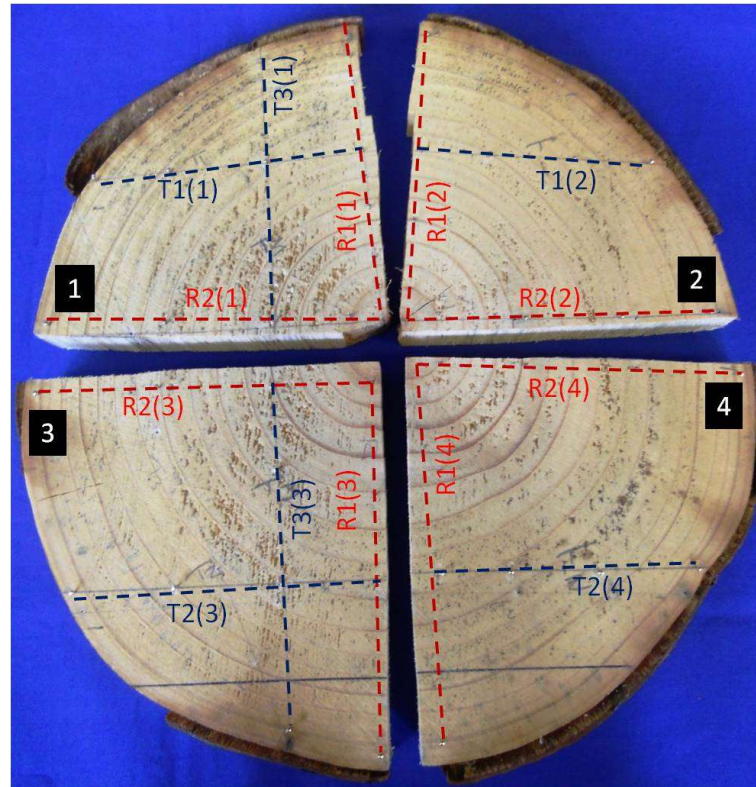
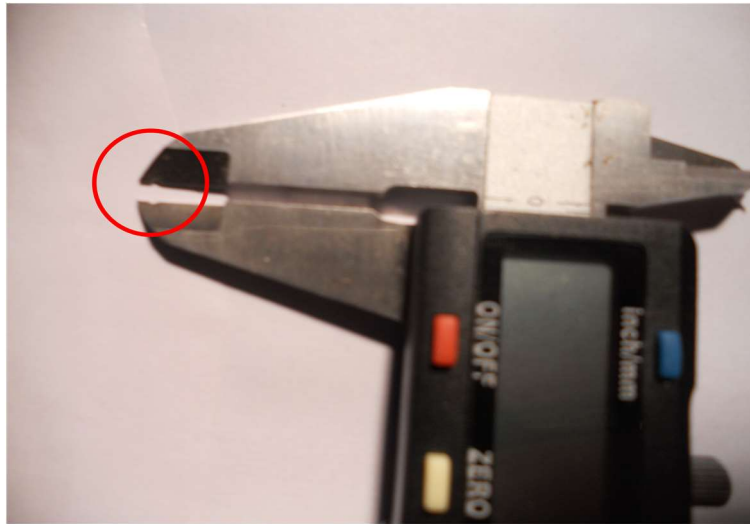


Figure 6.3. Sitka spruce disc split into quarters. Quarters are labelled 1-4, shown on black squares. The disc was re-pinned to give eight radial sections (red dashed lines) and six tangential sections (blue dashed lines) which were labelled as continuous lines and by quarter e.g. T1 (1) and T1 (2); T1 denotes the line, with the quarter ID in brackets.

### 6.2.1.2 Measurement

When re-saturated the samples (intact or quartered) were weighed prior to measurement and subsequently with each round of measurements. Between pin measurements were carried out using a digital calliper (Powerfix Profi Digital Calliper; Resolution: 0.01 mm, Accuracy: 0.10 mm  $\pm$  0.02 mm). The calliper was modified with a very small hole drilled near the tip of the measuring jaws (Figure 6.4). This allowed for accurate repeatability of measurements as the calliper could be secured to the pins at a precise location for each subsequent measurement. Pins were held in the calliper jaws as close to the disc surface as possible.



**Figure 6.4.** Digital calliper with small hole drilled in jaws, highlighted by red circle, to ensure repeatable measurement of pins.

## 6.2.2. Experiment 2

The fundamental nature of the second experiment was very much based on the preliminary experiment in terms of the method. Again, the discs were pinned, albeit in a slightly different arrangement. Additional radial lines were pinned to increase the measured surface area. Measurements of the saturated discs were taken regularly until equilibrium moisture content had been achieved. The aims are in principle the same as in experiment one but more directly focused upon the differences between radial and tangential shrinkage with regard to position in the disc.

### 6.2.2.1 Sampling

Samples were taken from trees felled at Harehope Forest, North West of Peebles in the Scottish Borders (55.41.42.N, 3.15.58W). Three Sitka spruce trees were selected for relative straightness and approximate diameter of 20cm at dbh. A set of three discs of approximately 20 mm each were removed by chainsaw at the dbh locus. A further three sets of discs were then removed at successive 1m intervals in the direction of the crown (Figure 6.5). The discs were sealed on site in plastic bags and transported to Forest Research, NRS, Bush Estate, Roslin where they were put in to cold storage.

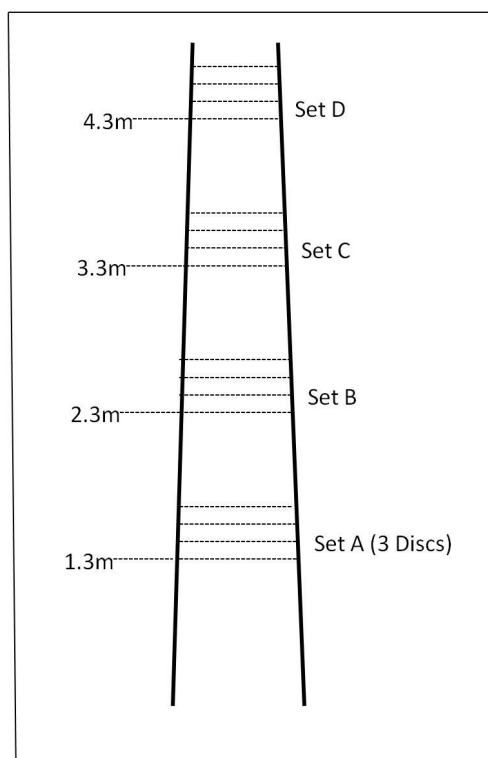


**Figure 6.5.** Removal of discs from logs of Sitka spruce. Four sets of three discs were taken from each log. Discs were removed by chainsaw at an approximate thickness of 20 mm. The first set was taken at 1.3m (dbh) and subsequent sets at 1m intervals.

### 6.2.2.2 Sample preparation

One disc from each set of three was selected to provide four (one from each height stage) from each tree. The selected discs were as free from knotting, branching or other blemishes as possible. All discs were intact in terms of showing no obvious signs of, or potential for cracking or splitting. At the time of preparation the discs had been preserved to as near the moisture content at felling as was possible. Each disc was marked to create eight sectors. Pins were inserted along the borders of each sector to enable the measurement of dimensional changes as the discs dried. The pins were tapped in with a hammer to be as perpendicular to the surface as possible. The pin was inserted entirely through the disc to restrict any tilting of the pin due to faster drying on the surface while ensuring that the tip did not penetrate the under surface. Eight pins were inserted around 2-3 rings from the bark on the dividing line between each of the sectors (outer pins). A further eight pins were inserted on the same dividing lines around 5-6 rings from the pith (inner pins). A single pin was located at the centre of the pith. Each of the eight outer sectors in the tangential plane were labelled *A – H* and each of the inner sectors, *I – P*. In the radial direction the dividing lines between outer and inner sectors were labelled *a – h* and the inner to centre sectors *i –*

*p.* The centre pin was labelled *z*. (Figure 6.6). Measurements were taken in accordance with the method set out in 6.2.1.2 for Experiment 1.

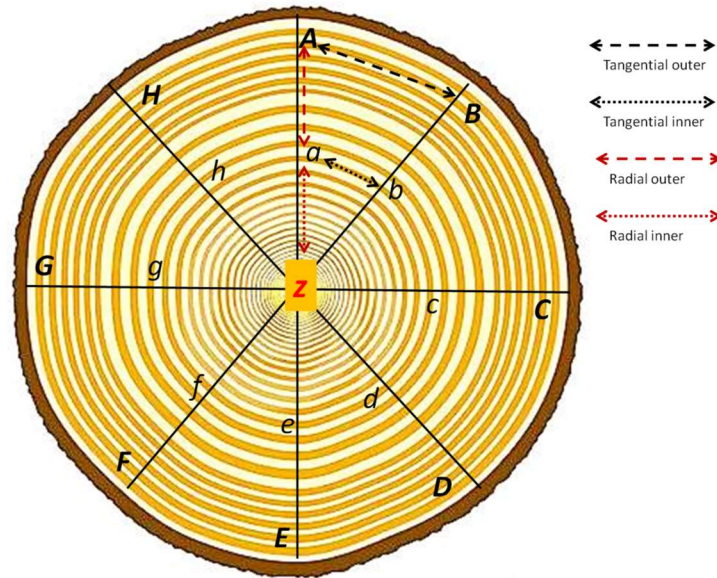


Figure 6.6. Layout of pinned disc. Outer pins labelled A-H, Inner pins a-h and centre pin z. Dotted lines show the range of measurements taken: Tangential outer; A-B, B-C, C-D, etc.; Tangential inner; a-b, b-c, c-d, etc.; Radial outer; (outer pin to inner pin), A-a, B-b, C-c, etc.; Radial inner; (inner pin to centre pin), a-z, b-z, c-z, etc.

### 6.2.2.3 Measurement and drying procedure

Measurements were taken daily from the day the pins were introduced. Estimations of when fibre saturation point had been reached (based on an approximate value of 30% moisture content) were made as the discs dried. This was calculated from saturated and oven dried weights which were obtained from an individual replicate disc for each of the experimental discs. The replicate discs were cut directly above or below the experimental discs and had been stored and treated in an identical manner. On reaching the estimated FSP weight, each disc was refrigerated at 5°C for 72 hours to allow even redistribution of moisture throughout the disc. When estimating the moisture content of the discs by weight only, there was no way of checking to what extent the initial moisture content was evenly distributed across the area of the disc, or whether the period allowed for redistribution of moisture was sufficient to equilibrate any discrepancies. Faster drying on the surfaces of the discs would be expected due to their immediate contact with the ambient conditions. The thickness of the discs (~20mm) would suggest a steady longitudinal moisture gradient being established in response to this. The aim of the period of refrigeration was to allow

equilibration across the thickness of the disc and to minimise problems with tilting of the pins caused by drying around the pin locus. It was also hoped that this would avoid fissures appearing in the discs at an early stage. Due to the rapid diffusion of moisture along the grain (Yerbury, 2015, unpublished data) this should have been achievable and there appeared to be no significant movement in any of the pins post refrigeration. Estimates of mean disc moisture content were calibrated after the completion of the experiment by oven drying of the actual samples. The mean calculated moisture content prior to refrigeration was 30% although this was over a rather wide range; 59.8 to 11.3%. These values were based on the calculations from the replicate discs which, in most cases, did not provide a good estimate. It is therefore difficult to assess the success or otherwise of this effect as only 25% of the discs came within a 10% range of the estimated FSP values of 30%. The distances between the pins were measured daily until it was estimated that the moisture content had equilibrated with the laboratory atmosphere. This was calculated as a decrease in moisture content of less than 2% in 24 hours over two measurement periods. Unexpectedly, with the exception of one disc, no significant cracks or fissures developed during drying.

## **6.3 Results**

### **6.3.1 Experiment 1 (Preliminary)**

The release of tangential tension in a disc could in principle result in either or both of two mechanisms: (1) greater shrinkage in the tangential than in the radial direction throughout the disc, and (2) an increase in shrinkage, in both of these directions, with distance from the centre of the disc. Mechanism (2) is understandable in terms of decreasing microfibril angle with distance from the centre. Tangential tension at the outer edge of a dried disc or log is released naturally by radial cracks if it exceeds the transverse breaking stress of the wood. Mechanism (1) is supported by long established evidence. As referenced in section 1.6, tangential shrinkage has consistently been shown to exceed radial shrinkage. In oven dried, medium density conifer wood estimates of shrinkage at 5-10% (tangential) and 2-6% (radial) have been reported (Walker, 2006a). A recent dedicated study by Dundar et al (2013) on this topic found tangential shrinkage to be greater than radial by 44% in small clear samples of Sitka spruce.

It is assumed that this differentiation in the magnitude of shrinkage is related to the behaviour of a number of combined factors, most significantly; differences in earlywood and latewood cell composition, variable microfibril angle and the directional geometric composition of collected cells. Studies of anisotropic shrinkage in Scots pine (*pinus sylvestris*) by Bonarski et al (2015) found that transverse shrinkage is 'governed mostly by a specific ultrastructural organisation of moderately organised cell wall compounds'.

As cells lose moisture the inter-cellular cohesion that binds the cellular matrix is weakened. Fissures in the structure develop that enable the release of tangential tension. If an individual disc is left to dry, this release can often be observed in the form of a V shaped crack; normally narrow at the pith and widening towards the bark. This occurrence will in turn lead to a less visible release of stresses throughout the disc. In figure 6.7 the results of swelling and shrinking in a disc is observed.

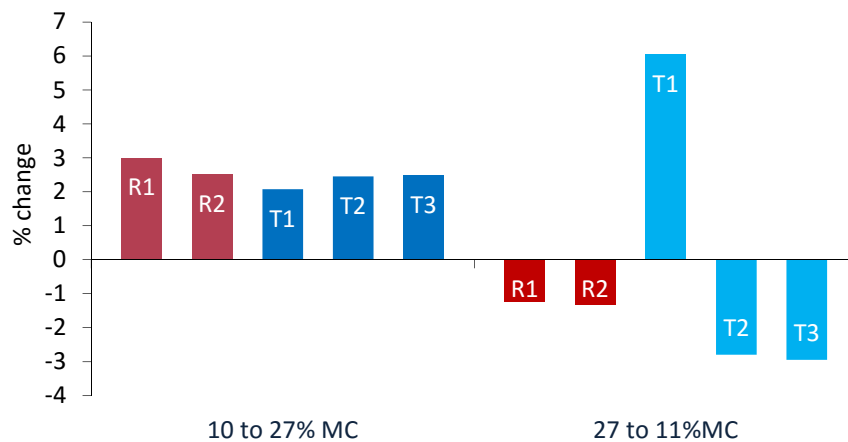


**Figure 6.7. Swelling and shrinking at two particular stages in the wetting/drying cycle of a disc. Left: swelling of an intact disc from 10 to 27% MC is approximately equal in radial and tangential directions while constrained by circular geometry, Right: shrinkage from 27 to 11% MC. Release of constraint within the disc caused by a radial split across T1 allows for tangential shrinkage to exceed radial. See Figure 6.3 for explanation of the radial and tangential measurements R1-R2 and T1-T3.**

On swelling the mean dimensional change in the radial direction is 11% greater than tangential. On drying, tangential shrinkage exceeds radial. The increase at T1 is the result of measurement taken across a V crack. With T1 removed the mean tangential shrinkage exceeds radial by 22.5%.

On completion of this experiment the disc was sawn into quarters and re-pinned in a similar fashion. The quarters were re-saturated and measurements taken as the discs dried. The results are shown in Figure 6.8.

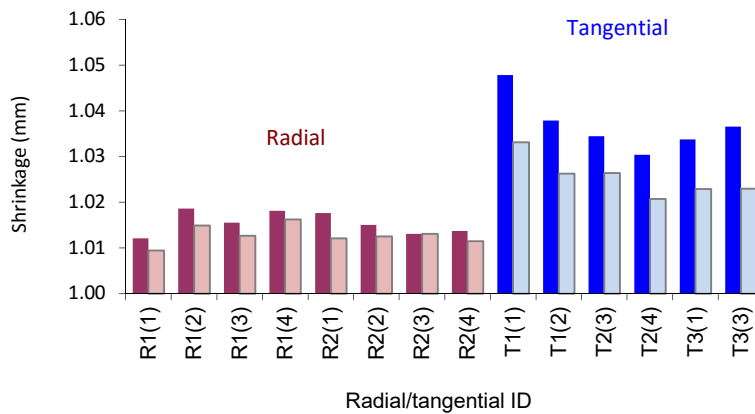


**Figure 6.8.** Radial and tangential shrinkage in quartered discs at 14% and 20% moisture content relative to dry. The darker coloured bars show the relative length at 20% MC and the lighter coloured bars the relative length at 14% MC. The identifiers on the x axis relate to the pinned lines on the original intact disc, numbers in brackets denote the numbered quarter of the disc.

The disparity of shrinkage between radial and tangential measurements clearly shows the effect of tension release in the tangential direction. The same data was analysed for variation between the inner and outer measurements (Figure 6.9).

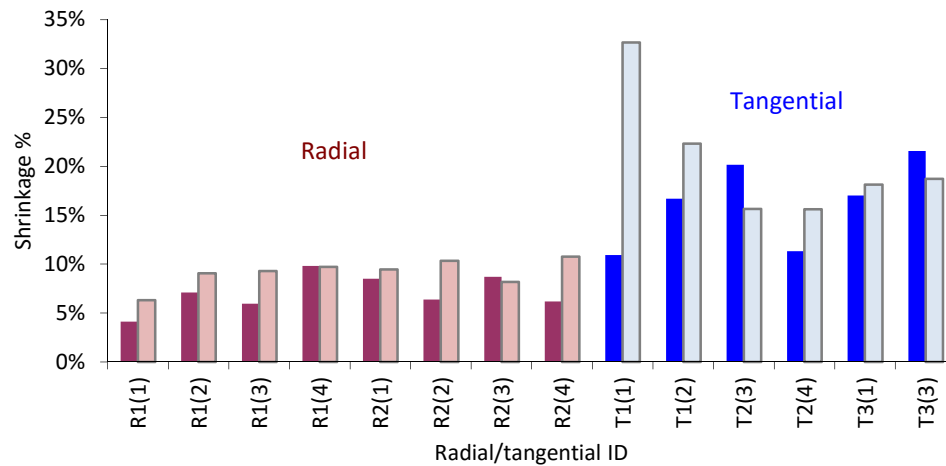


Figure 6.9. Variation in measurements taken near to the pith; inner (darker coloured bars) compared with those taken nearer the bark; outer (lighter coloured bars) in four quarters of a sawn disc.

The degree of shrinkage recorded for the outer sections of the quartered discs is greater than the inner sections and proportionately similar for both directions (radial: +29%, tangential: +26%). However, the trend is not evenly distributed throughout. Tangential shrinkage is greater than radial shrinkage by 70% and statistically, highly significant (ANOVA one-way,  $p < 0.001$ ). These results suggest that mechanism (1) may be predominant.

## 6.3.2 Experiment 2

### 6.3.2.1 Radial and tangential shrinkage with decreasing moisture content

The discs used in this experiment varied in size; dependant on their position with height within each tree. A number of the discs had small but potentially relevant differences in thickness. This had an impact on the rate of drying between discs as did the effect of visible surface drying compared to core drying. In order to present a comparable picture of between disc shrinkage the results have been interpolated to cover a range of values from fully re-saturated to zero percent moisture content. The mean start (saturated) and end (EMC) points for trees 1-3, deduced from the oven dried weights of the samples, were 125.5% and 11.1% moisture content respectively. Table 6.1 shows a more detailed breakdown of these values for each disc by position and for each tree.

**Table 6.1. Mean percentage moisture content by disc position (top table) and by tree (bottom table) showing values for start (saturated state) and end (equilibrium moisture content).**

Mean Disc MC%				
	A	B	C	D
Start	131.71	130.43	125.82	125.88
End	11.44	11.17	10.81	10.44

Mean tree MC%			
	1	2	3
Start	144.75	119.38	112.46
End	11.16	11.48	10.70

The following pages contain charts showing the interpolated values for radial and tangential shrinkage based upon the actual measured values (Figures 6.10 – 6.18). Charts for each individual disc are shown, A-D (butt to crown by height) for trees 1-3.. In some cases, the plotted lines for the different categories tend to merge which makes for a rather confused picture. This has been difficult to resolve without disturbing the consistency of the charts. In many cases the radial inner and tangential inner values are quite similar. This also occurs with the radial means and the tangential outer values and in some cases the tangential outer plot appears to be missing. In such cases the tangential plot lies directly under the radial mean with almost identical values. There also appears to be an amount of shrinkage occurring well before the fibre saturation point is reached and a merging of the plots as equilibrium moisture content is achieved and beyond. For clarity the charts are presented in larger format for the above reasons. The charts are annotated with the start point (saturated), end point (the recorded final equilibrium moisture content), the estimated sample fibre saturation point (Eq: when the sample was placed in refrigeration for 72 hours to equalise) and the general estimate of fibre saturation point at 30% moisture content (Est FSP). Progress is charted from right to left by time/decreasing moisture content. For continuity this is set at a maximum of 130%. In some samples the initial moisture content was higher than this figure but any omitted data at higher moisture content is considered not relevant to the results. Interpolated values are added beyond the end point to zero percent moisture content.

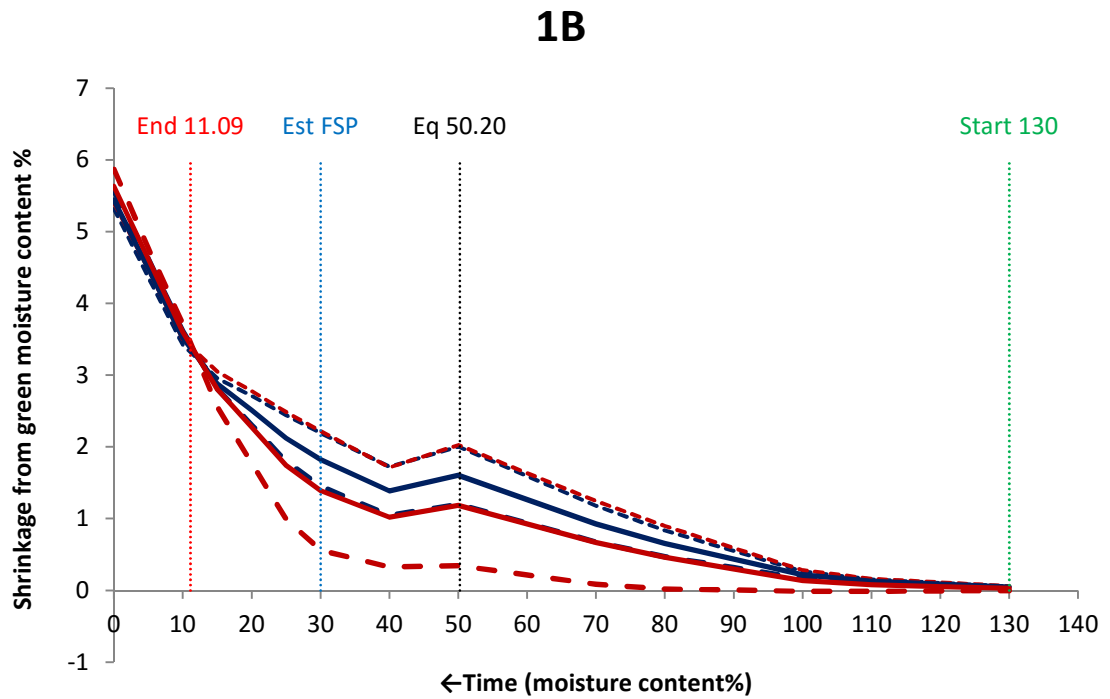
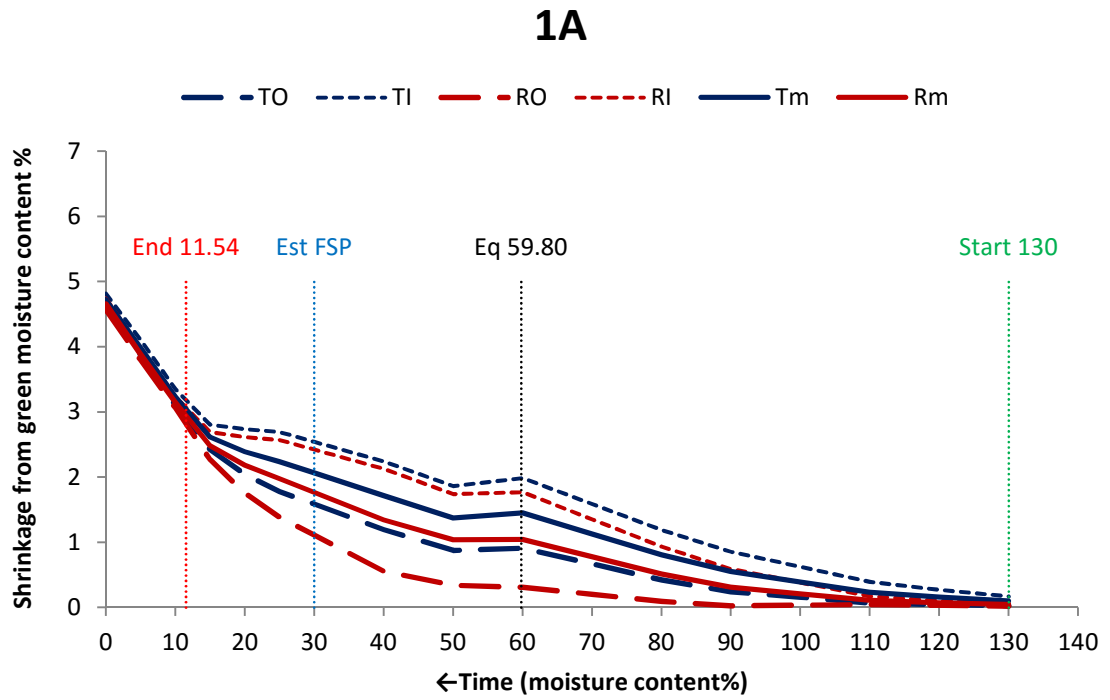


Figure 6.10. Plots of interpolated values for discs 1A and 1B of radial and tangential shrinkage from saturated to zero percent moisture content showing the outer, inner and mean values for both directions.

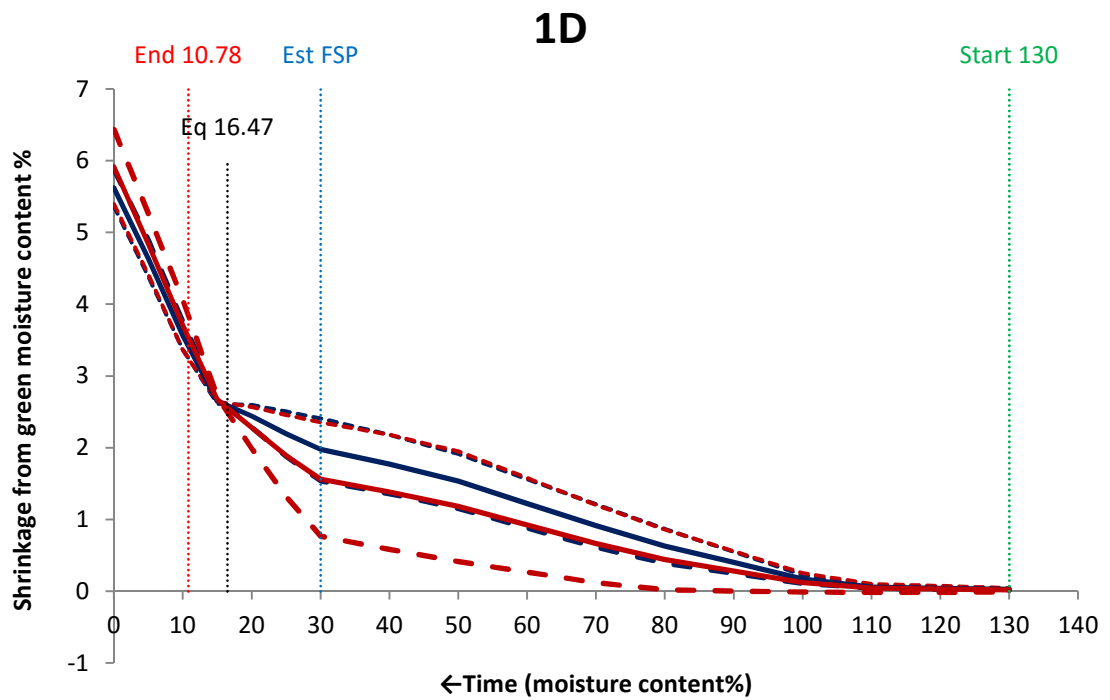
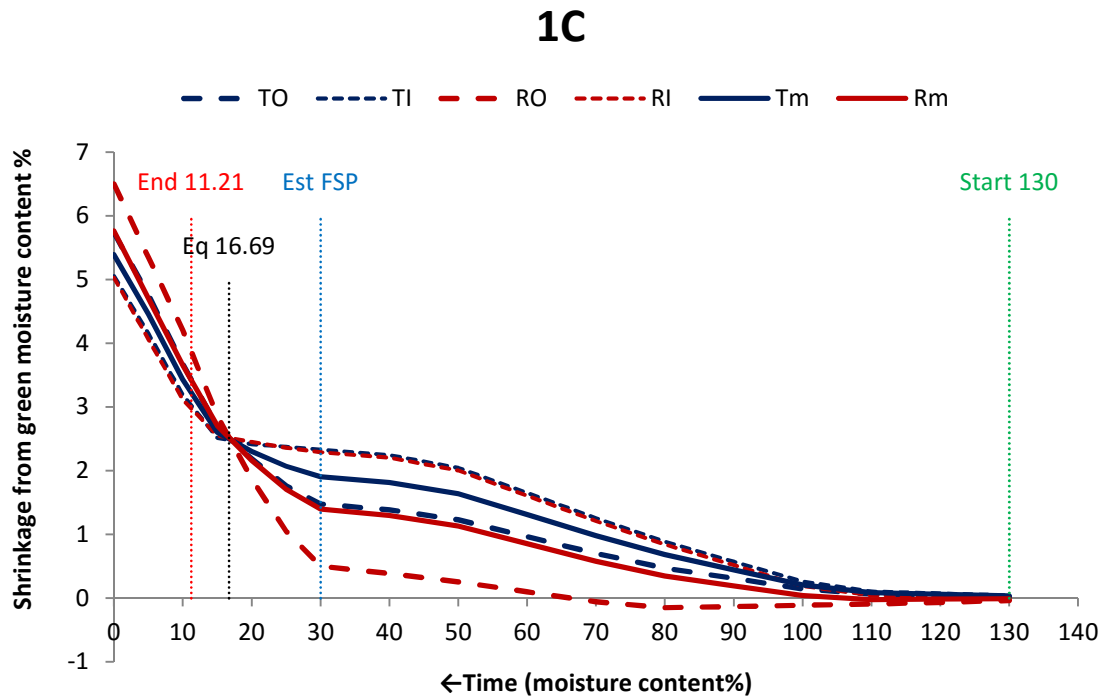
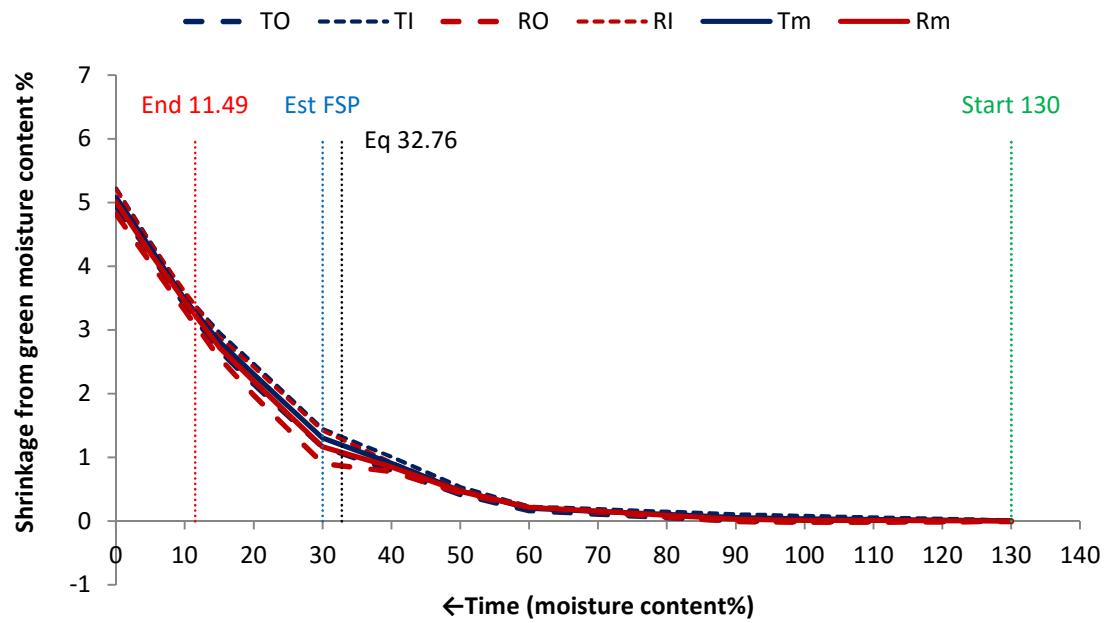


Figure 6.11. Plot of interpolated values for discs 1C and 1D of radial and tangential shrinkage from saturated to zero percent moisture content showing the outer, inner and mean values for both directions.

## 2A



## 2B

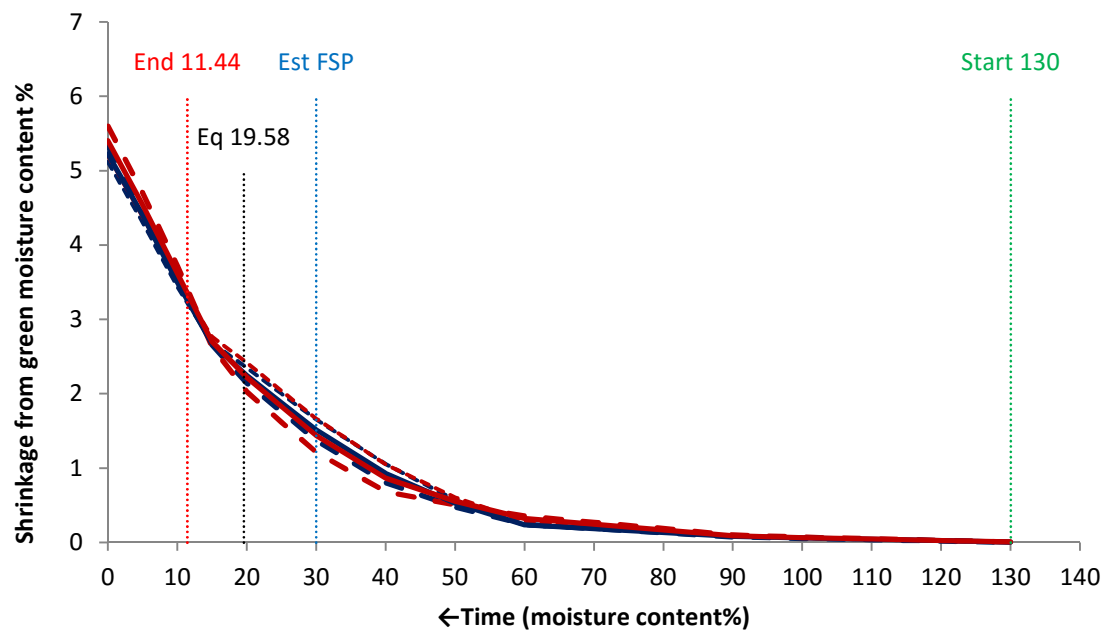
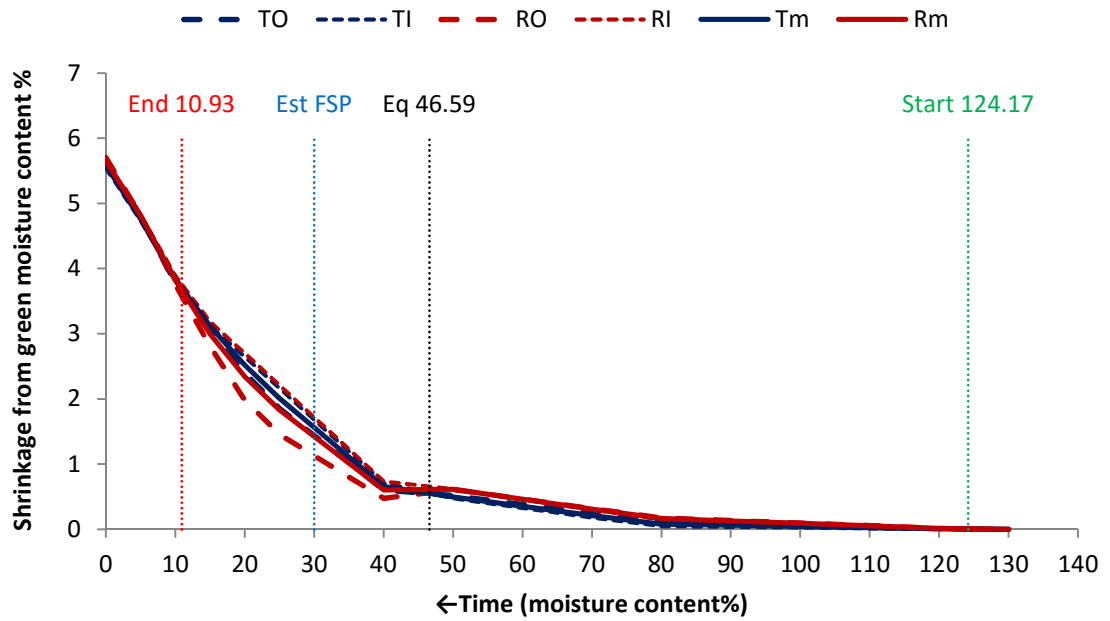


Figure 6.12. Plot of interpolated values for discs 2A and 2B of radial and tangential shrinkage from saturated to zero percent moisture content showing the outer, inner and mean values for both directions.

## 2C



## 2D

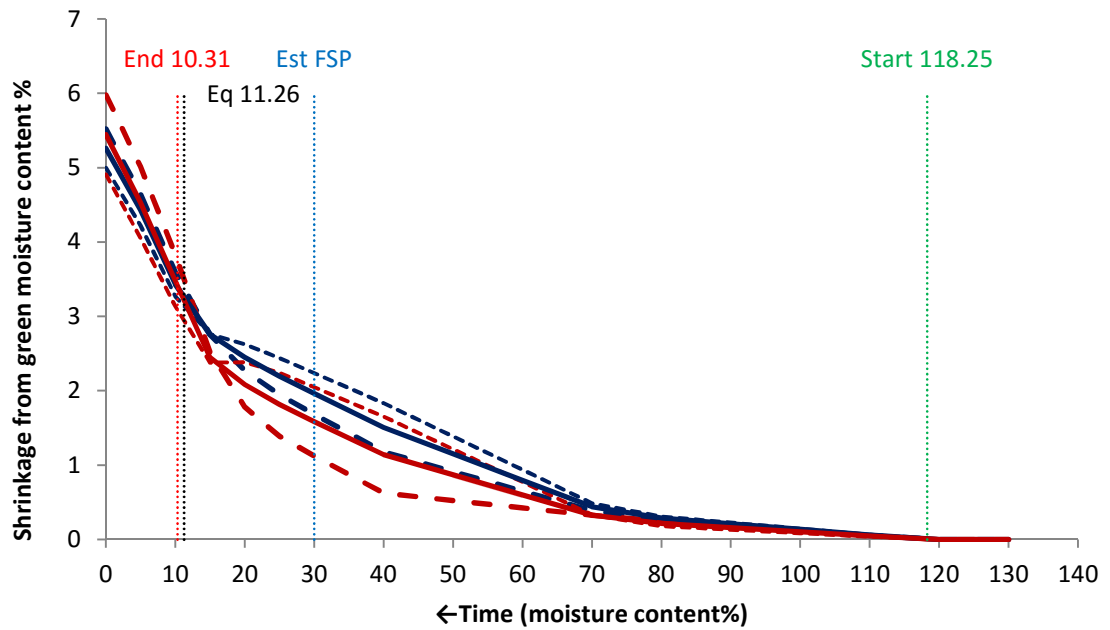
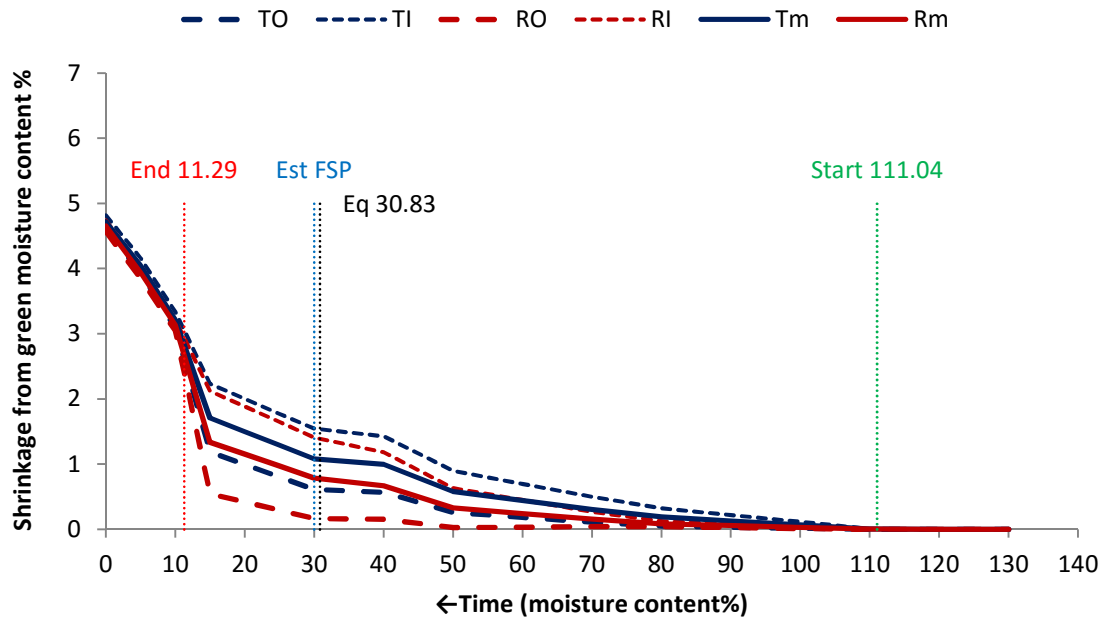


Figure 6.13. Plot of interpolated values for discs 2C and 2D of radial and tangential shrinkage from saturated to zero percent moisture content showing the outer, inner and mean values for both directions.

### 3A



### 3B

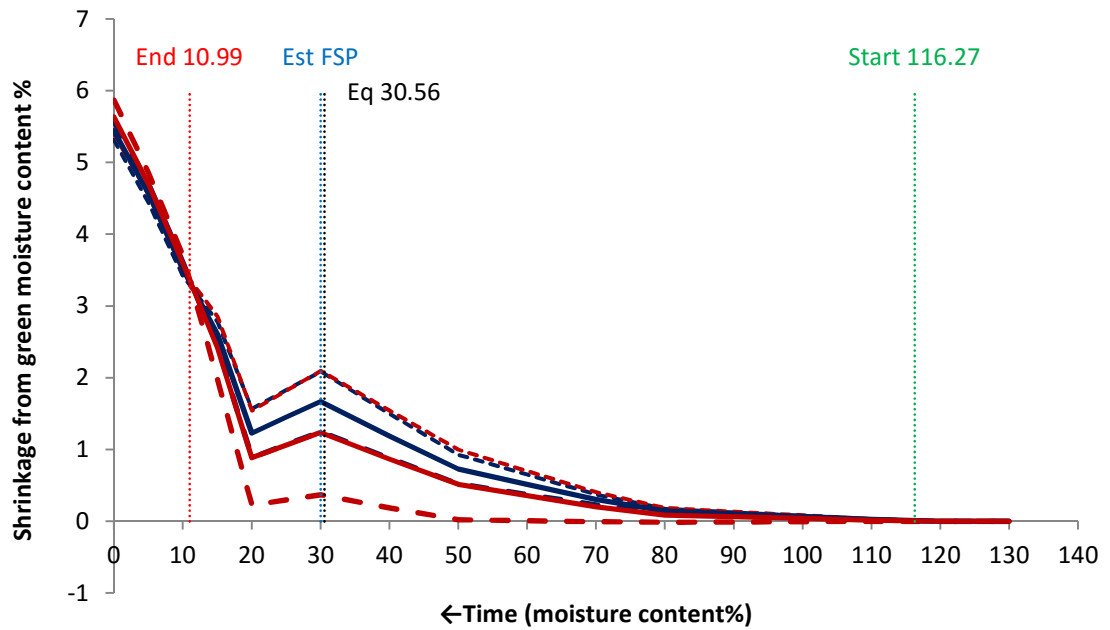
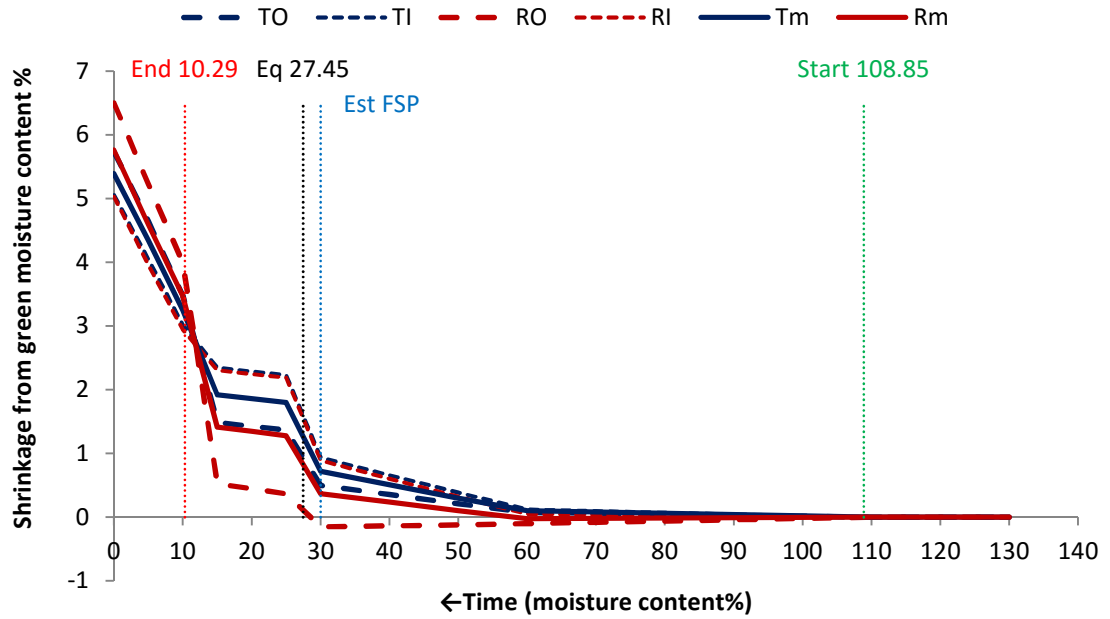


Figure 6.14. Plot of interpolated values for discs 3A and 3B of radial and tangential shrinkage from saturated to zero percent moisture content showing the outer, inner and mean values for both directions.

### 3C



### 3D

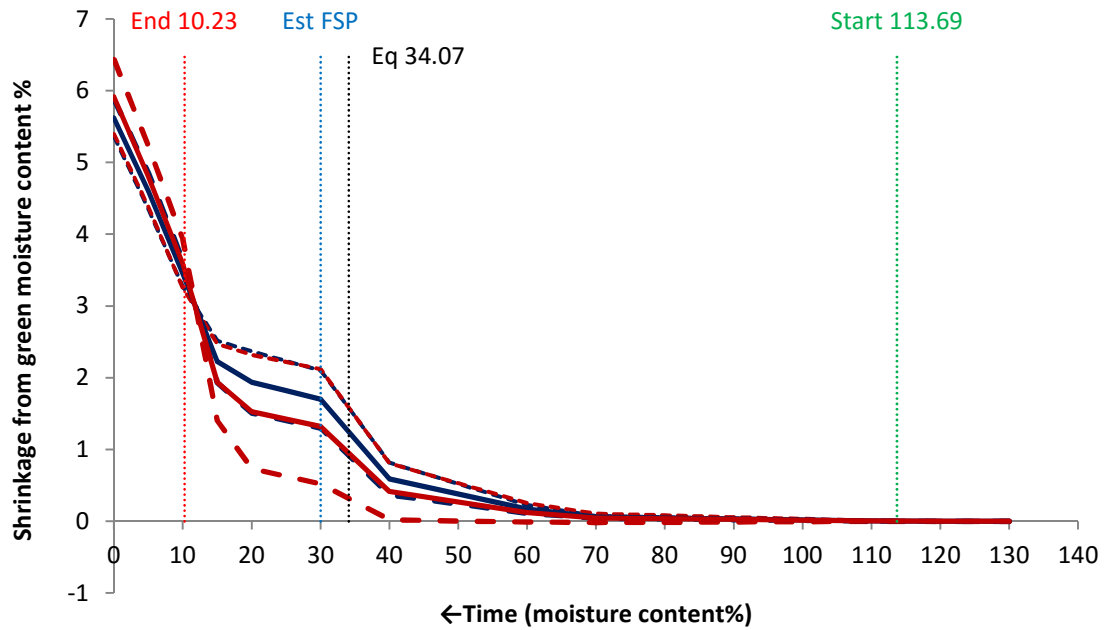


Figure 6.15. Plot of interpolated values for discs 3C and 3D of radial and tangential shrinkage from saturated to zero percent moisture content showing the outer, inner and mean values for both directions.

Figures 6.10 to 6.15 show interpolated plots for each individual disc showing shrinkage in relation to moisture content. No significant shrinkage should be expected until fibre saturation point has been reached. This is marked by a line at the assumed value of 30% moisture content on these plots although it is accepted that in individuals the actual value can be variable (higher or lower). In all of the plots there is a suggestion of shrinkage at high moisture content. In some cases this occurs at over 100% moisture content. It was expected that the pins may be less stable above fibre saturation point due to rapid moisture loss from the surfaces of the discs and the loss of free water from the cell lumen causing some minor external and internal movement of pins. Although all pins were checked post refrigeration and none seemed to be compromised it cannot be assumed that small changes in position did not occur. If this affected a number of pins it is possible the combined effect would suggest swelling or shrinkage. The presence of both positive and negative values at higher moisture content would suggest that this was the reason for this effect. In all of the interpolated plots this effect accounts for around 1%- 2% of the total mean shrinkage for all discs of 5.4%. Given that the total mean shrinkage for all discs from the measured data was 3.2% this may account for the discrepancy.

It is notable that the radial and tangential inner plots are very similar in the majority of the discs when compared with the relationship between the radial and tangential outer plots. This is due to the geometry of the discs where the inner measurements compare the radial and tangential distances within an intact circular geometry whereas the outer radial measurements do not account for the distance from the pith to the inner pin limit of the outer measurement (see Figure 6.6).

In trees 1 and 2, with the exception of disc 2A, the estimated fibre saturation point calculated from replicate discs was not accurate. However, all discs in tree 3 were relatively close to the estimate. This may reflect the truly variable nature of localised moisture distribution. It was thought that, given the proximity of the replicate discs, the estimated values would be within around 10% of the actual value and provide a reasonable indication of the FSP. Unfortunately this was not the case at all in trees 1 and 2 and in some cases the estimated FSP is significantly different from the observable break point on the chart. It can be assumed from this experience that the use of replicate discs for this purpose does not provide entirely reliable estimates of FSP in a global context.

In the Tree 1 plots, discs A and B visibly show a negative deviation in slope beyond their respective estimated Eq points where 72hrs of refrigeration had taken place. This is less

evident in C and D due to the low FSP estimates and perhaps as it occurs after significant shrinkage has developed. The dominance of the tangential mean shrinkage ( $T_m$ ) over radial mean ( $R_m$ ) shrinkage is apparent in all four discs. The shrinkage in the radial outer (RO) plots of B, C and D is seen to noticeably increase around the estimated FSP of 30% suggesting a common FSP between these discs. Beyond the divergence of the tangential and radial plots at around 10-15% MC, radial shrinkage appears to become greater than tangential with height.

The Tree 2 plots follow a similar pattern of tangential over radial shrinkage but with the exception of 2D, the plot values are much tighter than in Tree 1. There appears to be a less dramatic effect of decrease in the slope beyond the Eq points in discs A and C. This may suggest the presence of a more stable moisture gradient. As with the disc in Tree 1, the radial outer plot seems to show some evidence of the actual FSP by visibly deviating from the slope, particularly in 2C and 2D, at around 40% MC, suggesting a higher mean FSP than Tree 1. Once more there seems to be a switch from tangential to radial dominance in shrinkage at low moisture content.

In Tree 3 the dominance of tangential over radial shrinkage is similar to that of Tree 1. It is apparent in A, C and D that the Eq point does not correspond with the effect. The post moisture re-distribution period also seems more dramatic and prolonged than in either Tree 1 or 2. There is again some evidence of an actual FSP in the radial outer line but this may have been disturbed somewhat by the incorrect Eq points and as a result is difficult to determine, particularly in B, C and D. Again the switch to radial dominance with height is observed.

There is an overall effect of shrinkage with height in all trees and although this is sequentially regular in Tree 3 ( $A < B < C < D$ ) it is not in Trees 1 and 2. This is shown in Figure 6.16. The differences with height are not statistically significant.

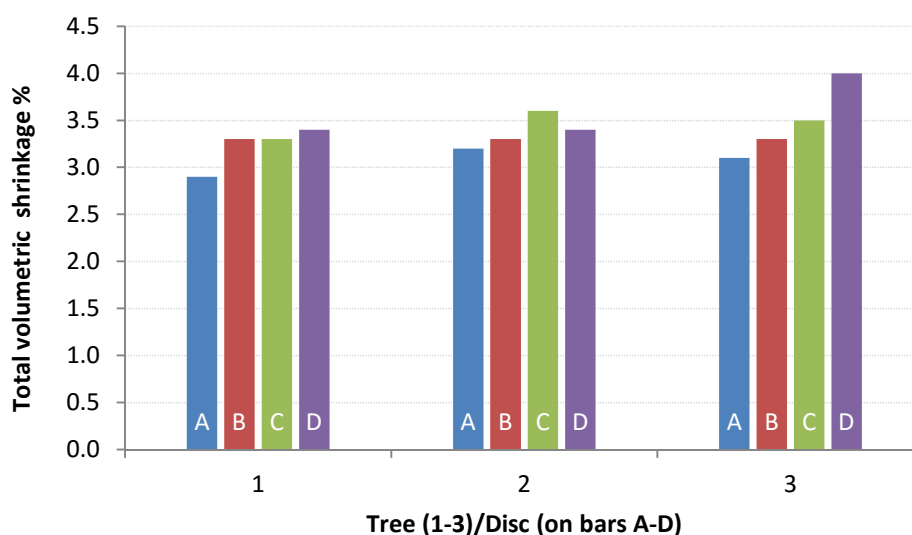


**Figure 6.16.** Difference in total volumetric shrinkage in trees 1-3 showing variation with height. Discs are labelled A-D; A being the closest to the butt and D the closest to the crown. An effect of increased shrinkage with height is evident but with the exception of the A discs consistently showing the lowest shrinkage no regular trend is apparent and the differences are not statistically significant.

In this experiment it was expected that around 50% of the discs would develop cracks and comparisons could be made between the samples to investigate the process of tension release, differences in radial and tangential shrinkage and the effect of decreasing moisture content. However, as only one of the discs developed a crack during drying the scope of this investigation was significantly limited. The method included a period where attempts were made to re-distribute moisture within the discs by refrigerating at 5°C for 72 hours. As charts 6.10 – 6.15 demonstrate, this did have an effect. This was in part an attempt to prevent premature fissures developing. It is conceivable that by allowing the re-distribution of moisture, the early development of fissures was averted but the experiment would have to be repeated with attention to this effect before this could be verified. It may simply have been a random occurrence.

### 6.3.2.2 Comparing radial and tangential shrinkage

As with Experiment 1, it was expected that the radial and tangential shrinkage within the restrained discs would be relatively equal. This is shown in Figure 6.17 with mean values for both categories in each individual disc. This shows the discs which remained intact and values for disc 3D (the only disc to crack) have been removed. Data used in this section is based on the measurement of shrinkage from saturated to equilibrium moisture content and not on the interpolated data used in the previous section.

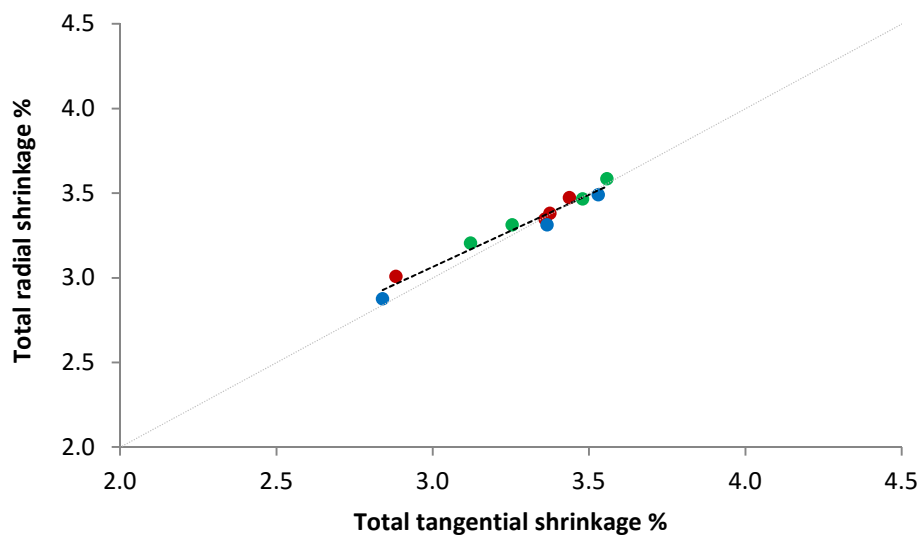


**Figure 6.17.** Mean values of tangential and radial shrinkage for the eleven out of twelve discs which remained intact within restrained geometry throughout the experiment. Trees are identified as 1 – blue, 2 – green and 3 - red. Disc 3D values have been removed as this disc developed a crack. This demonstrates the similarity in shrinkage in both planes. Correlation coefficient  $r = 0.98$ .

The differences between tangential and radial shrinkage after a disc has cracked and tension has been released is measurable in disc 3D. The crack developed in a quite peculiar manner; beginning as a fissure emanating from the pith towards the bark on one radius and after one day developing on both sides of the pith but not extending as far as the bark. Both sides then closed somewhat before the split on one side developed into a wider pith to bark crack of around 1cm at its widest point. The opposite radius remained as a considerable fissure but did not separate at the bark. Images of the crack development over the period are shown in Figure 6.18.

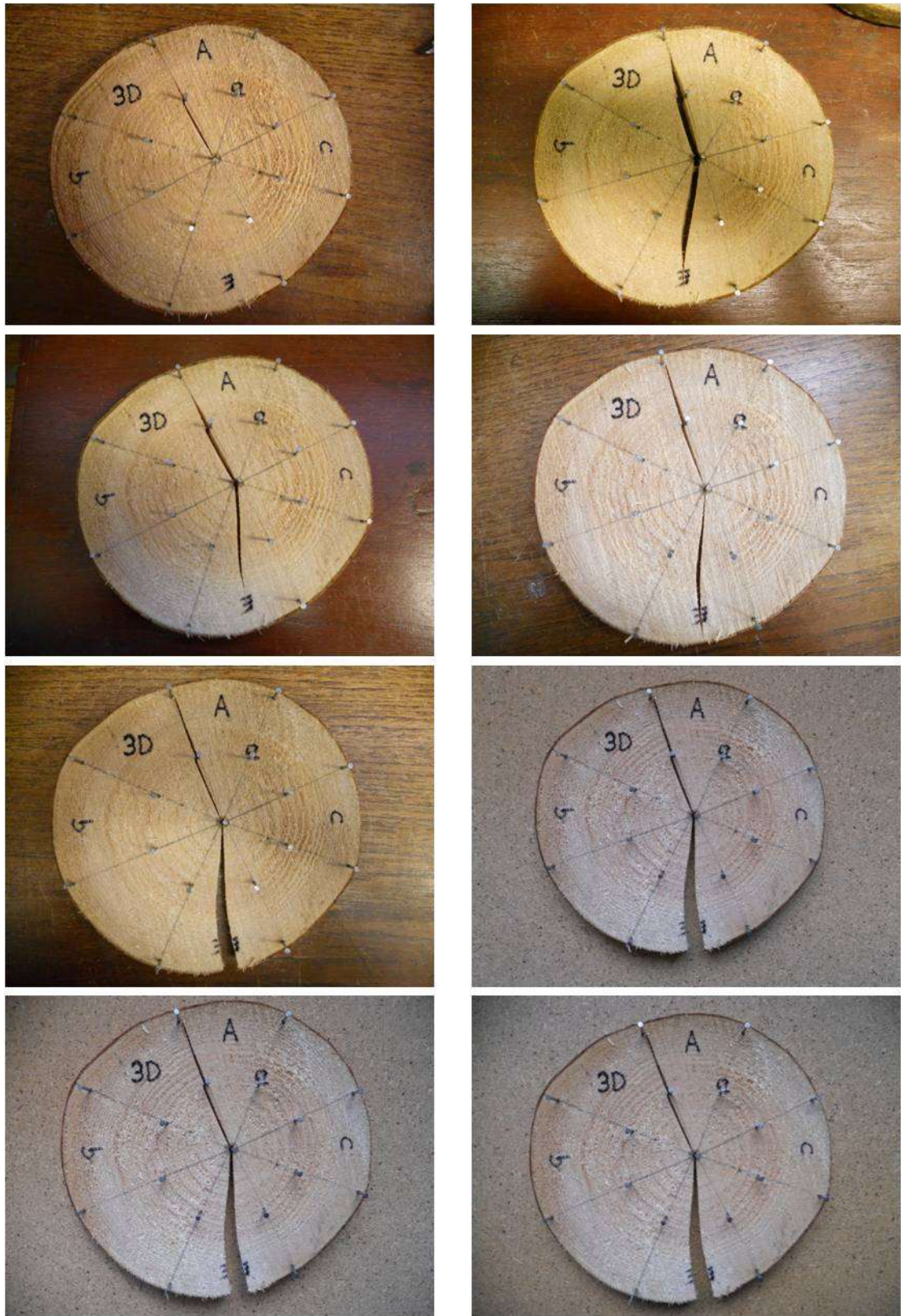


Figure 6.18. Images of crack development in Disc 3D. Recorded daily from day of discovery until crack settled. Images should be viewed from left to right by row (top to bottom) starting from top left image (day2) to the bottom right (day 9).

It is difficult to say if the insertion of pins contributes to the formation of fissures and this was not tested in this work. It is noted that the fissure initially develops along a line of three pins although this is not replicated on the opposite side. On day 2 a crack in 3D appears, emanating from the pith or heartwood area outwards towards the bark to the left of sector A. This is then replicated in the opposite radial direction through sector E on day 3 and larger openings develop on both sides while the circular geometry is still maintained at the bark. On day 4 the gap on both sides has closed somewhat. As the fissure elongates on both sides the outer bark is eventually separated through sector E. A 'V' crack is now evident from the pith through sector E to the bark with a fissure that does not break the bark running opposite along sector A. The gap in the 'V' crack widens slightly before reaching equilibrium moisture content on day 9.

Kang and Lee (2004) found a close relationship between differential tangential and radial shrinkage and the development of 'V' cracks in larch discs. Cracks were evident in discs which showed differential tangential shrinkage of over 2%. It is not clear if this was found in intact discs prior to cracking or after discs had cracked. The differential shrinkage in this experiment found values higher than 2% in a number of discs that did not crack. However, the Kang and Lee study was species specific and may not be of particular relevance to this work.

## **6.4 Discussion**

### **6.4.1 Method**

Experiment 1 was carried out early in this work, essentially as a preliminary trial and provided the basis for the subsequent Experiment 2 which was the final experiment in this research. The intention was to increase the sample size and fine tune the practical methodology and analytical process. It would have been interesting to be able to compare the results to the experimental work in the previous chapters but as there was no remaining sample material suited to this experiment other samples had to be acquired. The most disappointing, and unusual aspect of experiment 2 was the unexpected robustness of the discs. It was expected that a number of the twelve discs used would develop radial V

cracks which would allow for reasonable exploration of the effects of tension release in discs. This could have been done by comparing the relationship between radial and tangential shrinkage in terms of differential shrinkage under the constraint of an intact disc versus the differential shrinkage in cracked discs and provide a step towards a better understanding of why tangential shrinkage is so much greater than radial when tension is released. As only one of the discs developed such a crack, the lack of comparable data leaves the outcome of this experiment lacking any meaningful conclusions.

It would have been possible to induce cracks in the samples at a later stage but this would have bypassed some of the drying time and may not have provided answers to the relevant questions. Drying could also have been accelerated by periods of exposure to higher temperatures to induce cracks in the discs. The fact that the material was dried at ambient laboratory temperatures in the winter may not have been the ideal conditions in which to carry out this experiment. All of the above should be considered if a repeat of this experiment was planned at any time in the future. All this aside, the results do provide an insight into the patterns of anisotropic shrinkage in relation to moisture content and anatomical geometry. It also provides some reference to specific variation between radial and tangential shrinkage that was lacking in the transverse shrinkage data in Chapter 3.

This method of measurement is simple to replicate and provided the integrity of the pins is maintained the results are good.

#### **6.4.2 Experiment 1**

This experiment was very simple and was carried out to establish a method for measuring radial and tangential shrinkage in discs as they dried. It proposed two possible mechanisms for shrinkage in discs; (1) greater shrinkage in the tangential than in the radial direction throughout the disc, and (2) an increase in shrinkage, in both of these directions, with distance from the centre of the disc. Observations of shrinkage in the disc showed that shrinkage in both directions is relatively proportionate while the disc remains intact. On cracking, the tension release shifts the shrinkage in the tangential direction where the total shrinkage was significant and 70% greater than radial. Variation in shrinkage in either direction was not affected by radial position. The results would suggest mechanism (1) the controlling influence on shrinkage.

## 6.4.3 Experiment 2

### 6.4.3.1 Moisture content

The interpolated plots of moisture content against shrinkage show some small differences between trees in the percentage tangential shrinkage over radial but both follow a consistent slope from saturated to dry. The difference between radial and tangential is smaller in Tree 2 than the others. This may be simply due to differences in anatomy which affect the direction and magnitude of internal stresses. There is no evidence of any between disc differences in individual trees which may support this. Questions could be asked here as to why the majority of the discs did not crack. Is it possible that Sitka has a capacity for relaxation of internal stresses when dried at ambient temperatures? This could also explain the decrease in twist experience by battens during the storage period of the unrestrained drying experiment.

### 6.4.3.2 Shrinkage in intact discs

From the data accumulated it can be concluded that total shrinkage in intact discs, where the circular geometry is preserved is relatively similar between trees. In all three trees the measured total shrinkage was between 5.1 and 5.5%. Across all trees, discs closest to the butt end show the lowest amount of shrinkage. However, statistically there was no significant difference in shrinkage with height and there does not appear to be any underlying trend between discs. Comparing the tangential shrinkage on the outer edge of the disc and pith to bark radial shrinkage against the smaller tangential and radial inner circle, there is no significant variation. Again the total shrinkage between these two categories and between trees and discs appears random. This may simply reflect the anatomical differences that will exist between individuals where the unique nature of internal compressive and tensile stresses that develop between cells during growth will dictate the direction and magnitude of shrinkage within the contained geometry.

### 6.4.3.3 V cracks and shrinkage

Disc 3D was the only disc to develop a V crack. This became visible on day 2 of drying and appeared as a small, narrow fissure emanating from the pith to the first pin in the inner circle. This could perhaps be seen as an initial violent release of internal stresses, causing the wide gash across both radii.

In disc 3D the differential shrinkage between the tangential and radial data is considerable. The mean total tangential shrinkage (outer and inner) exceeds radial (total and inner) by 117% which compares with figures quoted by Kang and Lee (2004) of 138% (mean of five V cracked discs). Comparing the mean total shrinkage of discs 3A, 3B and 3C with 3D there is a 46% (outer) and 48% (inner) increase in tangential shrinkage and a 43% (inner) and 22% (total) decrease in radial shrinkage in 3D. To have been able to compare the data from Disc 3D with other cracked disc from different height within the tree or from other trees would have perhaps added to the conclusions of this experiment.

## 7. Discussion

### 7.1 Conclusions

The aim of this research was to investigate the mechanisms that generate twist in sawn timber. This was done by kiln drying battens of sawn Sitka spruce, unrestrained, to three drying targets at 20%, 15% and 8% MC, to promote maximum twist and, by recording changes in key properties that influence twist, explore relationships that may contribute to the development of twist. Grain angle and tangential shrinkage are known have a major influence on the development of twist (Johansson et al, 2001; Straze et al, 2011; Fonweban, 2013). Longitudinal shrinkage is often regarded as having a negligible influence on twist and is frequently overlooked as a contributing factor. These properties were measured and observed and relationships between them were investigated.

By drying the samples in three stages the effect of interrupting the drying process was small. The results show a predominance of twist in battens taken from the middle of logs where the pith is present. This is consistent with other research (Haslett et al 2001; Gorisek et al, 2005). Between tree and between position variation in measured twist at the first drying target of 20% moisture content reminded constant through 15% and 8% targets. This has practical applications as a simple predictive model for segregating out material prone to twist, prior to drying to lower moisture content. This could be of economic benefit to processors if the demand for timber dried to lower moisture content increases.

Two batches of battens, all sawn to contain the pith, were also dried under restraint to assess the effectiveness top load or strapping. The results show that battens containing the pith will twist regardless of how they are dried. The restrained battens did twist a little less but still, most failed to pass the grade for construction timber. The issue for processors is that the generally small diameter of logs they take delivery of minimises the options for cutting patterns that avoid the pith. With the exception of segregating out all material that contains the pith it is therefore unavoidable that twisted material will be present. Minimising twist could possibly increase the yield of construction grade timber.

Longitudinal shrinkage is often overlooked as a potential influence on twist and as a result is not routinely measured in studies of twist, with some notable exceptions (Backstrom and Johansson, 2006). In this work, the method developed for measuring longitudinal shrinkage worked well and produced good data. It was therefore possible to compare these results with the twist data. The relationship between longitudinal shrinkage and twist is shown to be strong ( $r = 0.8$ ).

Portable tools to record acoustic velocity ( $AV^2$ ) values in battens were used to investigate relationships with other properties. It is established that values for  $AV^2$  correlate well with measured values of MoE ( $r = 0.95$ ). There is also a strong relationship between  $AV^2$  and longitudinal shrinkage ( $r = 0.83$ ) and  $AV^2$  and twist ( $r = 0.73$  at 20% MC).

This work lacked data on microfibril angle. Measurement of microfibril angle can be costly and an inexpensive alternative which could provide good estimate of microfibril angle would be of particular use in a commercial setting. A relationship between microfibril angle and longitudinal shrinkage is known to exist (Sadoh and Kingston, 1967; Yamamoto et al, 2001). Further exploration of relationships between acoustic velocity/MoE, longitudinal shrinkage and microfibril angle to predict twist in sawn battens could be of benefit to processors and researchers.

The measurement of grain angle in this work was impeded by problems with the intended method (the current industry standard) to provide dependable, consistent results. Analysis of the data obtained from the alternate method was limited by the small sample size that was available. For these reasons, the results did not provide any conclusive evidence linking the influence of grain angle to the development of twist in this work. The available data does show that battens sawn further from the pith displayed a positive relationship with twist; increasing grain angle with increasing twist. A connection with grain angle at 30-70 mm from pith would coincide roughly with the part of the cross-section of a 100 x 50 mm batten that has a surface area most liable to distortion due to torsional leverage. In battens sawn from around the pith, twist was greater but the plotted data shows no relationship with the grain angle data. This suggests that grain angle at the pith is less predictable but confirms the theory that battens containing the pith will twist more.

The lack of whole tree data in the grain angle measurements from this method precludes being able to make any conclusive statements regarding directional change of the grain angle spiral with height. As stated in Chapter 5, discs from each annual growth increment

would be required for a full assessment of grain angle throughout any individual tree. Due to the unforeseen problems with the intended method, large sections of the trees measured in this work are not represented in the data and only a snapshot of the grain angle distribution is available. Evidence from the data does suggest that half of the trees used did switch the direction of their spiral (Figures 5.7 and 5.8). However, lacking the complete data for the whole tree, it is not possible to envisage the influence the change in the spiral direction would have on the development of twist. To avoid this problem, another method of measuring grain angle in sawn timber would be required if a relationship between grain angle and twist is to be fully explored.

Measurement of transverse shrinkage that was taken concurrently with longitudinal shrinkage segregated battens into those containing the pith and those that did not. The results showed a similar relationship with twist to that of the measured longitudinal shrinkage. However, as the transverse shrinkage could not be defined directionally as specifically radial or tangential, the relationship is unclear. Identifying purely radial and tangential faces on sawn timber is complex and could be seen as a limiting factor in determining the definitive direction of shrinkage in individual battens.

The experiment looking more specifically at tangential and radial shrinkage sought to address the question of why tangential shrinkage consistently exceeds that of radial (Kang and Lee, 2004; Wang et al, 2008). The method for measuring tangential and radial shrinkage in pinned discs is quite simple but worked well and provided robust data. The lack of comparable data in terms of discs that cracked and disc that did not somewhat negated the aims of the experiment. In the discs that did not crack, tangential and radial shrinkage continued in step with each other until equilibrium moisture content was reached. In the disc that did crack the increase in tangential shrinkage over radial was significant. Tangential shrinkage has been shown to be 1.5 to 2 times greater than radial shrinkage. Johansson et al (2001) found tangential shrinkage to be greater than radial by 110% in sticks of Norway spruce and Wang et al (2008) found 75% greater tangential shrinkage in small clears of radiata pine. In this work the difference in favour of tangential shrinkage was, on average, 117%. The release of the internal stresses in discs appears to be the results of the discrepancies between tangential and radial shrinkage rather than small differences in both with distance from the pith. The quantitative differences between radial and tangential shrinkage due to these internal stresses are not explained in this work. Due to the inherent nature of these stresses it may in future be possible to define them but limiting the extent of twist due to these stresses may not be possible.

Although the question of why tangential shrinkage is greater than radial remains unanswered there is current, ongoing work which seeks to find answers to this (Thomas, Jarvis and Altnar, unpublished data). The same process may also be applicable to the drying of logs or in standing trees. Drought crack has been a problem for standing trees in the drier eastern areas of Scotland for some time. Research of this nature may help to provide some answers as to why this occurs.

Parallel work on finite element modelling of twist (De Borst & Jarvis unpublished data) suggests that twist can be understood in terms of longitudinal shrinkage as a driving force and gradients of grain angle as a directing influence, setting up internal stresses that are partially relieved when they come into balance with the natural torsional stiffness of the batten. Finite element models of twist combined with numerical models for radial variation in stiffness may provide insights into how cutting patterns can be improved. The collection of data for grain angle, tangential, radial and longitudinal shrinkage similar to that produced in this work would be a good starting point for parameterisation of finite element models to predict the occurrence of twist.

## **7.2 Future work**

As mentioned in the previous section, there may be potential through finite element modelling to better understand the relationship between the known factors that contribute to the development of twist. Ultimately, this could possibly serve as a predictive tool which may be of great benefit to growers and producers to improve the quality and yield of construction grade timber. However, the design of such a model would be complex and further understanding of certain effects may require more research prior to any success in this area. It is evident that spiral grain angle and anisotropic shrinkage are the major influences on the development of twist. The interaction between both will add to the complexity of the design of any predictive model.

This work showed that a relationship between longitudinal shrinkage and twist exists but it is not fully understood to what extent the interaction between longitudinal and transverse (radial and tangential) shrinkage influences this relationship. The dominant plane of shrinkage in the transverse direction is difficult to define in sawn timber, particularly where data from multiple samples is involved. It could be assumed that most cutting

patterns would produce faces that are predominantly tangential in nature but further work in this area to more clearly define this may be of use. What we do know is the approximate magnitude and ratio of shrinkage in the longitudinal, radial and tangential directions and this appears to be relatively consistent in previous research on Sitka spruce. As longitudinal shrinkage is often regarded as having a negligible impact on twist, further investigation into the directional interaction effects of anisotropic shrinkage on twist development may be of use. Grain angle measurements could be regarded as more problematic. How grain angle develops between and within individual trees can vary considerably. A simple method to determine grain angle in sawn battens would be helpful. The current scribing method prescribed by the relevant standard may suffice on occasion but as was shown in this work, the volume of knotting that is often present in Sitka spruce can limit the reliability of this method. The method used in this work or a similar method may provide robust results for the purposes of modelling but a faster, reliable method of measuring grain angle in standing trees or logs may be required if the results of any model are to be put in to practice in a commercial setting.

Finite element models of distortion of sawn Norway spruce timber have been carried out previously (Ormarsson et al, 1999; Johansson and Ormarsson, 2009) and reference to these studies may be a good starting point for any similar work with Sitka spruce. Both found spiral grain angle to have a major influence on the development of twist as battens dried. Position within the log (i.e. distance from the pith) is also noted as a contributory factor as are the release of growth stresses and shrinkage.

It should therefore be possible to construct a manageable finite element model for Sitka spruce based on data for grain angle, longitudinal shrinkage and transverse shrinkage, perhaps from the data in this work or from further research based on the methods proposed in this work. Recent work by Jarvis (unpublished data) constructed very simple finite element models of this type where the inputs were simply a model for radial variation in spiral grain, the longitudinal shrinkage, the batten dimensions and position relative to the centre of the tree. However, until more is known about variation in spiral grain angle, the main purpose of such a finite element model would be to explore how varying the sawing pattern will affect the distribution of twisted battens.

## List of References

- Abe K, Yamamoto H (2006) Behavior of the cellulose microfibril in shrinking woods. *Journal of Wood Science* 52: 15-19
- Abimaje J, Baba AN (2014) An Assessment of timber as a sustainable building material in Nigeria. *International Journal of Civil Engineering, Construction and Estate Management* 2: 39-46
- Achim A, Gardiner B, Leban J-M, Daquitaine R (2006) Predicting the branching properties of Sitka spruce grown in Great Britain. *New Zealand Journal of Forestry Science* 36: 246-264
- Auty D, Achim A (2008) The relationship between standing tree acoustic assessment and timber quality in Scots pine and the practical implications for assessing timber quality from naturally regenerated stands. *Forestry* 81: 475-487
- Backstrom M, Johansson M (2006) Analytical model of twist in Norway spruce (*Picea abies*) timber. *Scandinavian Journal of Forest Research* 21: 54-62
- Backstrom M, Kliger IR (2009) Timber-framed partition walls and their restraining effect on warp in built-in wall studs - A model for spring. *Construction and Building Materials* 23: 71-77
- Backstrom M, Kliger R (2006) Restraining moisture-related twist in timber structures. *Holz Als Roh-Und Werkstoff* 64: 235-242
- Balodis V (1972) Influence of grain angle on twist in seasoned boards. *Wood Science* 5: 44-50
- Barber NF (1968) Theoretical model of shrinking wood. *Holzforschung* 22: 97-&
- Barber NF, Meylan BA (1964) The anisotropic shrinkage of wood. A theoretical model. *Holzforschung* 18: 146-156
- Barnett JR, Bonham VA (2004) Cellulose microfibril angle in the cell wall of wood fibres. *Biological Reviews* 79: 461-472
- Beauchamp K (2011) The biology of heartwood formation in Sitka spruce and Scots pine. PhD Thesis, University of Edinburgh
- Boone RS, Kozlik CJ, Bois PJ, Wengert EM (1988) Dry kiln schedules for commercial woods - temperate and tropical. General Technical Report FPL-GTR-57. Madison WI: Department of Agriculture, Forest Service, Forest Products Laboratory 158p
- Brazier JD (1965) An assessment of the incidence and significance of spiral grain in young conifer trees. *Forest Products Journal* 15: 308-312
- Buksnowitz C, Mueller U, Evans R, Teischinger A, Grabner M (2008) The potential of SilviScan's X-ray diffractometry method for the rapid assessment of spiral grain in softwood, evaluated by goniometric measurements. *Wood Science and Technology* 42: 95-102
- Cameron AD, Lee SJ, Livingston AK, Petty JA (2005) Influence of selective breeding on the development of juvenile wood in Sitka spruce. *Canadian Journal of Forest Research- Revue Canadienne De Recherche Forestiere* 35: 2951-2960
- Campbell NA, Reece JB (2002a) *Biology* (Sixth edition) Benjamin Cummings, San Fransisco 737p
- Campbell NA, Reece JB (2002a) *Biology* (Sixth edition) Benjamin Cummings, San Fransisco 734-738pp
- Caron-Decloquement A (2010) Extractives from Sitka spruce. PhD Thesis, University of Glasgow

- Carter P, Chauhan S, Walker J (2006) Sorting logs and lumber for stiffness using director HM200. *Wood and Fiber Science* 38: 49-54
- Cave ID (1972) Theory of shrinkage of wood. *Wood Science and Technology* 6: 284-292
- CEN (1997) Round and sawn timber-Method of measurement of features, EN1310:1997. European Committee for Standardisation, Brussels
- CEN (2010) Structural timber – Determination of characteristic values of mechanical properties and density, EN384:2010. European Committee for Standardisation, Brussels
- CEN (2011) Timber structures - Strength graded structural timber with rectangular cross section, EN14081-1:2005+A1:2011. European Committee for Standardisation, Brussels
- CEN (2012a) Timber structures - Strength graded structural timber with rectangular cross section - Part 3: Machine grading; additional requirements for factory production control EN14081-3:2012. European Committee for Standardisation, Brussels
- CEN (2012b) Timber structures – Structural timber and glued laminated timber – Determination of some physical and mechanical properties, EN408:2010+A1:2012. European Committee for Standardisation, Brussels
- Chauhan SS, Sharma M, Thomas J, Apiolaza LA, Collings DA, Walker JCF (2013) Methods for the very early selection of *Pinus radiata* D. Don. for solid wood products. *Annals of Forest Science* 70: 439-449
- Chauhan SS, Walker JCF (2011) Wood quality in artificially inclined 1-year-old trees of *Eucalyptus regnans* - differences in tension wood and opposite wood properties. *Canadian Journal of Forest Research-Revue Canadienne De Recherche Forestiere* 41: 930-937
- Chen ZQ, Karlsson B, Lundqvist SO, Garcia Gil MR, Olsson L, Wu HX (2015) Estimating solid wood properties using Pilodyn and acoustic velocity on standing trees of Norway spruce. *Annals of Forest Science* 72: 499-508
- Comstock GL, Cote WA (1968) Factors affecting permeability and pit aspiration in coniferous sapwood. *Wood Science and Technology* 2: 279-291
- Cooper G, Maun K (2004) DRYCON: Conclusions and Recommendations. Building Research Establishment, Construction Division, Watford WD25 9XX UK
- Cown D, Harrington J, Lee J, Moore J (2012) Assessing spiral grain by light transmission. *IAWA Journal* 33: 1-14
- Danborg F (1994) Drying properties and visual grading of juvenile wood from fast grown *picea-abies* and *picea-sitchensis*. *Scandinavian Journal of Forest Research* 9: 91-98
- Davis I (2009) Sustainable construction timber. Forestry Commission Scotland, Edinburgh
- Domec JC, Gartner BL (2002) How do water transport and water storage differ in coniferous earlywood and latewood? *Journal of Experimental Botany* 53: 2369-2379
- Donaldson L (2008) Microfibril angle: measurement, variation and relationships - a review. *Iawa Journal* 29: 345-386
- Donaldson L, Bardage S, Daniel G (2007) Three-dimensional imaging of a sawn surface: a comparison of confocal microscopy, scanning electron microscopy, and light microscopy combined with serial sectioning. *Wood Science and Technology* 41: 551-564
- Dundar T, Wang XP, Ross RJ (2013) Prediction of transverse shrinkages of young-growth Sitka spruce (*Picea sitchensis*) and western hemlock (*Tsuga heterophylla*) with ultrasonic measurements. *Wood Material Science and Engineering* 8: 234-241
- Ekevad M (2005) Twist of wood studs: dependence on spiral grain gradient. *Journal of Wood Science* 51: 455-461

- Erickson RW, Shmulsky R (2005) Warp reduction of red pine two-by-fours via restrained drying. *Forest Products Journal* 55: 84-86
- Esau K (1977a) *Anatomy of seed plants* (2<sup>nd</sup> Edition) John Wiley & Sons Inc, Hoboken, New Jersey, USA 77 p
- Esau K (1977b) *Anatomy of seed plants* (2<sup>nd</sup> Edition) John Wiley & Sons Inc, Hoboken, New Jersey, USA 302-303 pp
- Fang C-H, Guibal D, Clair B, Gril J, Liu Y-M, Lui S-Q (2008) Relationships between growth stress and wood properties in polar I-69 (*Populus deltoids* Bartr.cv"Lux" ex I-69/55). *Annals of Forest Science* 65: 307
- Feist WC, Tarkow H (1967) Polymer exclusion in wood substance: a new procedure for measuring fiber saturation points. *Forest Products Journal* 17: 65-68
- Fernandes AN, Thomas LH, Altaner CM, Callow P, Forsyth VT, Apperley DC, Kennedy CJ, Jarvis MC (2011) Nanostructure of cellulose microfibrils in spruce wood. *Proceedings of the National Academy of Sciences of the United States of America* 108: E1195-E1203
- Fonweban J, Mavrou I, Gardiner B, Macdonald E (2013) Modelling the effect of spacing and site exposure on spiral grain angle on Sitka spruce (*Picea sitchensis* (Bong.) Carr.) in Northern Britain. *Forestry* 86: 331-342
- Forsberg D (1999) Warp, in particular twist, of sawn wood of Norway spruce (*Picea abies*). *Acta Universitatis Agriculturae Sueciae - Silvestria*: 20 +80 +20 +23 pp.
- Forsberg D, Warensjo M (2001) Grain angle variation: A major determinant of twist in sawn *Picea abies* (L.) Karst. *Scandinavian Journal of Forest Research* 16: 269-277
- Forestry Commission Statistics 2014 (2014) [www.forestry.gov.uk/statistics](http://www.forestry.gov.uk/statistics)
- Fries A, Ulvcrona T, Wu HX, Kroon J (2014) Stem damage of lodgepole pine clonal cuttings in relation to wood fibre traits, acoustic velocity and spiral grain. *Scandinavian Journal of Forest Research* 29: 764-776
- Fruhwald E (2006) Improvement of shape stability by high-temperature treatment of Norway spruce - Effects of drying at 120 degrees C with and without restraint on twist. *Holz Als Roh-Und Werkstoff* 64: 24-29
- Fruhwald E (2007) Effect of high-temperature drying and restraint on twist of Norway spruce. *Drying Technology* 25: 489-496
- Fruhwald E (2007) Effects of high drying temperatures and restraint on twist of larch (*Larix*). *Wood Material Science and Engineering* 2: 55-65
- Gjerdrum J, Sall H, Storo HM (2002) Spiral grain in Norway spruce: constant change rate in grain angle in Scandinavian sawlogs. *Forestry* 75: 163-170
- Gorisek Z, Straze A, Bucar DG, Bucar B (2005) Influence of some anatomical and physical properties of wood on warp during kiln drying of spruce (*Picea abies* Karst.) and silver fir (*Abies alba* Mill.). In A Teischinger, ed, *Lignovisionen*, Vol 13. Institut fur Holzforschung und der Verband Holzwirte Osterreichs - VHO, Wien, Austria
- Hallingback HR, Jansson G, Hannrup B (2010a) Genetic correlations between spiral grain and growth and quality traits in *Picea abies*. *Canadian Journal of Forest Research-Revue Canadienne De Recherche Forestiere* 40: 173-183
- Hallingback HR, Jansson G, Hannrup B, Fries A (2010b) Which Annual Rings to Assess Grain Angles in Breeding of Scots Pine for Improved Shape Stability of Sawn Timber? *Silva Fennica* 44: 275-288

- Harris AS (1990) *Picea sitchensis*. In: Silvics of North America, Burns RM, Honkala BH (tech coords) Silvics of North America Vol 1. Conifers, Agriculture Handbook 654 U.S. Department of Agriculture, Forest Service, Washington, DC 2: 877 pp
- Harris JM (1965) Preliminary studies of spiral grain in radiata pine. Proceedings IUFRO Melbourne Sect 41, Vol 1, 23 p
- Harris JM, Meylan BA (1965) Influence of microfibril angle on longitudinal and tangential shrinkage in *pinus radiata*. *Holzforschung* 19: 144-&
- Harris J (1989a) Spiral Grain and Wave Phenomena in Wood Formation. Springer-Verlag, Berlin Heidelberg 2-5 pp
- Harris J (1989b) Spiral Grain and Wave Phenomena in Wood Formation. Springer-Verlag, Berlin Heidelberg 43 p
- Harris J (1989c) Spiral Grain and Wave Phenomena in Wood Formation. Springer-Verlag, Berlin Heidelberg 61 p
- Haslett AN, Dakin M (2001) Effect of pressure steaming on twist and stability of radiata pine lumber. *Forest Products Journal* 51: 85-87
- Haslett AN, Simpson IG, Kimberley MO (1992) Utilisation of 25-year-old *Pinus radiata*. Part 2: warp of structural timber in drying. *New Zealand Journal of Forestry Science* 21: 228-234
- Hill CAS, Norton A, Newman G (2009) The Water Vapor Sorption Behavior of Natural Fibers. *Journal of Applied Polymer Science* 112: 1524-1537
- Johansson M (2003) Prediction of bow and crook in timber studs based on variation in longitudinal shrinkage. *Wood and Fiber Science* 35: 445-455
- Johansson M, Kliger R (2002) Influence of material characteristics on warp in Norway spruce studs. *Wood and Fiber Science* 34: 325-336
- Johansson M, Kliger R, Perstorper M (1999) The influence of material variation on quality of Norway spruce timber. *Forest Research Bulletin*: 314-321
- Johansson M, Nystrom J, Ohman M (2003) Prediction of longitudinal shrinkage and bow in Norway spruce studs using scanning techniques. *Journal of Wood Science* 49: 291-297
- Johansson M, Ormarsson S (2009) Influence of growth stresses and material properties on distortion of sawn timber - numerical investigation. *Annals of Forest Science* 66: 10
- Johansson M, Perstorper M, Kliger R, Johansson G (2001) Distortion of Norway spruce timber Part 2. Modelling twist. *Holz Als Roh-Und Werkstoff* 59: 155-162
- Kang W, Lee NH (2004) Relationship between radial variations in shrinkage and drying defects of tree disks. *Journal of Wood Science* 50: 209-216
- Kennedy SG, Cameron AD, Lee SJ (2013) Genetic relationships between wood quality traits and diameter growth of juvenile core wood in Sitka spruce. *Canadian Journal of Forest Research* 43: 1-6
- Klaiber V, Seeling U (2004) The influence of drying method on the warp behavior of Norway spruce (*Picea abies* (L.) Karst.) sawn timber. *Forest Products Journal* 54: 79-87
- Kliger IR (2001) Spiral grain on logs under bark reveals twist-prone raw material. *Forest Products Journal* 51: 67-73
- Kliger IR, Nilsson N, Johansson M (2006) Pre-twisting during sawing results in straight studs. *Forest Products Journal* 56: 61-65
- Kliger R, Bengtsson C, Johansson M (2005) Comparison between HT-dried and LT-dried spruce timber in terms of shape and dimensional stability. *Holzforschung* 59: 647-653

- Kliger R, Johansson M, Perstorper M, Johansson G (2003) Distortion of Norway spruce timber - Part 3: Modelling bow and spring. *Holz Als Roh-Und Werkstoff* 61: 241-250
- Kowalski SJ, Pawlowski A (2011) Intermittent drying of initially saturated porous materials. *Chemical Engineering Science* 66: 1893-1905
- Kubler H (1991) Function of spiral grain in trees. *Trees-Structure and Function* 5: 125-135
- Kubojima Y, Kobayashi I, Yoshida T, Matsumoto H, Suzuki Y, Tonosaki M (2013) Twisting force during drying of wood. *European Journal of Wood and Wood Products* 71: 689-695
- Leonardon M, Altaner CM, Vihermaa L, Jarvis MC (2010) Wood shrinkage: influence of anatomy, cell wall architecture, chemical composition and cambial age. *European Journal of Wood and Wood Products* 68: 87-94
- Macdonald E, Hubert J (2002) A review of the effects of silviculture on timber quality of Sitka spruce. *Forestry* 75: 107-138
- MacDonald JAB (1967) Norway or Sika spruce? *Forestry* 40: 129-138
- Mackay JFG (1973) The influence of drying conditions and other factors on twist and torque in *Pinus radiata* studs. *Wood and Fiber* 4: 264-271
- Mavrou I (2007) Modelling spiral grain in *picea sitchensis*. MSc Thesis. University of York 25 p
- McLean JP, Canavan JW, Jarvis MC, de Borst K, Ridley-Ellis D (2014) SIRT (Strategic Integrated Timber Research, Distortion Project Report, internal report
- McLean JP, Moore JR, Gardiner BA, Lee SJ, Mochan SJ, Jarvis MC (2015) Variation of radial wood properties from genetically improved Sitka spruce growing in the UK. *Forestry* 89: 109-116
- Meylan BA (1972) Influence of microfibril angle on longitudinal shrinkage-moisture content relationship. *Wood Science and Technology* 6: 293-301
- Mochan S, Gardiner BA, Lee S (2008) Benefits of improved Sitka spruce: volume and quality of timber. Forestry Commission Research Note FCRN003. Forestry Commission, Edinburgh
- Mochan S, Moore J, Connolly T (2009) Using acoustic tools in forestry and the wood supply chain. Forestry Commission Technical Note FCTN018. Forestry Commission, Edinburgh
- Moore J (2011) Wood properties and uses of Sitka spruce in Britain. Forestry Commission Research Report. Forestry Commission, Edinburgh
- Moore J, Achim A, Lyon A, Mochan S, Gardiner B (2009) Effects of early re-spacing on the physical and mechanical properties of Sitka spruce structural timber. *Forest Ecology and Management* 258: 1174-1180
- Moore J, Gardiner B, Ridley-Ellis D, Jarvis M, Mochan S, Macdonald E (2009) Getting the most out of the United Kingdom's timber resource. *Scottish Forestry* 63: 3-8
- Moore JR, Lyon AJ, Lehneke S (2012) Effects of rotation length on the grade recovery and wood properties of Sitka spruce structural timber grown in Great Britain. *Annals of Forest Science* 69: 353-362
- Moore JR, Lyon AJ, Searles GJ, Lehneke SA, Ridley-Ellis DJ (2013) Within- and between-stand variation in selected properties of Sitka spruce sawn timber in the UK: implications for segregation and grade recovery. *Annals of Forest Science* 70: 403-415
- Moore JR, Mochan SJ, Bruechert F, Hapca AI, Ridley-Ellis DJ, Gardiner BA, Lee SJ (2009) Effects of genetics on the wood properties of Sitka spruce growing in the UK: bending strength and stiffness of structural timber. *Forestry* 82: 491-501

- Northcott PL (1957) Is spiral grain the normal growth pattern? *Forest Chron* 33: 335-352
- Nystrom J (2003) Automatic measurement of fiber orientation in softwoods by using the tracheid effect. *Computers and Electronics in Agriculture* 41: 91-99
- Ormarsson S, Dahlblom O, Petersson H (1999) A numerical study of the shape stability of sawn timber subjected to moisture variation. *Wood Science and Technology* 33: 407-423
- Pang S (2002) Predicting anisotropic shrinkage of softwood - Part 1: Theories. *Wood Science and Technology* 36: 75-91
- Passialis C, Kiriazakos A (2004) Juvenile and mature wood properties of naturally-grown fir trees. *Holz Als Roh-Und Werkstoff* 62: 476-478
- Perstorper M, Johansson M, Kliger R, Johansson G (2001) Distortion of Norway spruce timber - Part 1. Variation of relevant wood properties. *Holz Als Roh-Und Werkstoff* 59: 94-103
- Plomion C, Leprovost G, Stokes A (2001) Wood formation in trees. *Plant Physiology* 127: 1513-1523
- Ray D, Pyatt G, Broadwater M (2002) Modelling the future climatic suitability of plantation forest tree species. *Forestry Commission Bulletin* 125, Forestry Commission, Edinburgh, UK 151-167pp
- Reynolds TN (2010) Variables affecting the stiffness and distortion of Sitka spruce. PhD Thesis, Edinburgh Napier University, Edinburgh
- Rice RW (2000) Measurements of delayed warp in eastern spruce studs. *Drying Technology* 18: 1833-1847
- Ridley-Ellis D (2011) Introduction to Timber Grading; The European system of machine strength grading. Workshop presentation SIRT (Strategic Integrated Timber Research), Forest Products Research Institute, Edinburgh Napier University
- Riepen M, Tarvainen V, Aleon D (2004) Final report on STRAIGHT WP.2.1, TNO, Delft, The Netherlands
- Sadoh T, Kingston RT (1967) Longitudinal shrinkage of wood. Part II: The relation between longitudinal shrinkage and structure. *Wood Science and Technology* 1: 81-98
- Salin JG (2007) Drying of prone to twist boards in a pre-twisted position. *Drying Technology* 25: 475-481
- Salin J-G (2011) Fibre level modelling of free water behaviour during wood drying and wetting. *Maderas-Ciencia Y Tecnologia* 13: 153-162
- Sall H (2002) Spiral grain in Norway spruce. PhD Thesis, Vaxjo-Linnaeus University, Smaland, Sweden
- Samuel CJA, Fletcher AM, Lines R (2007) Choice of Sitka spruce seed origins for use in British forests. *Forestry Commission Bulletin*: xi + 111 pp.-xi + 111 pp.
- Schjaer GS, Orhan FB (2006) Measurement of wood grain angle, moisture content and density using microwaves. *Holz als Roh-Und Werkstoff* 64: 483-490
- Seeling U, Merforth C (2000) FRITS - a new equipment to measure distortion. *Holz Als Roh-Und Werkstoff* 58: 338-339
- Simpson WT, Tschernitz JL (1997) Effect of thickness on warp in high-temperature drying plantation-grown loblolly pine 2 by 4's. *Wood and Fibre Science* 30: 165-174
- Skaar C (1988) *Wood-Water Relations*. Springer-Verlag, Berlin Heidelberg 140-164pp
- Stevens WC, Johnston DD (1960) Distortion caused by spiral grain. *Timber Technology* 68: 217-218
- Straze A, Gorisek Z (2006) Drying characteristics of compression wood in Norway spruce (*Picea abies karst.*). *Wood Structure and Properties* 06 399-403

- Straze A, Kliger R, Johansson M, Gorisek Z (2011) The influence of material properties on the amount of twist of spruce wood during kiln drying. *European Journal of Wood and Wood Products* 69: 239-246
- Tarvainen V, Ranta-Maunus A, Hanhijarvi A, Forsen H (2006) The effect of drying and storage conditions on case hardening of Scots Pine and Norway spruce timber. *Maderas: Ciencia y Tecnologia* 8: 3-14
- Taylor AM, Gartner BL, Morrell JJ (2002) Heartwood formation and natural durability - a review. *Wood and Fibre Science* 34(4): 587-611
- Timell TE (1986) *Compression wood in gymnosperms 2*. Springer-Verlag, Heidelberg 150p
- Tranquart V (1995) Spiral grain in Sitka spruce. Unpublished MSc thesis. Bangor University
- Tronstad S (2005) Effect of top loading on the deformation of sawn timber during kiln drying. Rapport - Norsk Treteknisk Institutt: 99 pp.-99 pp.
- Vainio U, Andersson S, Serimaa R, Paakkari T, Saranpaa P, Treacy M, Evertsen J (2002) Variation of microfibril angle between four provenances of Sitka spruce (*Picea sitchensis* Bong. Carr.). *Plant Biology* 4: 27-33
- Walker JCF (2006a) *Primary Wood Processing, 2<sup>nd</sup> Edition*, Springer, Dordrecht, The Netherlands 52-56 pp
- Walker JCF (2006b) *Primary Wood Processing, 2<sup>nd</sup> Edition*, Springer, Dordrecht, The Netherlands 101 p
- Walker JCF (2006c) *Primary Wood Processing, 2<sup>nd</sup> Edition*, Springer, Dordrecht, The Netherlands 78 p
- Wang E, Chen T, Pang S, Karalus A (2008) Variation in anisotropic shrinkage of plantation grown *pinus radiata* wood. *Maderas-Ciencia Y Tecnologia* 10: 243-249
- Wang XP, Simpson WT (2006) Using acoustic analysis to pre-sort warp-prone ponderosa pine 2 by 4s before kiln-drying. *Wood and Fiber Science* 38: 206-214
- Warensjo M, Rune G (2004) Effect of compression wood and grain angle on deformations of studs from 22-year-old Scots pine trees. *Scandinavian Journal of Forest Research* 19: 48-54
- Wengert EM and Meyer D (1993) Causes and cures for warp in drying. University of Wisconsin, Forestry Facts 68
- Wilson K, White DJB (1986a) *The Anatomy of Wood: its Diversity and Variability*. Stobart & Son Ltd, 66-73 Worship Street, London 47-52 pp
- Wilson K, White DJB (1986b) *The Anatomy of Wood: its Diversity and Variability*. Stobart & Son Ltd, 66-73 Worship Street, London 151-156 pp
- Wilson K, White DJB (1986c) *The Anatomy of Wood: its Diversity and Variability*. Stobart & Son Ltd, 66-73 Worship Street, London 17-20 pp
- Xu P, Liu H, Evans R, Donaldson LA (2009) Longitudinal shrinkage behaviour of compression wood in radiata pine. *Wood Science and Technology* 43: 423-439
- Yamamoto H (1999) A model of the anisotropic swelling and shrinking process of wood. Part 1. Generalization of Barber's wood fiber model. *Wood Science and Technology* 33: 311-325
- Yamamoto H, Sassus F, Ninomiya J, Gril (2001) A model of the anisotropic swelling and shrinking process of wood. Part 2. A simulation of shrinking wood. *Wood Science and Technology* 35: 167-181

- Yamashita K, Katsuki T, Akashi K, Kubojima Y (2010) Wood properties of *Picea koyamae*: within-tree variation of grain angle, tracheid length, microfibril angle, wood density and shrinkage. *Bulletin of the Forestry and Forest Products Research Institute* 9: 19-29
- Yerbury MD, Cooper RJ (2010) Curve sawing spruce sawlogs containing sweep can reduce drying distortion when compared with conventional sawing. *Forestry* 83: 443-450
- Ying L, Kretschmann DE, Bendtsen BA (1994) Longitudinal shrinkage in fast-grown loblolly-pine plantation wood. *Forest Products Journal* 44: 58-62
- Ylinen A, Jumppanen P (1967) Theory of the shrinkage of wood. *Wood Science and Technology* 1: 241-252